PREPARATION AND CHARACTERIZATION OF CALCIUM COPPER TITANATE FILLED EPOXY COMPOSITES FOR EMBEDDED CAPACITOR APPLICATIONS

by

MOHD SAIDINA BIN DANDAN SATIA

Thesis submitted in fulfillment of the requirements
for the degree of
Master of Science

2015

ACKNOWLEDGEMENT

Bismillahirrahmanirrahim. With the name of Allah, The Most Beneficent and The Most Merciful. First of all, I would like to express my gratitude to Allah SWT for the blessing, strength, and each and every ni'mat He bestowed upon me. Alhamdulillah, I have this research completed. Besides that, I would like to express my deepest appreciation to my main supervisor, Professor Ir. Mariatti Jaafar @ Mustapha for her guidance, inspiration and supervision throughout this research. I would also like to extend my gratitude to my co-supervisor Dr. Julie Juliewatty Binti Mohamed for her continuous support in helping to complete my research project.

I also extend my acknowledgement to School of Materials and Mineral Resources Engineering, Universiti Sains Malaysia and the Dean, Professor Hanafi Ismail for provided good facilities to me during my studies here.

Not to forget, my warmest appreciation to all the SMMRE's staffs for their technical support, as well as to my postgraduate friends; Andre Ningkan, 'Irfan, Nurliyana, Chen Ling, Norshamira, Johari, Fariz, Wan Fahmin and Abdul Rashid who always available for discussions.

Warmest appreciation to my father, Hj. Dandan Satia Bin Bukah and my siblings, Mr. Saidani, Ms. Samee'ah, Ms. Syawalliah and Mr. Shahrul Affendi for their motivation, love and endless support.

Last but not least, special thanks to the Ministry of Higher Education, Malaysia and Explorating Research Grant Scheme (ERGS) for granting the research fund used for this project (Project No. 6730109).

TABLE OF CONTENTS

CHAPTER 3:MATERIALS AND METHODOLOGY

LIST OF TABLES

LIST OF FIGURES

LIST OF ABBREVIATIONS

PCB	Printed Circuit Board
$CaCu_3Ti_4O_{12}$ (CCTO)	Calcium Copper Titanate
$BaTiO_3$	Barium Titanate
GPTMS	3-glycidoxypropyltrimethoxysilane
TGA	Thermogravimetric Analysis
DMA	Dynamic Mechanical Analysis
TMA	Thermo-Mechanical Analysis
MLC	Multilayer Capacitor
DGEBA	Diglycidyl ether of bisphenol-A
NaOH	Sodium Hydroxide
CTE	Coefficient of Thermal Expansion
XRD	X-ray Diffraction
SEM	Scanning Electron Microscope
FTIR	Fourier-Transform Infrared
EDS	Energy Dispersive Spectroscopy
SC	Spin Coating
HP	Hot Press

LIST OF MAIN SYMBOLS

%	Percentage
°C	Degree Celsius
°C/min	Degree Celsius per minutes
MPa	Megapascal
g	Gram
nm	Nanometer
μm	Micrometer
mm	Millimeter
g/cm^3	Gram per cubic centimeters
vol %	Volume percent
$	U.S Dollar
s	Second
min	Minutes
h	Hour
ε	Permittivity
tan δ	Tangent loss
Hz	Hertz
MHz	Megahertz
GPa	Gigapascal
%	Percentage
F	Farads
F/m	Farads per meter
K	Kelvin

T_g	Glass Transition Temperature
$T_{5\%}$	Initial Degradation Temperature
T_{onset}	Onset Decomposition Temperature
T_c	Curie Temperature
kV/mm	Kilovolt per millimeter
J/cm^3	Joule per cubic centimeters
mPa.s	Millipascal-second
rpm	Rotation per minute
psi	Pounds per square inch
ml	Milliliter
cm^{-1}	One per centimeter

PENGHASILAN DAN PENCIRIAN KOMPOSIT EPOKSI TERISI KALSIUM KUPRUM TITANAT UNTUK APLIKASI KAPASITOR TERBENAM

ABSTRAK

Permintaan yang semakin meningkat untuk pengecilan peranti elektronik menawarkan pengurangan saiz yang ketara, prestasi dielektrik dan haba yang lebih baik, kebolehpercayaan dan kos yang lebih rendah. Komposit polimer-seramik telah dipilih sebagai bahan dielektrik yang paling sesuai untuk kapasitor terbenam. Dalam kajian ini, seramik seperti kalsium kuprum titanat, $CaCu_3Ti_4O_{12}$ (CCTO) dan barium titanat ($BaTiO_3$) telah digunakan sebagai pengisi dalam komposit epoksi filem nipis. Sifat-sifat komposit epoksi filem nipis dihasilkan berdasarkan muatan pengisi yang berbeza (5 hingga 20% isipadu), kaedah fabrikasi seperti salutan putaran (SC) dan tekan panas (HP), pengisi hibrid (CCTO dan $BaTiO_3$), rawatan permukaan pengisi dan pelbagai jenis resin epoksi (DER 332, Epolam 2015 dan OP 392) telah dikaji. Keputusan menunjukkan bahawa komposit CCTO/epoksi mempamerkan pemalar dielektrik, T_g dan kekonduksian haba yang lebih tinggi berbanding dengan epoksi tidak terisi dan komposit $BaTiO_3$/epoksi. Dalam siri kedua, pengisi CCTO untuk pengisian komposit epoksi telah dipilih untuk siasatan lanjutan. Komposit CCTO/epoksi dengan pengisian sehingga 40% isipadu dapat dihasilkan dengan menggunakan kaedah HP. Hasil ujian telah menunjukkan bahawa sifat-sifat komposit 40% isipadu CCTO/epoksi (HP) telah meningkat sebanyak 55% pemalar dielektrik dan 83% modulus simpanan, dan penurunan 69% pekali pengembangan haba berbanding dengan sifat-sifat komposit 20% isipadu CCTO/epoksi (SC). Pengisi Hibrid untuk pengisian komposit epoksi telah dihasilkan dan keputusan menunjukkan bahawa Hibrid 70:30 mempamerkan kesan hibrid yang positif berbanding dengan komposit pengisi tunggal; komposit filem nipis CCTO/epoksi dan $BaTiO_3$/epoksi. Selepas rawatan CCTO oleh ejen gandingan silana, sampel komposit epoksi terisi CCTO 10% yang terawat menunjukkan peningkatan yang memberangsangkan iaitu sebanyak 60% pemalar dielektrik berbanding komposit filem nipis CCTO/epoksi yang tidak terawat. Berdasarkan pelbagai resin epoksi, komposit filem nipis CCTO/epoksi OP 392 yang terawat mempamerkan kenaikan pemalar dielektrik sebanyak 10% dan susutan dalam pekali pengembangan haba sebanyak 38% berbanding dengan bahan dielektrik komersial, iaitu 3M Embedded Capacitor. Secara kesimpulannya, komposit filem nipis CCTO/epoksi OP 392 yang terawat menunjukkan prestasi yang baik dari segi pemalar dielektrik dan haba berbanding komposit CCTO yang tidak terawat, komposit hibrid dan lain-lain komposit terawat.

PREPARATION AND CHARACTERIZATION OF CALCIUM COPPER TITANATE FILLED EPOXY COMPOSITES FOR EMBEDDED CAPACITOR APPLICATIONS

ABSTRACT

Continuous miniaturization of electronic devices result in a high demand of embedded capacitor that offers significant reduction in size, better dielectric and thermal performance, reliability and lower cost. Polymer-ceramic composites have been considered as the most suitable dielectric materials for embedded capacitor. In this study, ceramics such as calcium copper titanate, $CaCu_3Ti_4O_{12}$ (CCTO) and barium titanate ($BaTiO_3$) were used as fillers in epoxy thin film composites. The properties of epoxy thin film composites fabricated based on different filler loading (5 to 20 vol%), fabrication methods such as spin coating (SC) and hot press (HP) methods, hybrid fillers (CCTO and $BaTiO_3$), surface treatment of filler and various types of epoxy resins (DER 332, Epolam 2015 and OP 392) were characterized. Results showed that CCTO/epoxy composite exhibited higher dielectric constant, T_g and thermal conductivity compared to those of unfilled epoxy and $BaTiO_3$/epoxy composites. In the second series, CCTO filler filled epoxy composite was chosen for further investigation. CCTO/epoxy composite with filler loading of up to 40 vol% was able to be produced by using HP method. It was found that 40 vol% CCTO/epoxy (HP) composite has increased 55% of dielectric constant and 83% of storage modulus, and decreased 69% of CTE compared to 20 vol% CCTO/epoxy (SC) composite. Hybrid fillers composites were fabricated and results indicated that Hybrid 70:30 showed positive hybrid effect compared to those of single filler composites; CCTO/epoxy and $BaTiO_3$/epoxy thin film composites. After treatment of CCTO by silane-based coupling agent, sample with 10% treated CCTO filled epoxy composite presented remarkable improvement with an increased 60% of dielectric constant than untreated CCTO/epoxy thin film composite. Based on various epoxy resins, treated CCTO/OP 392 epoxy thin film composite has improved 10% of dielectric constant and decreased 38% of CTE compared to 3M Embedded Capacitor. In short, treated CCTO filled OP 392 epoxy thin film composite exhibited good dielectric properties and thermal properties compared to those of untreated CCTO composites, hybrid fillers composites and other treated composites.

CHAPTER 1

INTRODUCTION

1.1 Background

Passive components such as resistors, capacitors and inductors are widely used in the microelectronic packaging industry (Wu et al., 2007). These components refer to the type of electrical components that cannot generate power. Nearly 80% of the printed circuit board (PCB) is occupied by passive components, therefore research on the passive component are still developing so that the number of passives is steadily growing with high functionality of electronic devices (Rao et. al, 2002). Most of the passive components used today are discrete surface mount passive components which is directly mount on the surface of a PCB. Among passive components, capacitor plays important role in electronic device which is used to store energy in electric field.

A capacitor is a passive two terminal component which is used to store electric charge. It has a sandwich type of structrue as illustrated in Figure 1.1. Stephen (2001) reported that the structure has two parallel conductive plates (T) and a dielectric in the middle with its capacitance value in Farads. It is then being fixed by the surface area of the conductive plates (S) and the distance of separation between them (D). A capacitor should provide high storage of charge, stable capacitance over a broad temperature range and low losses for the device to maintain its charge and to avoid self-heating. Moreover, other practical requirements are packaging and reliability at high temperature, as well as cost efficiency which excludes the used of expensive elements to a large extent.

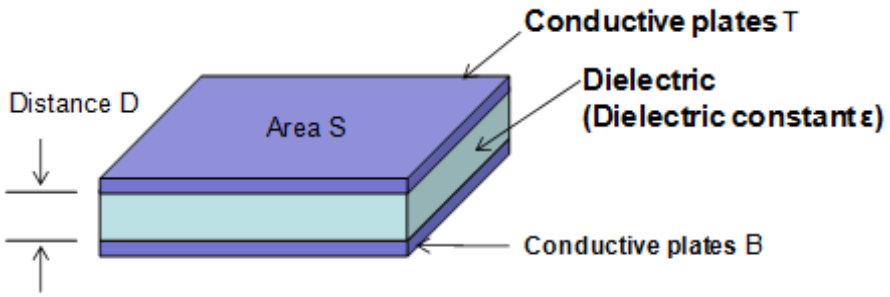

Figure 1.1: Structure of a capacitor

There are two types of capacitor that is widely used in the market, discrete capacitor and embedded capacitor. The primary advantages of embedded capacitor over discrete capacitor include size and weight reduction, better reliability, excellent electrical performance and easy processing. It is worth noting that composites consisting of the ceramic filler and polymer matrix have been considered as one of the most promising materials for embedded capacitors. Compared with the ceramic fillers, the polymer can be processed under low temperature and their processing method can be controlled easily. Besides, owing to their higher breakdown strength, the embedding polymer can improve the breakdown performance of embedded capacitors. The ceramic fillers have high dielectric permittivity, which can enhance the dielectric properties of the capacitors. Hwu et. al (2005), Yoon et. al (2009) and Luo et. al (2009) proved that by incorporating the ceramic fillers into polymer matrix can well combine their advantages to optimize overall properties of embedded capacitor.

Previous studies reported that epoxy resin is one of the most common type of thermosetting resin used in electronic packaging applications. Epoxy resin offers advantages in terms of flexibility, compatibility, low processing temperature and can be easily fabricated into various shapes. However, the dielectric constant of epoxy

resin is low which is not suitable to be used as dielectric material for embedded capacitor. Therefore, by incorporating epoxy resin with ceramic filler can produce epoxy composites with high dielectric constant (Alam et. al, 2011).

Based on the dielectric constant value, one of the most promising materials that can be used as ceramic fillers in epoxy resin is Calcium Copper Titanate, $CaCu_3Ti_4O_{12}$ (CCTO). CCTO ceramic which has centrosymmetric *bcc* structure (space group Im3, lattice parameter a ≈ 0.7391nm, and Z = 2), has been used as a filler due to lead-free, environment friendly and high dielectric constant ceramic which is about ~ 10^5 (Subramanian et. al, 2000; Homes et. al, 2001).

1.2 Problem Statements

Recently, the miniaturization in electronic devices has been a clear trend in the market due to the demand on the compactness, better performance, light weight and low cost of electronics. This phenomenon has driven changes in the electronic packaging requirements from discrete capacitor to embedded capacitor. Embedded planar capacitors are thin laminates embedded inside a substrate or PCB that serve both as a power or ground plane and as a parallel plate capacitor. As reported by Lee et al. (2007), Xu et al. (2007) and Das et al. (2008), polymer-ceramic composites have been pursued as the most promising dielectric materials for embedded capacitors in the organic package due to lower procesing temperature (<250°C), high flexibility and lower cost.

Pure ceramics such as Barium Titanate, $BaTiO_3$ has high dielectric constant which is about ~1000, but pure $BaTiO_3$ is still not suitable to be used as dielectric material as the processing temperature of $BaTiO_3$ is higher than PCB manufacturing

process and incorporation of $BaTiO_3$ ceramic into epoxy resin produced composites with low dielectric constant which is about 8 (measured at 100 Hz) at 20 vol% loading of $BaTiO_3$ filler (Duran et al., 2002; Zhang et al., 2014). Due to that, CCTO has received great attention by many researchers because of its giant dielectric constant which is about ~10 000 as compared to $BaTiO_3$ ceramic (Subramanian et al., 2000; Homes et al., 2001). According to the previous reports, by increasing CCTO loadings in polymer matrix system, dielectric properties of composites can be improved (Ramajo et al., 2008; Thomas et al., 2013). However, reports on thermal properties of CCTO filler filled epoxy matrix are very limited. Thermal properties such as glass transition temperature (T_g), storage modulus and thermal stability of CCTO/epoxy composite are important to be identified for electronic applications.

A combination of fillers in certain polymer matrices or hybrid composites is getting acceptance from many researchers (Weon and Sue, 2006; Deshmukh et al., 2011). Hybrid composites produce significant effects because the combination of two types of fillers may balance the performance of polymer composites that cannot be obtained when only a single filler is used (Kord, 2011). According to Etika et al. (2009), Helmi et al. (2013) and Luo et al. (2014), addition of hybrid fillers into polymer matrix can greatly enhance the properties of the composites as compared to single filler. This could be due to different shape, aspect ratio and dispersion characteristics of the two different fillers that could improve the properties of the composites.

Apart from that, the fabrication methods of epoxy thin film composites, filler treatment, types of epoxy resins, filler-matrix adhesion, filler dispersion in epoxy matrix and types of epoxy resins used in the preparation of epoxy composites play an

important role in determining the final properties of the composites. Based on the literature studies, the silane-based coupling agent showed an improvement in the properties of the polymer composites compared to untreated polymer composites due to better dispersion of filler in epoxy matrix (Todd and Shi, 2003; Hirano et al., 2012; Yang et al., 2013). The silane-based coupling agent acts as a bridge in between the filler and the matrix which then enhanced the filler-matrix bonding and subsequently improve the final properties of the composites. Electronic packaging application requires properties such as high dielectric constant, low dielectric loss, good mechanical strength, high thermal stability, high T_g and low CTE value. Therefore, in this study, those properties have been investigated.

1.3 Objectives

The present study mainly investigates the effect of incorporation ceramic filler in epoxy matrix system. The knowledge obtained from this investigation will be useful in selecting the most desirable dielectric materials with excellent dielectric, tensile and thermal properties for embedded capacitor. The main objectives of the present study are as follows:

1. To study the effect of different filler types and filler loading range on the dielectric, tensile and thermal properties of epoxy thin film composites
2. To compare the effect of spin coating method and hot press method on the dielectric and thermal properties of ceramic filler filled epoxy thin film composites
3. To investigate the effect of hybrid fillers on the dielectric and thermal properties of epoxy thin film composites

4. To determine the effect of silane coupling agent on the properties of CCTO/epoxy thin film composites
5. To compare the effect of various epoxy resins on the dielectric and thermal properties of CCTO filled epoxy thin film composites

1.4 Scope of Work

The present studies focus on the production of epoxy thin film composites by studying the filler types and loading range. Two types of filler, namely CCTO and $BaTiO_3$ ceramics are used in this study. The loading of the ceramic filler in the epoxy resin is varied from 5 vol% to 20 vol%. Besides that, unfilled epoxy is also prepared for comparison purpose. The second phase of study concentrates on the effect of several fabrication methods on the final properties of composites. CCTO ceramic is further used as a filler for the preparation of epoxy composites at two different fabrication methods which includes spin coating method and hot pressing method. This study is continued by studying the effect of hybrid fillers, which is believed can improve the properties of epoxy thin film composites. 20 vol% of hybrid fillers (CCTO and $BaTiO_3$ ceramics) are used at different ratio of hybrid fillers of CCTO: $BaTiO_3$ which is varied from 30:70, 50:50 and 70:30, respectively. Moreover, silane-based coupling agent known as 3-glycidoxypropyltrimethoxysilane (GPTMS) is chosen in order to improve the interfacial adhesion between CCTO filler and epoxy resin. Lastly, CCTO filler was used as a filler in two types of epoxy resins; Epolam 2015 and OP 392. Comparison of properties of the epoxy thin film composites with epoxy DER 332 thin film composite were made.

The present study is mainly focused on the investigation of dielectric, tensile and thermal properties of the composites using various characterization techniques such as dielectric properties analyzer, tensile properties analyzer, TGA, DMA, TMA and thermal conductivity analyzer. The results are also supported by the morphology of fractured samples of the composites.

1.5 Dissertation Overview

Chapter 1 starts with a brief introduction of passive components which is important in electronic packaging applications. This chapter also includes some of the problem statements for passive components, especially capacitors. The objectives of the research project are described in this chapter.

Chapter 2 consists of literature review on the recent progress made in embedded capacitor research area which includes the definition, classification and applications.

Chapter 3 describes the overall research flowchart in the present study, followed by materials used in the experiment and experimental procedures. The characterization methods are also discussed in this chapter.

Chapter 4 reports the characterization of raw materials used in the preparation of ceramic filler filled epoxy thin film composites. This chapter is further divided into four parts. The first part discussing the effect of filler types and loading range on the properties of epoxy composites. The second part describes the effect of fabrication methods on the dielectric and thermal properties of epoxy composites, followed by the effect of hybrid fillers on the properties of epoxy thin film composites. Next, the properties of treated CCTO in epoxy thin film composites are

studied and compared with the untreated CCTO/epoxy thin film composites. Lastly, the properties of epoxy thin film composites fabricated by using different types of epoxy resins are compared.

Chapter 5 presents the conclusions from this research and also some recommendations for future studies in this related field.

CHAPTER 2

LITERATURE REVIEW

2.1 Passive Devices

Passives often called as the key functional elements in all electronic systems. It represent a world wide market of $20 billion per year as illustrated in Figure 2.1. Passives refer to resistors, capacitors and inductors, and usually exist in all of the electronic system to provide impedance, current-to-voltage phase angle and energy storage. Moreover, passive components are nonswitching, have no gain and cannot amplify as compared to active components. These components perform vital functions such as bias, decoupling, filtering and terminations in order to provide proper operations of all electronic systems. There are more than ten discrete passives used for every active component in a typical system which account for 90% of components, 40% of board area and 30% of solder joints in typical systems (Tummala, 2001; Ramkumar et al., 2006; Bhalerao, 2008; Lu, 2008).

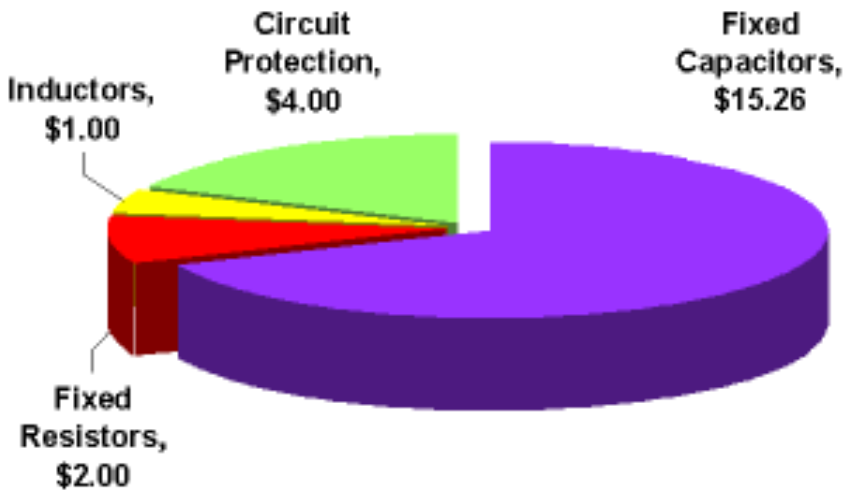

Figure 2.1: World passive components market ($billions) (Pfahl and McElroy, 2005)

As the trend towards miniaturization, lighter weight, faster, high reliability and low cost electronic devices increases over the years, passive technology has switched from discrete passives to integrated passives and recently, embedded passives. Embedded passives have been introduced in which the passive components are embedded or buried within the board itself as depicts in Figure 2.2. This is an alternative to smaller discrete passives and complex integrated passives. It provides many advantages such as reduction in size and weight, improved reliability and speed, improve performance and reduced cost as compared to discrete passives and integrated passives (Lu and Wong, 2008).

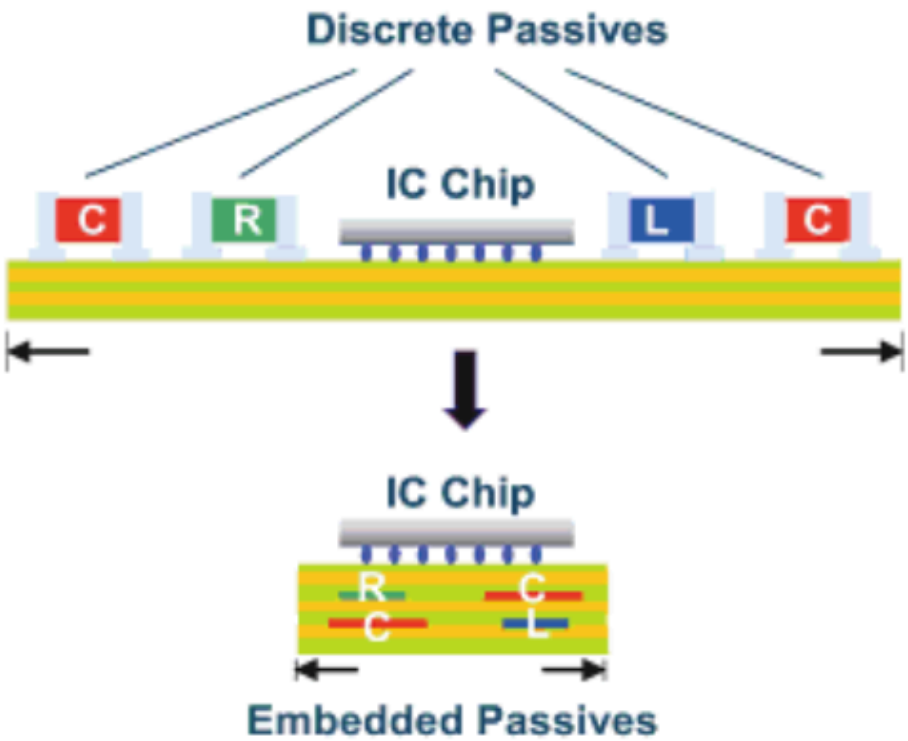

Figure 2.2: Schematic representation of the size advantages of the embedded passives as compared to discrete passives (Lu and Wong, 2008)

Table 2.1 shows the comparison between discrete passives and embedded passives. Despite of numerous advantages that have been offered by embbeded passives, they still have limitations too. It shows that the rework and manufacturing costs of embedded passives are low except the components and materials costs. Gerke (2005) illustrated that once the materials and design are set, the manufacturing and other costs associated with assembly are small. Furthermore, the overall risk of embedded technologies are high even the design flexibility is little, this is because if the passive values are incorrect, the board will have to be scrapped.

Table 2.1: Comparison between discrete passives and embedded passives (Gerke, 2005)

	Discrete Passives	**Embedded Passives**
Overall cost	High	Low
Circut board cost	High	Low
Manufacturing cost	High	Low
Board area consumed	Large	Small
Machine set-up time	Long	Fast
Yield	Low	High
Electrical performance (especially at high frequency)	Good	Better
Components costs	Low	High
Materials costs	Low	High
Design flexibility	Large	Little
Risk	Low	High

2.2 Capacitors

A capacitor is defined as two conductors (conductive plates) which separated by a non-conductive region also known as dielectric as illustrated in Figure 2.3 (i). The conductors may be plates, foil, solid shapes or even wires, whereby for dielectric, it can be glass, air, vacuum, paper, oxide layer on metal (as in electrolytic capacitors), flat thin paper or film, placed or even wound on the conductors. Figure 2.3 (ii) shows the general symbol used for capacitor. Generally, a capacitor is used to store and release electrical energy. It can also be used to smooth out current fluctuations, store and release a high voltage or block DC voltage.

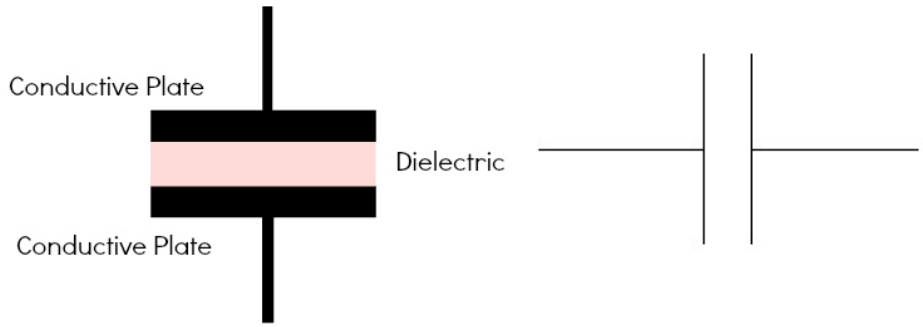

(i) (ii)

Figure 2.3: (i) Structure of a capacitor and (ii) general symbol used for capacitor

Paraelectrics and ferroelectrics are the main types of dielectric materials. Paraelectric materials tend to have much lower dielectric constant than those of ferroelectric materials but they are more stable with respect to temperature, frequency, film thickness, bias, voltage and time. Therefore, paraelectrics are more suitable for high tolerance applications including filtering, timing and more. Whereby for ferroelectrics, it would be preferred for decoupling because of higher dielectric constants and less tolerance. Table 2.2 presents various dielectric materials

and their properties. Paraelectrics and ferroelectrics can be further divided into four classes such as thin film oxides, unfilled polymers, ferroelectrics and ferroelectric filled polymers (Ulrich, 2000; Rao, 2001; Pfahl and McElroy, 2005).

Table 2.2: Various dielectric materials and their properties (Ulrich and Brown, 2006)

Dielectric Materials	**Dielectric Constant**
Epoxies	3 – 5
Unlimited laminated polymer	4
Ferroelectric filled polymer	50
Spin-on BCB	2.7
SiO_2	3.7
Al_2O_3	9
Ta_2O_5	24
TiO_2	40
$BaTiO_3$	~ 1000

The examples of paraelectric materials are thin film oxides and unfilled polymers. Thin film oxides such as SiO_2, Ta_2O_5, TiO_2, Al_2O_3 and BCB have higher dielectric constant than those of unfilled polymers. However, unfilled polymers offer simple processing conditions and lower processing cost per area as compared to thin film oxides. Ferroelectrics such as barium titanate, $BaTiO_3$ offer very high dielectric constant and therefore, possesses the highest energy density in ferroelectric materials which is useful for energy storage applications. However, $BaTiO_3$ is strongly affected by environment and operating condition such as temperature, frequency,

voltage and time. It also cannot be directly implemented on the organic substrates as the material must be annealed onto a separate copper foil first and oxygen is required during firing process. Ferroelectric filled polymers are the combinations of paraelectrics and ferroelectrics. Few advantages can be obtained by combining both types such as high dielectric constant and compatible processing conditions for organic substrates. For example, by adding ferroelectric material such as $BaTiO_3$ into paraelectric material such as epoxy resin or polyimide, relatively high dielectric constant can be obtained at low processing temperature.

2.2.1 Types of Capacitors

Capacitors have been created in various physical forms which presently exists in today's electronic market. There are two types of capacitors such as discrete capacitors and embedded capacitors. These topics will be discussed in the next sections.

2.2.1.1 Discrete Capacitors

The discrete capacitors are known as single component or integrated arrays that are enclosed in a single enclosure and mounted on an interconnecting substrate. This type of capacitors are the most common form of capacitors widely used in today's electronics. The examples of discrete capacitors including film capacitors, ceramic capacitors, mica capacitors, electrolytic capacitor and solid tantalum capacitors (Sarjeant et al., 1999; Jain and Rymaszewski, 2003).

A film capacitors can be described as non-polarized capacitors with an insulating plastic film as the dielectric and electrode plates. Various plastic films

have been used for film capacitors such as polypropylene, polyester, polycarbonate and polyimide. However, polypropylene and polyester become the most popular materials for surface-mount film capacitors (Cozzolino and Ewell, 2002).

Meanwhile for ceramic capacitors, it refers to non-polarized fixed capacitor made from two or more alternating layers of ceramic and metal in which the ceramic material acts as the dielectric and the metal acts as the electrodes. The main types of ceramic capacitor that is often used in electronic equipments are the multi-layer ceramic capacitor which is also known as MLCC (Pabst and Gregorová, 2007).

However, in the latest technology, as the demand to miniaturize the devices increase, discrete capacitors can be no longer fit to the trend of technology. These discrete capacitors not only occupies large surface area of the substrate, but also provide low electrical and reliability performance due to increment of interconnection length and number of solder joint. Therefore, to solve these problems, embedded passive component technology was introduced (Rao et. al, 2002).

2.2.1.2 Embedded Capacitors

Embedded capacitors are basically integrated inside the substrate in which can bring miniaturization to corresponding devices and therefore it will replace current discrete capacitors and can be used in the next generation modern electronics (Choa et al., 2004; Zhang et al., 2012). Embedded capacitors offer many advantages such as size reduction, cost reduction, improve in electrical performance and also improve the reliability performance of an electronic system due to elimination of the solder joints that are required by discrete components (Sandborn, 2003; Choa et. al,

2004; Lu et. al, 2007; Lu and Wong, 2008; Wu et. al, 2009). Figure 2.4 shows the cross sectional view of an embedded capacitor and the summarized advantages of embedding thin film capacitors in a microelectronics packaging (Kim et al., 2009).

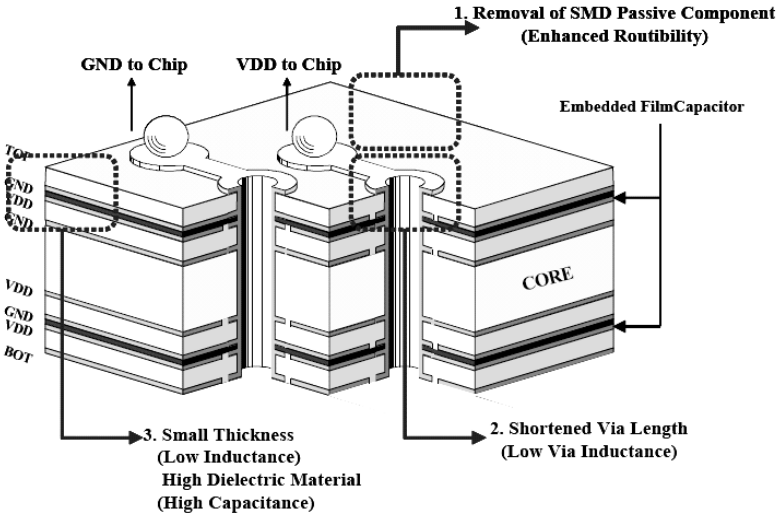

Figure 2.4: Cross-section view of an embedded capacitor and its advantages (Yoon et al., 2009)

In previous works, ceramic materials are usually considered to possess giant dielectric constant and low dielectric loss. Cho et al. (2004) reported that $BaTiO_3$ was chosen as a ceramic material due to its high dielectric constant. The dielectric constant of bulk $BaTiO_3$ ceramics increased with decreasing of grain sizes up to approximately 700nm. However, ceramic materials posses high sintering temperature, high production cost and poor processability. Therefore, it is not suitable to be used as dielectric materials for embedded capacitors (Bhattacharya et al., 2000). Meanwhile, polymers are flexible in nature, can be processed at much lower temperature, low dissipation factors, high dielectric breakdown strength and good dielectric stability over a wide range of frequencies and temperatures (Bai et

al., 2000).

Generally, to embed capacitor into the substrate, the dielectric materials must be easily processed in a manner compatible with the low-temperature manufacturing process of an organic substrate. Due to that, ceramic filler filed polymer system become one of the most promising materials for embedded capacitor. It utilizes high dielectric constant of ceramic powders and good processability of polymers resulting in lower temperature process about less than 250 °C and lower cost (Bhattacharya et al., 2000; Bhattacharya et al 2001; Rao et al., 2002).

2.3 Dielectric Mechanisms

The following topics discussed about the basic concepts with suitable examples of capacitance, dielectric constant and dielectric loss.

2.3.1 Capacitance and Dielectric Constant

The ability of a capacitor to store an electric charge is called capacitance (C). Capacitance can be simply stated as the amount of charge that a capacitor is capable of holding per unit of voltage applied. It is measured in units called farads (F), basically describes as the number of coulombs of charge that can be placed on each conductor causes a voltage of one volt across the device. Capacitance in the range of picofarad (10^{-12}) to microfarad (10^{-6}) are widely used for typical electrical circuit (Adhami et al., 2007; Deshpande, 2012; Erjavec, 2013). Equation 2.1 shows how capacitance with a vacuum dielectric layer, C_o is related to stored charge and applied voltage.

$$C = \frac{Q}{\Delta V} = \frac{Q}{Qd/\varepsilon_0 A} = \frac{\varepsilon_0 A}{d} \quad (2.1)$$

where Q is the charge applied, V is the voltage applied, ε_0 is the vacuum permittivity (8.854 x 10^{-12} F/m), A is the area of the electrical conductor and d is the distance between the conductors. Noted that, the capacitance can be maximized if the capacitor plates have larger area and the distance between the conductors are placed together as close as possible.

The dielectric constant (k or ε_r) is known as relative permittivity in which the ratio of permittivity of dielectric medium over permittivity of a vacuum (Sharif, 2010; Fariz, 2013). It also represents the ability of a capacitor to store charge in a capacitor. The relationship between capacitance (C) and dielectric constant (k or ε_r) are shown in Equation 2.2.

$$C = \frac{\varepsilon_0 \varepsilon_r A}{d} \quad (2.2)$$

It is evident that the larger the dielectric constant, the more the charge the capacitor can store in a given field and the higher the capacitance at a given space. Therefore, it is crucial to have materials with high dielectric constant for the application of capacitor.

2.3.2 Dielectric Loss

The dielectric loss is a measure of the energy so dissipated in the dielectric in the form of heat. It also can be called as dissipation factor or loss tangent (tan δ). Dielectric loss can be further separated into two forms including relaxation effect and

conduction loss. Fowler (1994) and Sirdeshmukh et al. (2006) stated that dielectric loss occurs because of the dipoles that continually reorient with the field. A little electric energy will be dissipated or converted into the heat energy on every time the molecular structure of the dielectric material has to adjust to a new polarity. This phenomenon is known as relaxation effect.

The dielectric loss is also influenced by the flow of charge passing through the material which causes energy dissipation. This phenomenon is often called as the conduction loss. It usually shows a linear log (tan δ) against frequency plot, whereby the loss caused by the relaxation effect shows a maximum at a certain frequency (Sirdeshmukh et al., 2006).

2.4 Filler/Polymer Thin Film Composites

Polymer composites can be described as materials which consists normally of two discrete phases, a continuous matrix phase which is often a resin and a discontinuous filler phase made up of discrete particles (Han, 1981). The reinforcement materials which are stiffer and stronger than the matrix are impregnated in order to enhance mechanical and physical properties of the composite materials and also to reduce the production cost by replacing expensive resins with inexpensive solid particles. As reported by Charles (2005), the miniaturization in the electronics industry and the evolution of packaging from bulk packaging to thin film packaging takes place in line with Moore's law.

According to ASTM D882-02, the material is considered as a thin film when the thickness is not greater than 0.25 mm. Polymer thin films have numerous applications such as multicolour photographic printing, paints, adhesives, index-

matched optical coatings and photoresists (Ade et al., 1998). Currently, thin film composites composed of polymers as matrix and ceramics as reinforcement are being developed in order to improve the electrical performance and reduce assembly cost as compared to traditional discrete capacitor technology (Rao and Wong, 2004). The ceramic fillers and epoxy resin that been used in polymer thin film composites are explained in the following sub-topics.

2.4.1 Fillers

Fillers often describe as a variety of solid particulate materials such as inorganic or organic that may be irregular, acicular, fibrous or plate-like in shape and which are used in reasonably large volume loadings in plastics. Pigments and elastomeric matrices are not normally included in this definition. Moreover, fillers were considered as an additives due to its unfavorable geometrical features, surface area or surface chemical composition which might increase the modulus of the polymer, whereas tensile strength and elongation at break will remain unchanged or decreased. Besides that, addition of fillers into matrix system can reduce the cost of materials by replacing the more expensive polymer, increased dielectric properties due to giant dielectric constant possesed by the filler and increased thermal conductivity due to faster molding cycles (Xanthos, 2005).

2.4.1.1 Calcium Copper Titanate

Calcium Copper Titanate, $CaCu_3Ti_4O_{12}$ (CCTO) is a family member of $ACu_3Ti_4O_{12}$ that was first discovered by Deschanvres et al. (1967). CCTO has a body-centered cubic, *bcc* structure with a lattice parameter of 0.7391 nm at room

temperature (Prakash & Varma, 2007), with four ATiO$_3$ perovskite-type structures per unit cell (He et al., 2002) as shown in Figure 2.5.

Unlike other ferroelectric materials such as $BaTiO_3$ which displays a peak in its dielectric properties near the curie temperature, T_c, the dielectric constant of CCTO is almost constant over a wide range of temperature from 100 to 400 K (Ramirez et al., 2000). Due to its unusual dielectric property which exhibits large dielectric constant (~10^5) and low dielectric loss at room temperature, lead free and also environment friendly, CCTO has attracted a great attention by many researchers (Subramanian et al., 2000; Homes et al., 2001).

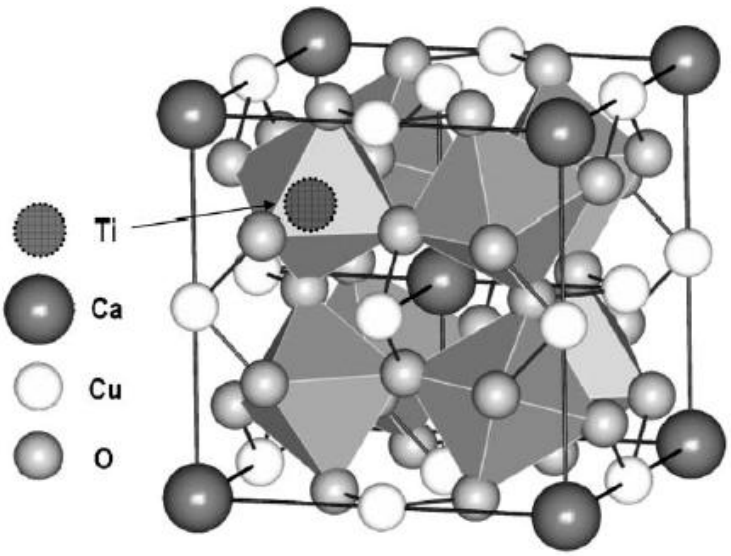

Figure 2.5: Structure of CCTO (Manik and Pradhan, 2006)

2.4.1.2 Barium Titanate

Barium Titanate, $BaTiO_3$ is a very well known dielectric material as compared to $CaCu_3Ti_4O_{12}$ because it has been widely used since the early part of the Second World War (Haertling, 1999). $BaTiO_3$ is a ferroelectric material that has

perovskite structure, with the chemical formula ABO_3, as illustrated in Figure 2.6 (Vijatovic et al., 2008).

Ferroelectric $BaTiO_3$ has a Curie temperature, T_c of 120 °C, possesses a high dielectric constant at room temperature which is about ~1000 and low dielectric loss (Duran et al., 2002). Due to its good characteristics, $BaTiO_3$ has become one of the most important ferroelectric ceramics and widely used in numerous applications such as capacitors and multilayer capacitors (MLCs). Meanwhile doped $BaTiO_3$ has been used in semiconductors, PTC thermistors and piezoelectric devices.

However, one of the crucial challenges with $BaTiO_3$ is the way to reduce the change in the dielectric constant around the T_c while increasing the mean dielectric constant at temperatures far from the T_c. Weber et al. (2001), Benlahrache et al. (2004) and Lin et al. (2004) found that adding dopants such as La helps to reduce these problems.

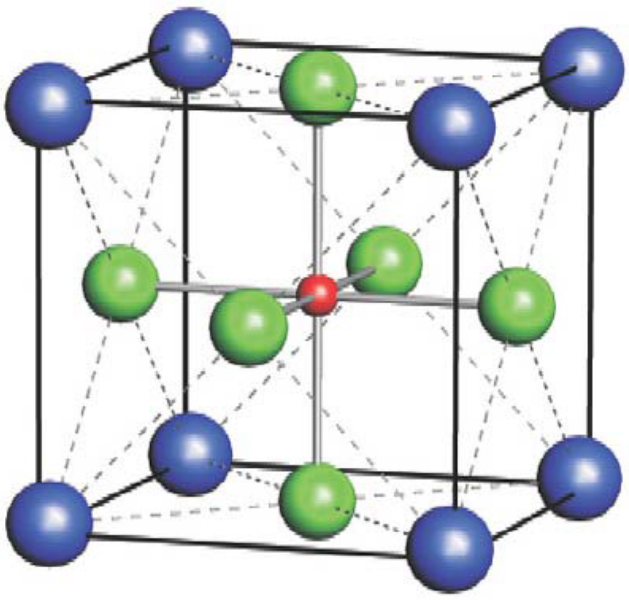

Figure 2.6: Structure of $BaTiO_3$ (Vijatovic et al., 2008)

2.4.1.3 Mica

Mica is a dielectric material that is widely used in electronics industry as mica capacitors and in electrical industry as an insulator. The most common type of mica is muscovite and phlogopite. Mica consists of 37 minerals, known as phyllosilicates which have a layered or platy texture (Carter and Norto, 2013). Mica possesses a combination of chemical, physical, electrical, thermal, and mechanical properties that are not found in any other materials.

Thermally, mica possesses excellent stability, fire proof and can resist temperature in the range of 600 – 900 °C. Chemically, they are exceptionally stable and are described as being virtually inert to various solvents, alkalies and acids except strong hydrofluoric and concentrated sulphuric acids. Electrically, they exhibit high dielectric strength, uniform dielectric constant in the range between 3 – 6, low power loss (high Q factor) and high electrical resistivity. Mechanically, micas are relatively flexible but maintain a robust strength within the film plane (Hepburn et al., 2000).

2.4.1.4 Glass-Ceramic Materials

Glass–ceramic materials are made as a glass, printed and the crystallized during the firing process. The crystalline phase that forms is dispersed uniformly throughout the glassy matrix so that the resultant material has very uniform properties. There are few major advantages of glass-ceramic materials such as higher softening point than the parent glass, stable under multiple refirings as long as it is not fired higher than the original processing temperature and the glass-ceramics

crossovers have less tendency to form pinholes, thus minimizing short circuits (Doane and Franzon, 1993).

Glass-ceramic materials are normally eletrical insulators with high resistivity, low dielectric constant which is about <10 and low loss factors (Holand and Beall, 2012). Titanates and niobates based glass–ceramic materials are the most studied materials. As an important titanates based system, (Ba, Sr)TiO_3 based glass–ceramics can exhibit high dielectric constant and high breakdown strength through the addition of the other oxide and fluoride components and the adjustment of Ba/Sr and Ba/Ti ratios. Gorzkowski et al. (2007) and Han et al. (2012) reported that high dielectric constant of ~1000 and high breakdown strength of 80 kV/mm but low energy density of 0.3 – 0.9 J/cm^3 can be found in (Ba, Sr)TiO_3 based glass–ceramics.

2.4.2 Hybrid Fillers

The incorporation of two or more types of inorganic fillers into a single polymeric system has lead to the development of hybrid composites. Growth of hybrid systems have been particularly rapid in the last decade due to the demand for high-performance engineering materials, especially where low weight is one of the main requirement. There are several advantages of incorporating hybrid fillers at different compositions into the matrix systems such as diluting a more expensive reinforcement of filler with cheaper materials, facilitating the design of materials with special characteristics and improving properties of the composites (Leong et al., 2004).

Although individual classes of fillers can contribute to some desirable properties, the main concern in composites is in optimizing the different

contributions from different types of fillers (Wei et al. 2006). Different shape, filler size, aspect ratio and distribution or dispersion characteristics of two inorganic fillers might affect the final properties of the composites.

According to Helmi et al. (2013), the hybrid compounds can be potentially used as polymer composite reinforcement in order to improve the properties of the composites. Luo et al. (2014) reported that a high dielectric constant of about 160 has been obtained for the $BaTiO_3$-Ag hybrid particles-filled polymer composites with 56.8 vol% $BaTiO_3$-Ag hybrid particles loading. The high dielectric constant and low loss tangent were observed as the hybrid structure of conductive particles deposited on ceramic particles.

Moreover, Liu and Grunlan (2007) and Etika et al. (2009) studied on the effect of hybrid fillers filled polymer matrix on the dynamic-mechanical analysis of the polymer composites. It showed that the introduction of a small number of hybrid fillers, significantly increased the modulus of elasticity as compared to single filler filled polymer matrix.

2.4.3 Thermosetting Polymers

Thermosetting polymers are polymers with three-dimensional networks of crosslinking bonds between chains. They are known as network polymers or cross-linked thermosets and widely used in electronic packaging due to excellent in thermal stability and dielectric properties. Thermoset resins can be in dry (powder) or wet (solution or dispersion) form. They may be compounded with catalysts, accelerators, lubricants, fillers and other processing additives. Catalysts cause cross linking, whereas accelerators promote and modify the curing reaction. Lubricants

help in processing and facilitate mold release. The most widely used thermosetting resins are epoxy, phenolic and polyimide (Lampman, 2003).

2.4.3.1 Epoxy Resin

Epoxy polymers (also called polyepoxides) are thermosetting polymers formed from the reaction of an epoxy resin with a curing agent (also called hardener) which contain more than one epoxide group (Dunn, 2003; Paipetis and Kostopoulos, 2012). The epoxide group is also called as oxirane ring that contains an oxygen atom bonded with two carbon atoms, as shown in Figure 2.7. Epoxy has a wide range of applications which include fiber reinforced plastics materials, encapsulation or casting of various electrical and electronic components, and more (Voo, 2012). Moreover, epoxy is one of the most primarily used polymers in electronic industry with a dielectric constant value of 6, especially for embedded capacitor applications because of its compatibility with printed wiring board manufacturing process (Lu, 2008). Epoxy resins are unique among thermosetting resins because of its excellent properties including high strength, good chemical and corrosion resistance, good mechanical and thermal properties, excellent adhesion to various substrates, low shrinkage during curing, high flexibility, good electrical properties and process versatility (Kroschwitz et al., 2004; Augustsson, 2004).

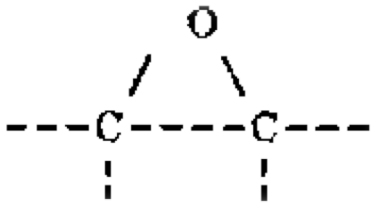

Figure 2.7: Chemical structure of epoxy group (Bhatnagar, 1996)

There are two main categories of epoxy resins, i.e. glycidyl epoxy and non-glycidyl epoxy resins, as schematically presented in Figure 2.8. The glycidyl epoxies are classified as glycidyl-ether, glycidyl-ester and glycidyl-amine. Whereas, non-glycidyl epoxies can be further classified as either aliphatic or cycloaliphatic epoxy resins. Each differs in the way that the epoxies are prepared. Glycidyl epoxies are prepared from a condensation reaction of dihydroxy compound, dibasic acid or a diamine and epichlorohydrin. Meanwhile non-glycidyl epoxies are prepared by peroxidation of an olefinic double bond (David, 2003; Whittie et al., 2011; Paipetis and Kostopoulos, 2012).

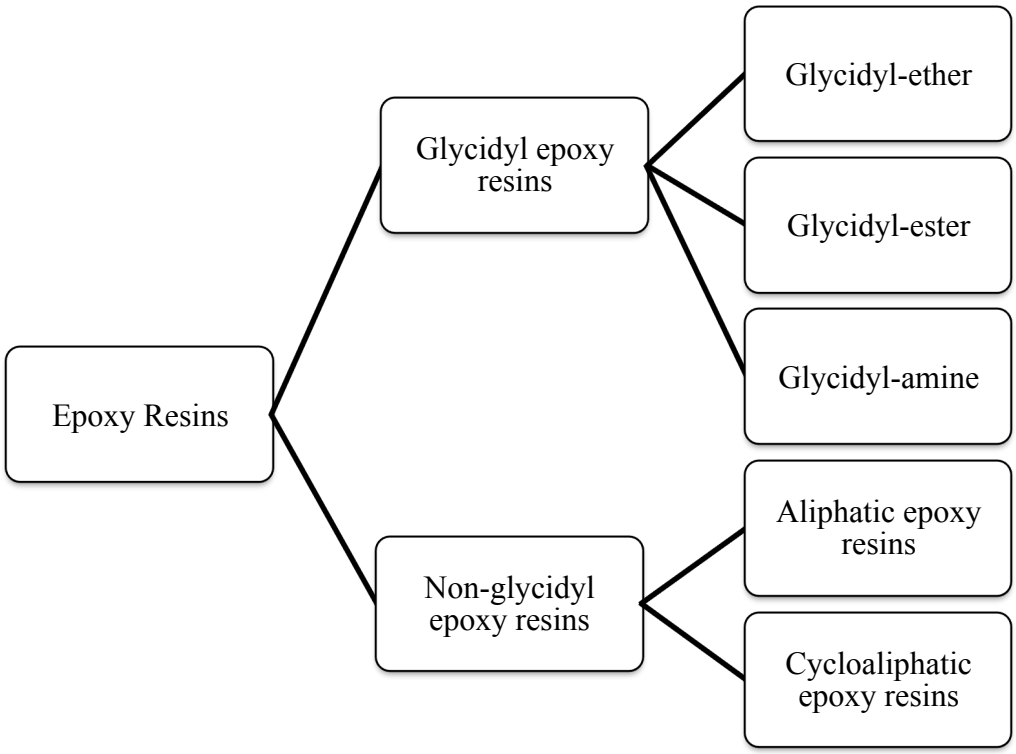

Figure 2.8: The summarized of the main categories of epoxy resins

The most commonly used epoxy resins are diglycidyl ether of bisphenol-A (DGEBA) and novolac epoxy resins. The DGEBA epoxy resin is formed from the reaction of epichlorydrin with bisphenol-A in the presence of a basic catalyst such as sodium hydroxide, NaOH, as illustrated in Figure 2.9. The molecular weight of the epoxy resin can affect the physical and chemical properties of the cured materials. It is often desirable to use high molecular weight in order to produce materials with sufficient toughness and flexibility. DGEBA is the most preferable type of epoxy resin to be used in electronic packaging applications due to its superior performance with the reinforcement (Dufton, 2000; David, 2003).

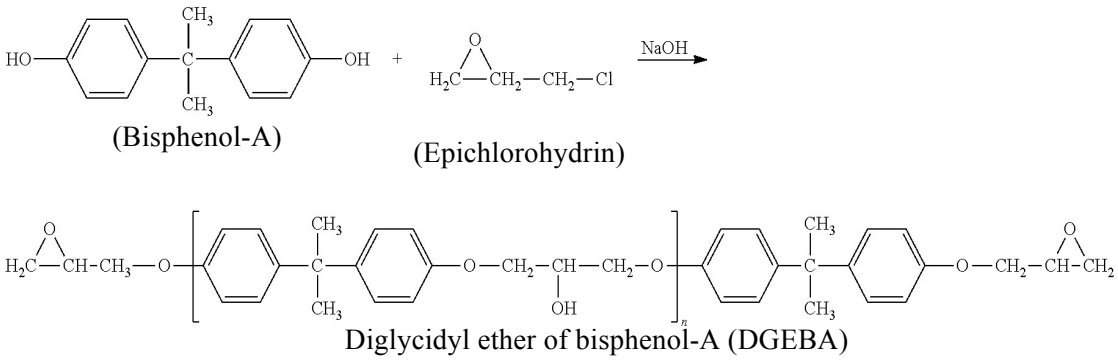

Figure 2.9: Reaction of epichlorydrin and bisphenol-A (Paipetis and Kostopoulos, 2012; Dodiuk and Goodman, 2013)

The novolac epoxy resins are prepared by reaction of phenolic novolac resin with epichlorohydrin in the presence of sodium hydroxide, NaOH. Whereas, the phenolic novolac resins formed from the reaction of phenols with formaldehyde in the presence of an acidic catalyst. The chemical structure of novolac epoxy resin is presented in Figure 2.10. These epoxy resins are also used in electronic applications

due to its excellent performance at elevated temperature, good dielectric properties, chemical resistance and mechanical properties (Dufton, 2000, Park, 2014).

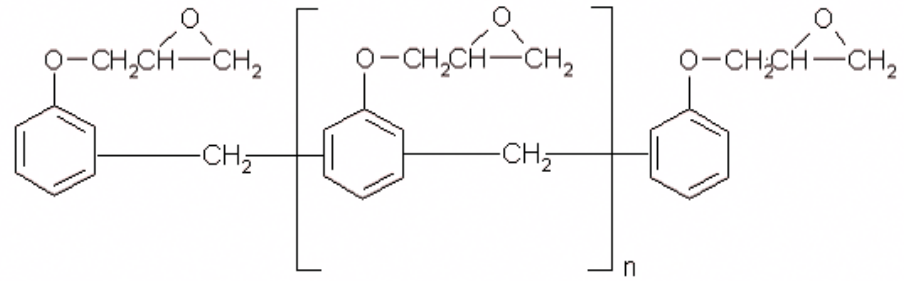

Figure 2.10: The chemical structure of novolac epoxy resin (Paipetis and Kostopoulos, 2012)

Aliphatic and cycloaliphatic epoxy resins represented non-glycidyl epoxy resins. According to Dufton (2000), many aliphatic backbones that contain OH units; i.e. alcohols, glycols and polyols can be epoxidised by reaction with epichlorohydrin. Meanwhile, cycloaliphatic resins are produced by peracetic acid oxidation of cycloaliphatic olefins. These resins are widely used in electronic applications due to good stability to UV light and electrical properties.

Epoxy resins must be cured with a hardener which is also known as co-reactant, crosslinking agent or catalyst in order to become a thermoset resin that provides the desired physical properties. There are four main categories of curing agents, namely amines, anhydrides, imidazoles and catalytic agents, as presented in Figure 2.11. The glass transition temperature (T_g), general structure and properties of the produced epoxy polymer depend greatly on the nature of the curing agent such as molecular weight, degree of crystallinity and chemical structure which includes

aromatic, cycloaliphatic and aliphatic (Dufton, 2000; Paipetis and Kostopoulos, 2012; Muhammad Firdaus, 2014).

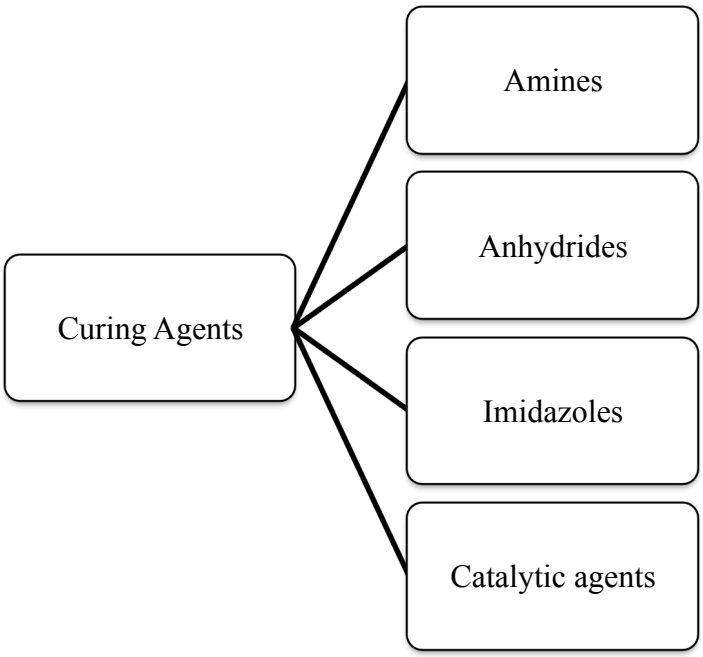

Figure 2.11: The summarized of the main categories of curing agents

Amines such as aliphatic amine offers low viscosity and good chemical resistance, whereas aromatic amine offers high T_g, good chemical resistance and electrical properties. For anhydrides, it offers high heat stability, good chemical resistance and heat resistance. However, it requires accelerator in order to be cured, long duration process and high temperature curing. For imidazoles and catalytic agents, both possessing high chemical resistance but poor moisture resistance (Teh, 2008; Foo, 2012, Muhammad Firdaus, 2014).

2.4.3.2 Phenolic Resin

Phenolic resin is a heat-cured plastic formed from the reaction between phenol and formaldehyde. Formaldehyde is a common raw material for this type of resin but others related chemicals can be used. Phenolic resins are available in flake, powder and liquid (solution emulsion) form to meet a variety of mechanical and electrical requirements. It is hard, heat resistant and can be mixed with a wide range of materials for industrial and residential uses. A phenol is an aromatic hydrocarbon, which means it contains a group of six carbons linked in a circular arrangement, as shown in Figure 2.12. This molecular shape permits the molecule to link to other molecules at selected sites around the ring. An aldehyde provides a linking molecule that creates a regular pattern or grid of phenol groups. The reaction occurs with heat and creates a very strong, stable polymer called a thermoset plastic (Manfred and Markus, 2010).

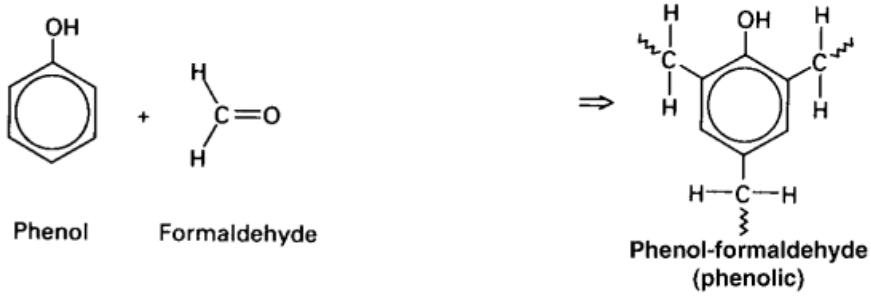

Figure 2.12: The chemical structure of phenolic resin (Lampman, 2003)

Phenolic resin board is widely used for electronic circuit boards and often mixed with small amounts of natural or synthetic fibers in order to avoid breakage as the resin can be very brittle when cured. The boards do not conduct electricity, and will resist heat generated by electronic equipment (NPCS Board of Consultants & Engineers, 2007).

2.4.3.3 Polyimide

Polyimide (PI) is a polymer of imide monomers. Polyimides have been classified as thermally stable polymers that are often based on stiff aromatic backbones. Figure 2.13 illustrates the structure of polyimides. Thermosetting polyimides are known for thermal stability, good chemical resistance and excellent mechanical properties. Polyimides exhibit good tensile strength (84 – 118 MPa), % elongation (8 – 12%), modulus (1.5 – 2.3 GPa) and stable up to 400 °C (Sarojadevi and Bhuvana, 2009). However, the dielectric constant of polyimides are low which is about 3.5. The decreased dielectric constant may be attributed to the pendant group and halo substituent present in it which the resulted in less efficient chain packing and increased free volume (Sarojadevi et al., 2009).

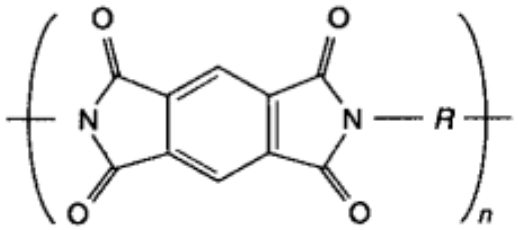

Figure 2.13: The chemical structure of polyimide (Lampman, 2003)

The polyimides are lightweight, flexible, resistant to heat and chemicals. Therefore, it can be used in the electronics industry for flexible cables, as an insulating film on magnet wire and for medical tubing. For example, in a laptop computer, the cable that connects the main logic board to the display (which must flex every time the laptop is opened or closed) is often a polyimide base with copper conductors (Lu and Wong, 2008).

2.5 Factors that Influence the Properties of Ceramic Fillers Filled Polymer Thin Film Composites

The potential factors that might affect the final properties of ceramic fillers filled polymer thin film composites have been studied and investigated in the previous works. Some of the researchers have suggested the way to improve the properties, especially dielectric, tensile and thermal properties. There are few factors that can affect the properties of the composites, including the filler loadings, the fabrication methods and the presence coupling agent.

2.5.1 Effect of Filler Loadings

Based on previous works, the dielectric properties of epoxy thin film composites were found to increase and improve with increasing of filler loadings (Ramajo et al., 2007; Prakash and Varma, 2007; Ramajo et al., 2008; Thomas et al., 2010; Yang et al., 2011). The dielectric constant increased as the CCTO loadings increased in the polymer but decreased as the frequency increased. The same scenario can be found in the dielectric loss of the composites. This result was obtained mainly due to the effect of interfacial polarization associated with the fillers (Prakash and Varma, 2007).

Teh et al. (2008), Voo et al. (2012) and Thomas et al. (2013) reported that the thermal properties such as thermal conductivity, thermal stability, thermal expansion behavior and dynamic behavior of epoxy thin film composites showed positive results and improved as the filler loadings increased. It was found that the tendency to form agglomerates increased as the filler loadings increased. According to

Kochetov et al. (2009), the agglomerates can act as regions of heat conduction resulting in a rapid increase in thermal conductivity.

Meanwhile for thermal stability of the polymer composites, filler loadings are important for determining the stability of the composites up to 150 – 200 °C which shows the application temperature of the materials. It was found that there is an increased in the decomposition temperature as the filler loadings increased in the polymer system. The improvement of thermal stability may be contributed by the interaction between filler and polymer matrix and also good dispersion state of the filler in the polymer matrix (Leszczynska et al., 2007).

Furthermore, thermal expansion behavior is a critical material property in electronic applications as the low coefficient of thermal expansion (CTE) is required for dimensional stability. According to Sun et al. (2006), incorporation of well-dispersed inorganic particles into a polymer matrix has been claimed to be an effective method in improving the performance of the CTE of the polymer composites. Similar observation were found by Teh et al. (2008) and Thomas et al. (2013), where the CTE reduces with the addition of fillers into the polymer system.

The glass transition temperature and dynamic mechanical behavior of the polymer composites can be measured by dynamic mechanical analysis (DMA). Amorphous polymers have different glass transition temperatures, T_g, above its T_g the material will be in rubbery stage and below its T_g the material will be in glassy behavior. Above its T_g, the stiffness of the material will drop dramatically and the loss modulus reaches a maximum (Agarwal et al., 2013). The incorporation of fillers into the polymer system can increase the T_g and stiffness of the polymer composites substantially. This is an indication of filler to matrix interaction which restricts

molecular mobility and increased the crosslink density (Miyagawa et al., 2005; Teh et al., 2008; Margem et al., 2010).

The tensile properties of epoxy thin film composites can be improved by the addition of filler materials. Increasing the filler loadings into the polymer system increases the tensile modulus in comparison with unfilled epoxy. However, the tensile strength and elongation at break of epoxy thin film composites reduced as the filler loadings increased. This might be due to the high viscosity of the matrix that make the fillers difficult to disperse uniformly in the matrix when the filler loadings are higher, it leads to agglomeration and also contributed to thin film brittleness. Besides that, there is a possibility of voids formation during the fabrication process of the composites (Choi et al., 2005; Chua, 2010; Voo et al., 2012; Ng, 2013).

2.5.2 The Fabrication Methods

A wide variety of fabrication methods to produce polymer composites are available. Each method has its own uniqueness over the others. However, each fabrication method still has its limitation. In order to achieve the desired film with good dielectric, tensile and thermal properties of epoxy thin film composites, further understanding on the characteristics, advantages and limitations of each of the fabrication method is necessary. The usual methods for thin film fabrication are spin coating (Voo et al., 2012), hot press and tape casting (Seema et al., 2007), dip coating (Li et al., 2010), solvent casting method (Nan, 2006), drop coating method (Cui, 2011) and more.

2.5.2.1 Spin Coating

The pioneering analysis of spin coating was performed more than fifty years ago by Emslie et al. (1958) who considered the spreading of a thin axisymmetric film of Newtonian fluid on a planner substrate rotation with constant angular velocity. Furthermore, this method can also be described as the process of applying a solution to a horizontal rotating disc which then results in injection and evaporation of the solvent and finally, leaves a liquid or solid film (Wang, 2007). Spin coating is considered as one of the most simplest and easy method to produce polymer thin film composites. It offer numerous advantages over the others including reproducible, homogeneous and uniform thin films over the wafers with thickness ranging from micrometers to nanometers.

The spin coating process can be further divided into four stages sketched in Figure 2.14 which are deposition, spin-up, spin-off and lastly, evaporation of solvents. Noted that the first three stages are commonly sequential but spin-off and evaporation are normally overlap. The final coating thickness is fully depending on stage 3 and stage 4. These four stages are described as follows (Lawrence, 1988; Sahu et al., 2009):

i. Starting phase where solvent is put on the substrate. Spreading of the solvent takes places due to centrifugal force and height is reduced to critical height.
ii. The substrate is accelerated up to its final, desired and rotation speed. The rotation of the turntable leads to the loss of material from substrate and therefore, formed the thin films with homogeneous thickness.

iii. The substrate is further spinning at a constant rate and fluid viscous forces dominate fluid thinning behavior. Subsequent reduction in film height is dominated by the evaporation of the solvent.

iv. The drying process begins after the spin-off stage ends. At this stage, centrifugal out flow stops and futher shrinkage is due to solvent loss which results in the formation of thin film on the substrate.

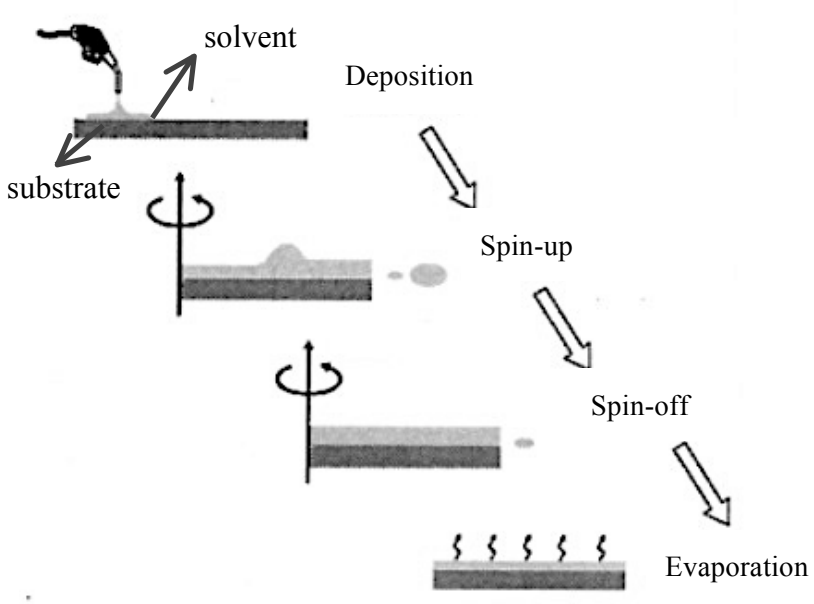

Figure 2.14: Spin coating process (Sahu et al., 2009)

The final film thickness and other desirable properties will depend on the spin rate, solution viscosity, solution concentration, amount of deposited solution, the rate at which the solution is deposited, history of rotational acceleration prior to the final acceleration and the total spin time. Spin coating is widely used in various applications including coating of photoresist on silicon wafers, sensors, protective coatings, paint coatings, optical coatings and membranes.

2.5.2.2 Hot Press

The hot press method which is also known as compression molding method is widely used to produce conventional polymer composites because this method is simple, reliable and fast to suit the industrial production cycle for large parts (Lee, 1990). Due to faster reaction, more pressure is required to force the solvent to fill the tool before it becomes too viscous as the solvent started to cured.

The hot press method required simple steps as the material for this method is placed onto the cavity of the mold and selected pressure is then applied to force the material into contact with all mold areas. The heat and pressure are well maintained until the molded material has fully cured. This process employs thermosetting resins in a partially cured stage, either in the form of granules, putty-like masses or even preforms (Thomas, 2013).

As reported by Seema et al. (2007), hot press method offers better thickness uniformity and denser composites which provide better significant to dielectric and thermal properties of the polymer composites. However, this fabrication method is quite costly due to higher pressure is required in the production of the polymer composites.

2.5.2.3 Dip Coating

The dip coating method is a simple and effective low-cost production of making thin films on substrates with a complicated shape. In a dip coating process, the substrate is immersed into a dip tank containing the coating solution and then slowly taken out or withdrawn from the solution with a uniform velocity (Tjong and Mai, 2010). There are five simple steps in dip coating which includes immersion,

start-up, deposition, drainage and evaporation, as shown in Figure 2.15. With volatile solvents such as alcohols, evaporation usually accompanies start-up, deposition and drainage. Meanwhile, the continuous dip coating process as illustrated in Figure 2.15 (f) is considered simpler because it separates immersion from the other stages, essentially eliminates start-up, hides drainage in the deposited film and restricts evaporation to the deposition stage and afterward (Brinker and Scherer, 1990; Rahaman, 2007).

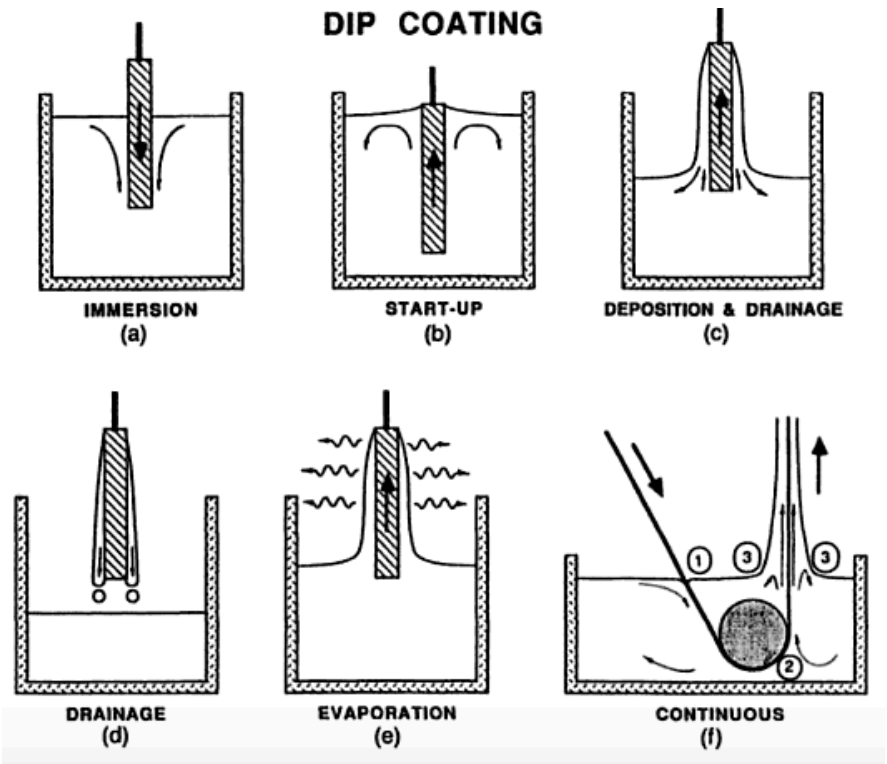

Figure 2.15: Dip coating process; (a-e) batch, (f) continuous (Rahaman, 2007)

The thin film thickness is determined by the balance of forces at the stagnation point on the liquid surface. The rate of withdrawal of the part from the tank is an important factor to consider for good results. Uniform thickness can be produced at slow withdrawal rate whereby, thin at the top and thick at the bottom

coatings are often produced at rapid withdrawal which in several cases a bead of coating remains at the bottom edge of the part that blisters on curing. Besides that, fluid viscosity, fluid density and surface tension are the factors that contribute to the thickness of thin films (Voo, 2012).

2.5.2.4 Solvent Casting

Solvent casting method is considered as the oldest technology in thin films manufacturing which was developed more than hundred years ago driven by the needs of the emerging photographic industry. In the solvent casting process, the polymer solution is coated onto a substrate or the substrate is dipped into the polymer solution and drawing off the solvent to leave a polymer thin film on the substrate. Figure 2.16 shows the solvent casting film system.

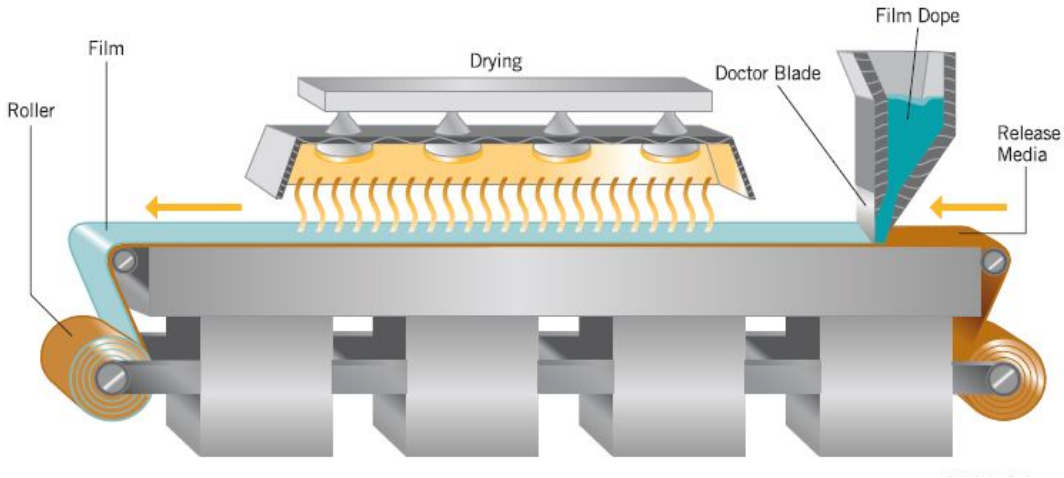

Figure 2.16: Solvent casting film system (Particle Sciences, 2010)

It offers several advantages such as excellent transparency, low haze, isotropic orientation, low optical retardation and also the unique process drying in a liquid on a surface without applying further mechanical or thermal stress. However,

this method does not produce films with uniform thickness and the reproducibility is inadequate in most cases. Moreover, only few selected materials can be further processed into films and slow production speed hindered for mass application by solvent casting method (Siemann, 2005; Tiwari et al., 2012). Table 2.3 summarized the comparison of the fabrication of thin film methods. It can be seen that spin coating method offers numerous advantages as compared to other fabrication methods.

Table 2.3: Comparison of thin film fabrication methods (Nan, 2006; Yimsiri and Mackley, 2006; Seema et al., 2007)

Method	Spin coating	Hot press	Dip coating	Solvent casting
Fabrication control	Complex	Simple	Complex	Simple
Thickness control	Good control with spin rate	Good control	Poor	Poor
Thickness of product	Nano to micron	Micron	Nano to micron	Micron
Substrate or shape	Flat substrate	Flat substrate	Irregular shape	Flat substrate
Uniformity of film	Good	Good	Poor	Poor
Production rate	Fast	Slower than spin coating	Slow	Fast
Cost	Expensive	Expensive	Less expensive	Cheapest

Commercialize	Easy due to controlled thickness and production rate	Difficult due to slow production rate	Difficult due to variability in thickness uniformity	Difficult due to difficulty in thickness controlled

2.5.3 Filler Surface Treatment

A lot of works have been done to improve the dielectric and thermal properties of epoxy thin film composites (Todd and Shi, 2003; Ramajo et al., 2007; Hirano et al., 2012; Yang et al., 2013). This is due to the difference in surface characteristic of inorganic reinforcing material and the organic matrix which inhibit the reinforcement to disperse uniformly in the matrix system, thus greatly affects the performance of the composite (Pongdhorn, 2004). To modify the interface between inorganic phase and the polymer matrix, many additives have been developed such as coupling agents. A coupling agent is an additive which promotes the development of a strong bond between the filler surface and the polymer (Shi, 2006).

Among these additives, silane coupling agents have gained more attention over the others as the coupling agents possess a special structure with two different functional groups, one is attached to the polymer matrix and another one is attached to the inorganic filler which leads to covalent bonds linking the reinforcement and the matrix (Chao and Liang, 2009).

Typically, silane coupling agents have the general structure $(X)_3Si(CH_2)_3$-Y. The silicon functional group X is a hydrolyzable group chosen to react with surface

hydroxyl groups of the filler to produce a stable bond and it is usually amine, acyloxy, halogen or alkoxy. Meanwhile, R is a nonhydrolyzable organic radical that may possess a functionality which enables the coupling agent to bond with organic resins and polymers. Most of the widely used organosilanes have one organic substituent.

Reaction of these silanes involves four steps as illustrated in Figure 2.17. Initially, hydrolysis of the alkoxy (X) groups occurs. It is after the first and second alkoxy groups are hydrolyzed that condensation to oligomers follows. The oligomers then hydrogen bonded with OH groups of the substrate. Finally during drying or curing, a covalent linkage is formed with the substrate with concomitant loss of water. Although described sequentially, these reactions can occur simultaneously after the initial hydrolysis step. At the interface, there is usually only one bond from each silicon of the organosilane to the substrate surface. The two remaining silanol groups are present either in condensed or free form. The R group remains available for covalent reaction or physical interaction with other phases (Witucki, 1992).

A study on the influence of a silane coupling agent on the dielectric properties of CCTO/PVDF composites was reported by Yang et al. (2013). Silane coupling agent (Si69) at few concentrations were used. The dielectric constant of the composites with addition of Si69 silane coupling agent shown a dramatic increased, which is probably due to good compatibility between Si69 silane coupling agent and the polymer system which leads to a homogeneous structure in the CCTO@Si69/PVDF composites. Si69 act as a bridge in between the reinforcement and the matrix. Similar observation has been reported by Todd and Shi (2003). The addition of GPTMS silane coupling agent increased the interphase dielectric constant

of silica-filled epoxy composites due to the chemical interaction between the coupling agent and the surface of the filler particles. This can be explained by the introduction of polar groups and siloxane bonds to the polymer backbone near the surface of the filler which then increases the molecular polarizability and therefore increases the interphase dielectric constant.

According to the study by Hirano et al. (2012), the use of silane coupling agent had a significant thermal properties improvement. However, excess of silane coupling agent should be avoided due to negative impact in the final properties of the composites. Nevertheless, there was no investigation on the thermal expansion of treated fillers filled epoxy composites.

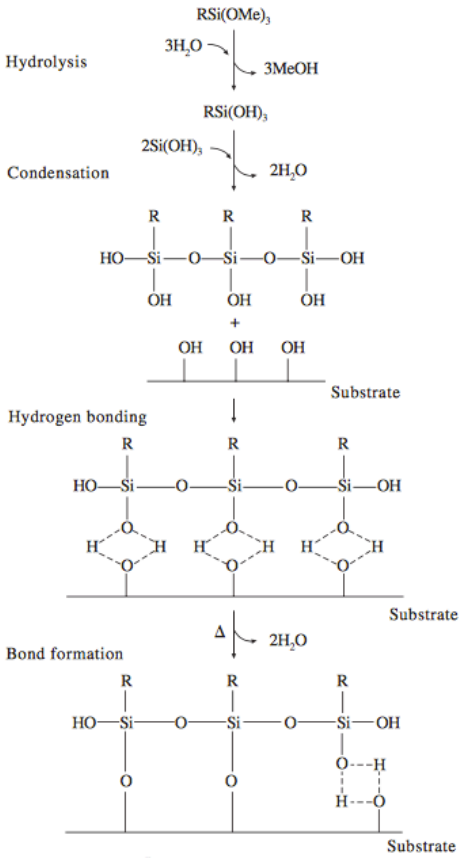

Figure 2.17: Reaction process of silane coupling agents (Arkles, 1977)

2.6 Research Gap

An overview of research work from previous and current studies are presented in Table 2.4. Based on the previous studies, most of the reports mainly emphasized on the dielectric properties of untreated and treated CCTO composites and there were no reports specifically focused on the thermal properties of untreated and treated CCTO/epoxy thin film composites (Ramajo et al., 2007; Prakash and Varma, 2007; Thomas et al., 2010; Yang et al., 2011; Yang et al., 2013; Feng et al., 2014).

Study on thermal properties is important in determining composites with excellent thermal stability, dynamic mechanical properties and thermomechanical properties for embedded capacitor application. Besides that, to enable the dielectric materials to be embedded inside the PCB substrate, the thickness of the composite should be less than 0.25 mm. Various fabrication methods such as casting and hot press were used in the previous studies to produce epoxy composite (refer to Table 2.4). In Table 2.4, it is found that CCTO and $BaTiO_3$ fillers were used in various polymer matrices to produce products for electronic applications. The size of the fillers used in the previous works is in micro size and the loading varies from 0 to 55 vol%. Composites fabricated by casting and hot press methods were able to be produced using filler loading up to 55 vol%. However the thickness of the sample is more than 0.25 mm, which is cannot be considered as thin film.

Table 2.4: Overview of research work

Composites	Filler loading	Fabrication method	Thickness (mm)	Properties investigated	Reference
CCTO/epoxy and $BaTiO_3$/epoxy Composites	5 - 15 vol%	Casting	-	Dielectric properties	Ramajo et al., 2007
CCTO/epoxy Composites	0 - 40 vol%	Casting	2	Dielectric properties	Prakash and Varma, 2007
Poly(vinylidene fluoride)/ CCTO Composites	0 - 55 vol%	Hot press	0.5	Dielectric properties	Thomas et al., 2010
CCTO/ Poly(vinylidene fluoride) Composites	0 - 55 vol%	Hot press	0.8	Dielectric properties	Yang et al., 2011
Poly(methyl methacrylate)/ CCTO Composites	0 - 38 vol%	Hot press	1.0	Thermal stability and dielectric properties	Thomas et al., 2013
Bis[3(triethoxysilyl) propyl]tetrasulfide treated CCTO/ PVDF Composites	5.5 - 22.5 vol%	Hot press	0.8	Dielectric properties	Yang et al., 2013
N-methylpyrrolidone treated CCTO/PEN Composite Films	5 - 20 wt%	Casting	-	Dielectric, tensile and thermal properties	Feng et al., 2014

CHAPTER 3

MATERIALS AND METHODOLOGY

3.1 Introduction

The present research mainly focuses on the dielectric, tensile and thermal properties of inorganic fillers such as CCTO and $BaTiO_3$ (control sample) filled epoxy thin film composites. This preliminary study is divided into three sections. The raw materials and chemicals used throughout the experimental work are discussed in Section 3.2. Section 3.3 covers the information about the methodology and processing method. Section 3.4 shows the principles of characterization that are used to characterize the CCTO and $BaTiO_3$ (control sample) filled epoxy thin film composites.

3.2 Materials

The starting materials that being used to produce epoxy thin film composites are listed in the following paragraphs. Note that all the materials are commercial products except CCTO powder, which was synthesized manually using solid-state reaction based on previous work by Julie et al. (2006).

3.2.1 Epoxy Resin

The epoxy resin (D.E.R.^{TM} 332) primarily used in this study was supplied by Penchem Technologies Sdn. Bhd. It is also known as bisphenol-A diglycidyl ether that appears as a colourless viscous liquid and meet the requirements of electronic packaging industry due to its high purity, dimensional stability, high physical

strength and excellent chemical resistance. For comparison purpose, epoxy resin type Epolam 2015 (Resin) supplied by Advance Moulding Chemicals Sdn. Bhd. and epoxy resin type OP 392 (Part A) supplied by Penchem Technologies Sdn. Bhd were used. Table 3.1 presents the general properties of various epoxy resins.

Table 3.1: General properties of various epoxy resins (Materials Safety Data Sheet)

Properties	**D.E.R.™ 332**	**Epolam 2015 (Resin)**	**OP 392 (Part A)**
Category	Glycidyl-ether	Glycidyl-ether	Glycidyl-ether
Appearance	Liquid	Liquid	Liquid
Viscosity at 25°C (mPa.s)	4000-6000	1550	2430
Color	Colorless	Light amber	Blue
Density (g/cm$^{3)}$	1.16	1.15	1.18
Glass Transition Temperature, T_g (°C)	60	88	140

3.2.2 Curing Agent

The main type of curing agent used was polyetheramine D230 supplied by BASF Corporation. This liquid consists of polyether and amine groups in its structure which is made up of amine aliphatic group. For comparison purpose, curing agent type Epolam 2015 (Hardener) supplied by Advance Moulding Chemicals Sdn. Bhd. and epoxy resin type OP 392 (Part B) supplied by Penchem Technologies Sdn. Bhd were used. The properties of various curing agents are listed in Table 3.2.

Table 3.2: General properties of various curing agents (Materials Safety Data Sheet)

Properties	D230	Epolam 2015 (Hardener)	OP 392 (Part B)
Chemical Type	Amine	Amine	Anhydride
Appearance	Colorless Liquid	Colorless Liquid	Blue Liquid
Viscosity at 25°C (mPa.s)	9-10	70	160
Density ($g/cm^{3)}$	1.16	0.95	1.16

3.2.3 Calcium Copper Titanate

Calcium copper titanate, $CaCu_3Ti_4O_{12}$ (CCTO) powders were prepared using solid state reaction method which has been reported by Julie et al. (2006). The starting materials of CaO (Aldrich, 99%), TiO_2 (Merck, 99%), and CuO (Aldrich, 99%) were weighted according to the stoichiometric ratios of CCTO. The starting materials were dry ball milled for 24 hours using zirconia balls as medium.

Calcination process takes place after mixing process. The milled powders were calcined using Electrical Carbolite Furnace (model: CWF 1100) at 900 °C for 12 hours. The calcined powders of CCTO have turned from black to brown solid color. The calcined powders were then ground by using agate mortar and been used as fillers for production of epoxy thin film composites. The general properties of CCTO powders are shown in Table 3.3. Average size was measured and discussed in Section 4.2.

Table 3.3: General properties of CCTO powders (Materials Safety Data Sheet)

Properties	Units	Description/ Value
Physical State	-	Powder
Color	-	Dark Brown
Density	g/cm^3	4.7
Dielectric Constant	-	10^5

3.2.4 Barium Titanate

The micron-sized barium titanate, $BaTiO_3$ powders supplied by Aldrich, Inc. were used as a filler in the production of epoxy thin film composites which act as a control sample. The properties of the composites were compared with properties of CCTO/epoxy thin film composites. Table 3.4 shows the properties of $BaTiO_3$ powders. Average size was measured and discussed in Section 4.2.

Table 3.4: General properties of $BaTiO_3$ powders (Materials Safety Data Sheet)

Properties	Units	Description/ Value
Physical State	-	Powder
Color	-	White
Density	g/cm^3	6.08
Dielectric Constant	-	1000

3.2.5 Silane-based Coupling Agent

In the fouth stage of research, the CCTO powders were treated with silane-based coupling agent known as 3-glycidoxypropyltrimethoxysilane (GPTMS). It was

supplied by Aldrich Inc. in liquid form. It was used to improve the surface adhesion between CCTO filler and epoxy matrix. The general properties of GPTMS is shown in Table 3.5. Figure 3.1 depicts the chemical structure of GPTMS silane-based coupling agent.

Table 3.5: General properties of GPTMS (Materials Safety Data Sheet)

Properties	**Units**	**Description/Value**
Physical State	-	Liquid
Color	-	Colorless
Density	g/cm^3	1.07
Flash Point	°C	122

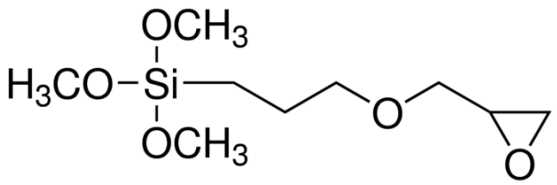

Figure 3.1: The chemical structure of GPTMS silane-based coupling agent

3.2.6 Ethanol

Ethanol with a chemical structure of CH_3CH_2OH was supplied by BDH. It is used for dilution of GPTMS silane-based coupling agent due to incomplete wetting of filler by relatively little amount of coupling agent. Ethanol can be completely evaporated during the drying process of treated CCTO at 100 °C due to its lower boiling point which is about 78.3 °C.

3.3 Experimental Methods

The experimental methods are divided into two stages, namely synthesis of CCTO and production of epoxy thin film composites. The production of epoxy thin film composites are further divided into four parts. Part 1 involves the preparation of epoxy thin film composites at different filler types and loading range. Whereby Part 2 includes the preparation of epoxy thin film composites at different fabrication methods. Followed by the preparation of hybrid fillers filled epoxy thin film composites at Part 3 and Part 4 involves the preparation of treated CCTO filled epoxy thin film composites. Lastly, Part 5 includes the preparation of treated CCTO/epoxy thin film composites by using different types of epoxy resins. Further explaination regarding the methodologies are described in the following sections.

3.3.1 Synthesis of CCTO

CCTO powders were prepared using the conventional solid-state reaction method based on previous work (Julie et al., 2006). All the starting materials used were CaO, TiO_2 and CuO, respectively. According to stoichiometric ratios of CCTO, an appropriate amount of CaO, TiO_2 and CuO were weighted and these materials were mechanically dry ball milled for 24 hours using zirconia balls with weight ratio of ball to powder was 10:1. The powder was then calcined in air at 900 °C for 12 hours using a Carbolite Furnace. The heating and cooling rate used was 5 °C/min. The calcined powders were ground in an agate mortar and further characterized by using XRD, Particle Size Analyzer and SEM.

3.3.2 Production of Epoxy Thin Film Composites

3.3.2.1 Different Filler Types and Loading Range

In this study, there are five stages involved in the preparation of epoxy thin film composites; weighing, mixing, vacuum, spin coating and curing. Appendix A depicts formulation used and the quantities of epoxy resin, curing agent and ceramic fillers such as CCTO and $BaTiO_3$ required to produce the epoxy thin film composite samples.

The loading of the ceramic filler in the epoxy resin DER 332 was varied from 5 vol% to 20 vol%. The mixing of epoxy resin and ceramic filler was carried out using the ultrasonic agitation method. The mixture of epoxy and ceramic filler was sonicated manually at room temperature for 10 min with 50% amplitude and 0.5 sonication cycle in order to achieve uniform and homogenous dispersion of ceramic filler in the epoxy resin. Once the sonication was completed, the curing agent was added at a ratio of 100:32 by weight (epoxy: curing agent) followed by further sonicated for another 10 min. The temperature of the mixture increased during sonication process, thus effect the curing process. To prevent the mixture from easily cured, it was immersed in an ice water bath in order to reduce the temperature, as shown in Figure 3.2. The mixture was then placed in a vacuum oven for 1 h of degassing to remove the air entrapped in the mixture during mixing and the final mixtures were spin coated at rate of 250 rpm to 750 rpm for 180 s.

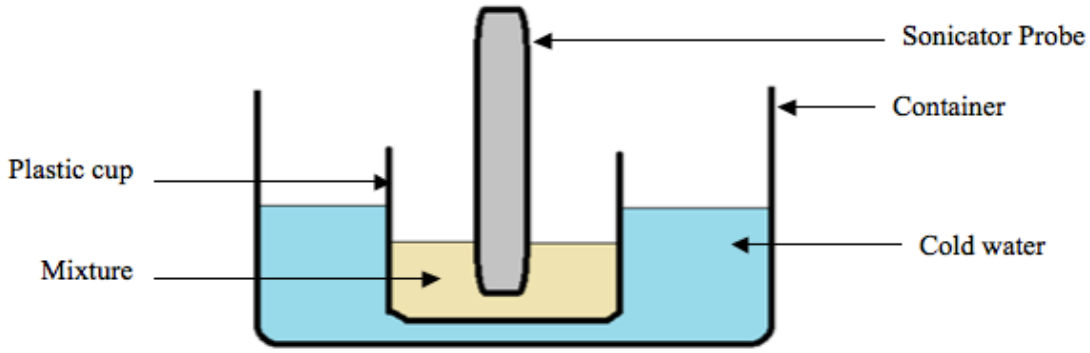

Figure 3.2: Schematic diagram of an ice water bath sonication process

Finally, the epoxy thin film composites produced by spin coated was cured at 80 °C for 2 h. Flexible CCTO/epoxy and $BaTiO_3$/epoxy thin film composites with thicknesses ranging from 30 μm to 70 μm were produced as shown in Figure 3.3 (a) and (b), respectively.

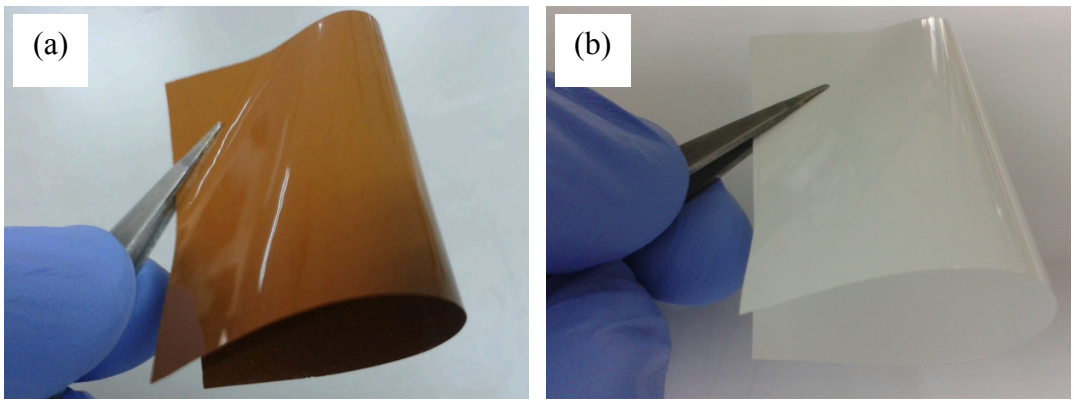

Figure 3.3: Flexible epoxy thin film composites filled with (a) CCTO and (b) $BaTiO_3$ ceramics

3.3.2.2 Different Fabrication Methods

CCTO ceramic was further used as a filler for the preparation of epoxy composites at two different fabrication methods; spin coating method and hot pressing method due to its excellent dielectric properties and thermal properties as compared to $BaTiO_3$ ceramic. The same procedures and parameters of spin coating method as mentioned in Section 3.3.2.1 were used in this study. Figure 3.4 shows the diagram of spin coating method.

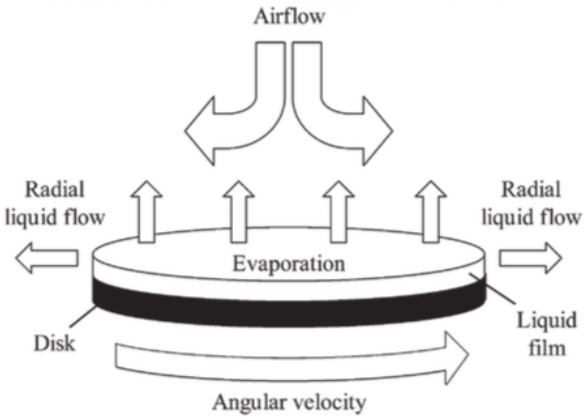

Figure 3.4: Spin coating method

Meanwhile for hot pressing method, the final mixture of CCTO and epoxy resin produced using the same procedure as mentioned previously in Section 3.3.2.1 was poured onto the centre of stainless steel sheet (mold) in between two teflon sheets, as shown in Figure 3.5. The mold and teflon were supported by steel plates and placed on the hot-press machine at temperature of 80 °C under the applied pressure of 300 psi for 2 hours. The whole steel plates were then wrapped and covered with the vacuum bag plastic in order to prevent the excess mixture from split out. The thickness of CCTO/epoxy composites produced by hot-pressing method ranging from 30 mm to 45 mm.

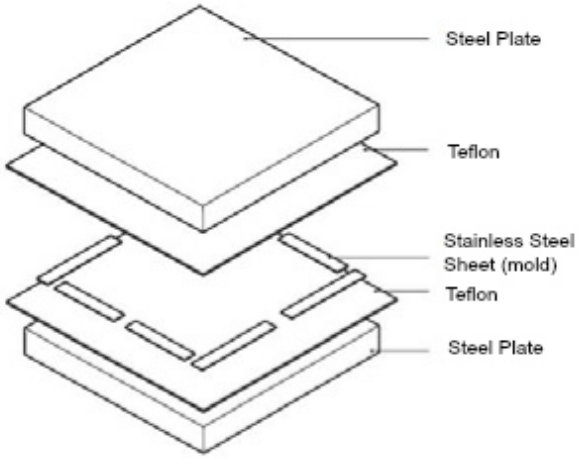

Figure 3.5: Hot pressing method

3.3.2.3 Hybrid Fillers

Best filler loading was selected from Part 1 and used in this study of hybrid fillers filled epoxy thin film composites. The selection of filler loading was based on the excellent dielectric properties, tensile properties and thermal properties shown by both CCTO/epoxy and $BaTiO_3$/epoxy thin film composites. Composites based on epoxy resin as matrix and 20 vol% of hybrid fillers (CCTO and $BaTiO_3$) as reinforcement were prepared with the same procedure as discussed in Section 3.3.2.1. Appendix B presents the quantities of epoxy resin, curing agent and hybrid fillers (CCTO and $BaTiO_3$) used to produce hybrid fillers/epoxy thin film composite samples. Ratio of hybrid fillers of CCTO: $BaTiO_3$ was varied from 30:70, 50:50 and, 70:30, respectively. Flexible hybrid fillers filled epoxy thin film composites with thicknesses ranging from 90 μm to 130 μm were produced as shown in Figure 3.6 (a), (b) and (c), respectively.

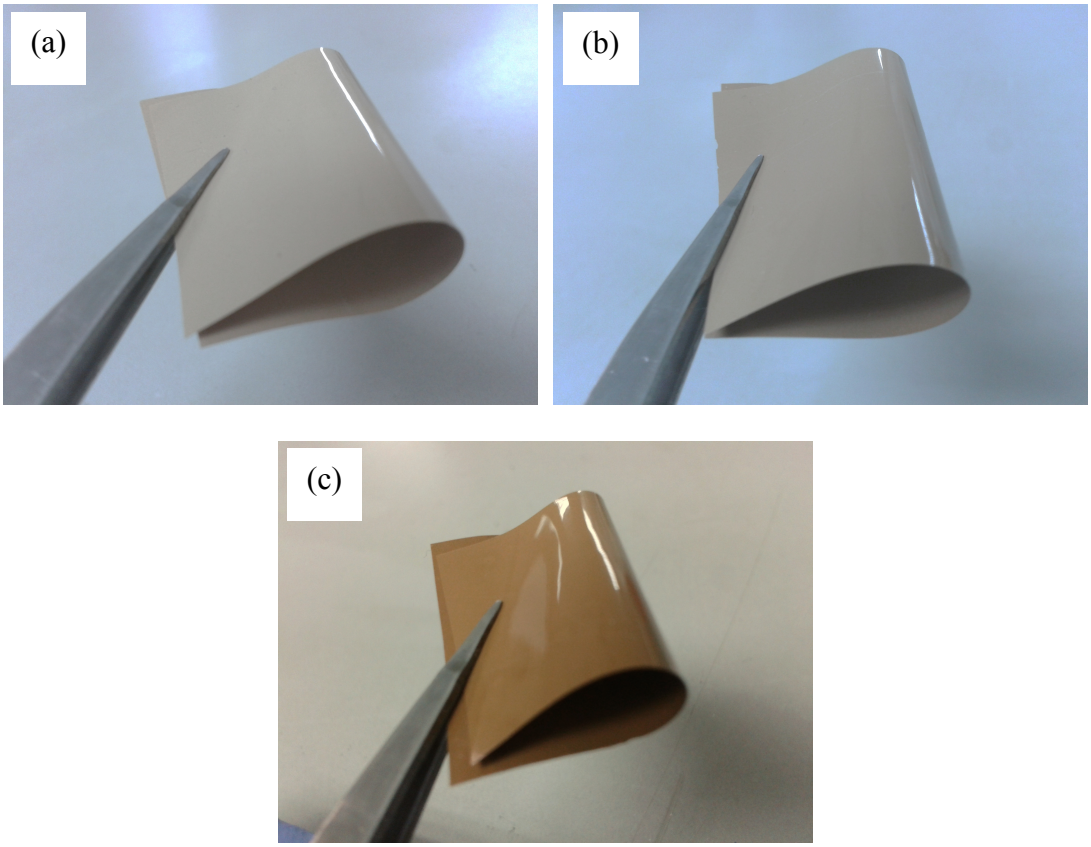

Figure 3.6: Flexible epoxy thin film composites filled with hybrid fillers with the ratio of CCTO: $BaTiO_3$ was varied from (a) 30:70, (b) 50:50 and (c) 70:30

3.3.2.4 Treated CCTO Fillers

After the first and second stage of study on filler types, loading range and fabrication methods, two predicative characterization methods had been conducted to narrow down the scope of research study in the forth stage. This stage focuses on the effect of treated CCTO filled epoxy thin film composites. Investigation and comparison with the untreated CCTO/epoxy thin film composites was carried out.

The filler loading of CCTO ceramic was fixed at 20 vol%. The silane coupling agent (GPTMS) was varied at 1%, 5% and 10%, respectively. Due to the relatively small amount of GPTMS, it needs to be diluted in ethanol to make up 1%, 5% and 10% solution in order to completely wet the filler surfaces. Appendix C

shows the calculated amount of ethanol (in weight) required to dilute the GPTMS based on previous work by Tee et al. (2007). After weighing, ethanol was poured into a 50 ml beaker containing the corresponding amount of GPTMS followed by stirred at a speed of 480 rpm for 15 minutes to achieve a homogeneous solution. After the preparation of GPTMS solution in ethanol solvent, the CCTO filler was introduced into the solution and further 15 minutes of stirring at 480 rpm with 30 °C was carried out. Next, the ultrasonic wave was used to treat the CCTO/GPTMS/ethanol suspension for 30 minutes at room temperature and ultrasonic power of 100%. Lastly, the treated suspension was dried in oven at 100 °C for 90 minutes before being ground to powder form for the following process.

The treated CCTO ceramics were ready to be used for the preparation of epoxy thin film composites. The same procedure was used as mentioned in Section 3.3.2.1. Three specimens at the same concentration of CCTO (20 vol%) were produced at different concentration of GPTMS; 1%, 5% and 10%, respectively. The properties of the specimens such as dielectric and thermal were compared.

3.3.2.5 Fabrication of Composites Using Various Epoxy Resins

In the final stage of the present research, the treated CCTO filled epoxy thin film composites were fabricated by using different types of epoxy resins; DER 332, Epolam 2015 and OP 392. The properties of epoxy Epolam 2015 and epoxy OP 392 thin film composites were compared with the properties of epoxy DER 332 thin film composite. The concentration of CCTO ceramic and silane coupling agent were fixed at 20 vol% and 10%, respectively.

For epoxy resin type Epolam 2015, the same procedures and parameters of

spin coating method to produce treated CCTO/epoxy thin film composite as mentioned in Section 3.3.2.4 were used in this study. Whereby for epoxy type OP 392, similar procedures and parameters were carried out to produce the treated composite except the curing agent was added at a ratio of 1:1 by weight (epoxy: curing agent). The epoxy thin film composites then produced by spin coated and precured at 125 °C for 1 h and finally, postcured at 135 °C for 2 h.

Figure 3.7 shows the overall research flowchart, which had been divided into three stages. Stage 1 involves the synthesis of CCTO and characterization of CCTO and $BaTiO_3$ ceramics. Stage 2 is further divided into four parts: the first part is to produce epoxy thin film composites at different filler types and loading range, the second part is to produce CCTO/epoxy thin film composites at different fabrication methods. The following part is to produce hybrid fillers filled epoxy thin film composites and produce treated CCTO filled epoxy thin film composites. Lastly, the fifth part is to produce CCTO/epoxy thin film composites by using various epoxy resins. Stage 3 presents the testing and characterizations used to characterized the properties of epoxy thin film composites.

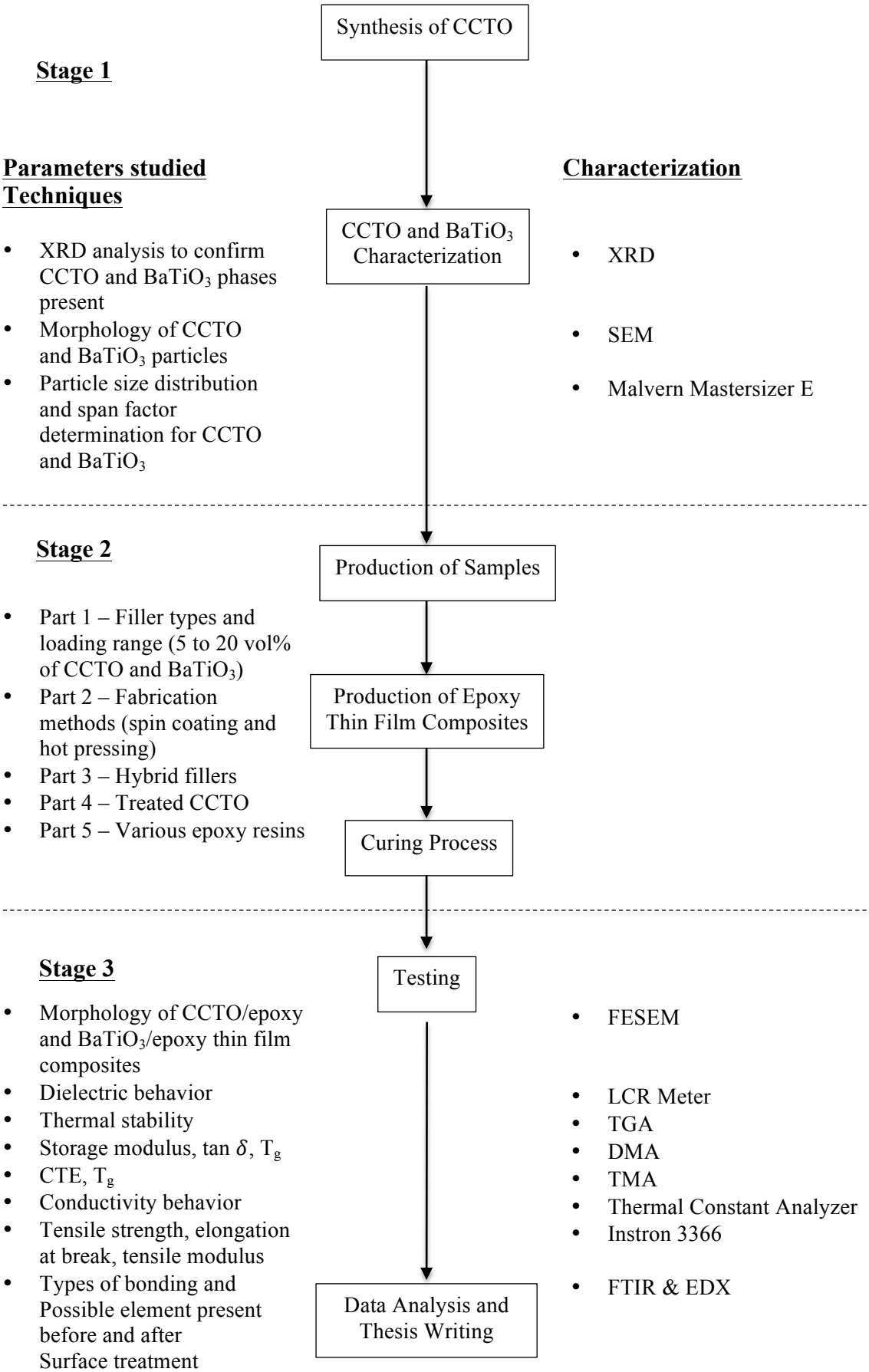

Figure 3.7: Overall research flowchart

3.4 Characterization Techniques

Characterization techniques can be divided into phase structure analysis, particle size analysis, functional groups and chemical characteristics analysis and, morphologies of the raw materials and epoxy composites. The results have been further supported with the characterization of epoxy composites using dielectric, tensile and thermal properties measurement. Dielectric properties measurement involved the analysis of dielectic constant and dielectric loss using LCR Meter. Tensile properties measurement is mainly used to characterize tensile strength, elongation at break and elastic modulus of the epoxy thin film composites were obtained from the experiment. Meanwhile thermal properties measurement can be further divided into thermal conductivity, thermogravimetric analysis, dynamic mechanical analysis and coefficient of thermal expansion analysis. These characterizations and testing are important in this study because it may help to reduce the overall research cost and also can be used to match the data with the overall research targets.

3.4.1 Phase Structure Analysis

X-ray Diffraction (XRD) analysis is an effective non-destructive analysis of crystalline materials from the millimetre down to the nanometre scale. It is very well-known technique due to its versatility that can provide detailed information about the phase and crystal structure of material. The results of XRD patterns were further compared and analyzed to the International Centre for Diffraction Data (ICDD) by using the EVA software (Bruker). The X-ray analysis data was collected in the form of intensity peak against diffraction angle, 2θ. The relation between wavelength and

diffraction angle was determined by using Bragg's Law in Equation 3.1.

$$n\ \lambda = 2\ d \sin\theta \tag{3.1}$$

The variable n is an integer, λ is the wavelength of incident x-rays beam, d is the distance between atomic layers and θ is the diffraction angles.

In this study, XRD (model: BRUKER AXS D8 Diffractometer) is used to determine and confirm the phase formation of the synthesized CCTO powder and $BaTiO_3$ powder. The analysis was carried out using Cu Kα radiation with the scan range (2θ) from 10° to 90° and wavelength at 1.5406Å.

3.4.2 Microstructures and Element Composition Analysis

The Scanning Electron Microscope (SEM) is a type of non-destructive characterization method that can be used to determine the microstructure of the samples. It is very well-known microscope as compared to optical microscope due to the ability to observe the sample with high magnification and produce high resolution image. SEM characterization is based on electron beam that pass through an evacuated column which then focused into the specimen surface. Secondary electrons (SE) was used in this characterization. Prior to SEM analysis, the ceramic powders and fractured samples of the composites were mounted on aluminium stubs and coated with gold to make it electrically conductive. It was carried out in order to prevent electrostatic charging and poor resolution while examined.

For this study, the microstructure and morphology of CCTO and $BaTiO_3$ ceramics, and fractured samples of the composites were observed using SEM

machine (model: Zeiss SUPRA 35VP) at operating power of 5.0kV with magnification of 1500x, 5000x and 10000x, respectively.

Meanwhile, for the Energy Dispersive Spectroscopy (EDS), it is used for the elemental analysis and chemical characterization of a sample such as Atomic % and Weight %. In this project, Zeiss SUPRA 35VP machine was used to identify the presence of silicon (Si) element on the surface of CCTO filler after chemically treated by GPTMS.

3.4.3 Particle Size Analysis

The particle size distributions of the synthesized CCTO powder and $BaTiO_3$ powder were measured using the particle size analyzer (Malvern MasterSizer E version 1.2b). It was determined by a laser scattering technique on the test particles in a liquid medium. About 3 g of each ceramic filler was tested and the result was displayed in a cumulative graph plot. Furthermore, the width of the particle distribution was measured by the span factor. The span factor was calculated by using Equation 3.2.

$$\text{Span Factor} = \frac{d_{90} - d_{10}}{d_{50}} \tag{3.2}$$

3.4.4 Functional Groups and Chemical Characteristics Analysis

Fourier-Transform Infrared Spectroscopy (FTIR) is a powerful analytical tool for characterizing and identifying inorganic and organic molecules. The chemical bonds and the molecules structure of organic compounds can be determined using the infrared (IR) spectrum. In this present study, FTIR was carried out to get some

informations regarding the functional groups and chemical characteristics of the epoxy thin film composites, before and after the surface treatment of CCTO filler. Perkin Elmer with the model Spectrum One was used with a typical wave number range of 400 – 4000 cm^{-1} in open air environment at reflectance mode and 16 scans.

3.5 Dielectric Properties Measurement

For preparation of diectric properties measurement, the thickness of the sample was measured using micrometer screw gauge. Next, the surface of the sample was evenly swapped with silver paste at both sides (a) and (b) as illustrated in Figure 3.8. The swapping was done carefully in order to prevent the silver paste overflow at (c) and (d) sides of the composite. This is to provide electrical contact between probe and the sample. The samples were then air-dried for 30 minutes before being cutted into the square shape with a dimension of 1 cm x 1 cm.

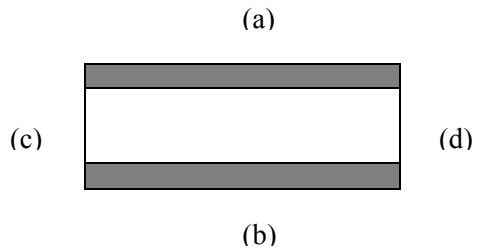

Figure 3.8: The surface of epoxy thin film composites being swapped by silver paste

The measurement of dielectric properties which includes the dielectric constant and dielectric loss of epoxy thin film composite was done using Agilent LCR Meter. The measurement frequency was set from 100 Hz to 1 MHz which then provides the capacitance and dielectric loss data. The dielectric constant data was calculated by using Equation 3.3.

$$k = \frac{C\,d}{A\,\varepsilon} \tag{3.3}$$

Where: k = Dielectric Constant

C = Capacitance, (F)

d = thickness of the sample, (m)

A = Area of the sample, (m^2)

ε_0 = Permittivity of free space taken as 8.8543 x 10^{-12} F/m

3.6 Tensile Properties Measurement

The tensile properties of CCTO/epoxy and $BaTiO_3$/epoxy thin film composites were measured according to ASTM D882-02 at a constant crosshead speed rate of 1 mm/min using an Instron 3366 machine. A total of five rectangular specimens were prepared with a dimension of 1 cm x 15 cm and the thickness were measured using micrometer screw gauge. The average values from the five specimens were reported.

From the data obtained, the stress-strain curve was plotted and the following properties such as; tensile strength, elongation at break and elastic modulus were obtained from Equations 3.4, 3.5 and 3.6, respectively. Equations 3.7 and 3.8 were used to calculate the stress (σ) and stain (ε) values followed by plotting the stress-strain curve. The tensile strength is the stress at the highest point of the curve in accordance with Equation 3.4. The elongation at break is where the strain is at the maximum and can be determined by using Equation 3.5. Meanwhile for the elastic modulus, it is obtained from the slope of the curve in the elastic region and can be calculated using Equation 3.6.

$$\text{Tensile Strength} = \frac{\text{Maximum load}}{\text{Surface area}} \ (\text{Unit} = \text{MPa}) \quad (3.4)$$

$$\text{Elongation at Break} = \text{Maximum strain X 100\% (Unit = mm)} \quad (3.5)$$

$$\text{Elastic Modulus, E} = \frac{\text{Stress}}{\text{Strain}} \ (\text{Unit} = \text{MPa}) \quad (3.6)$$

$$\text{Stress, } \sigma = \frac{\text{Load or Force}}{\text{Area}} \ (\text{Unit} = \text{MPa}) \quad (3.7)$$

$$\text{Strain, } \mathcal{E} = \frac{\text{Displacement}}{\text{Original length}} \quad (3.8)$$

3.7 Thermal Properties Measurement

3.7.1 Thermal Conductivity

The hot disk method for measuring thermal conductivity is an experimental technique designed for the estimation of the thermal transport properties of solid samples. The thermal conductivity of CCTO/epoxy and $BaTiO_3$/epoxy thin film composites were determined using Hot Disk Thermal Constant Analyzer (model: TPS 2500 S Thermal Conductivity System), which is conducted in accordance to ISO 22007-2:2008. The sensor probe with a diameter of 30 mm x 30 mm is placed in between two pieces of epoxy thin film composites and pressed by a metal block.

For this testing, specimens with a dimension of 35 mm x 35 mm square shape were used in the measurement. This is to cover the entire surface of the sensor area for a higher efficiency measurement. Average thickness of the sample was measured and the measurement was conducted in room temperature.

3.7.2 Thermogravimetric Analysis

Thermogravimetric Analysis (TGA) is a technique in which the mass of the sample is monitored against time or temperature of the sample. TGA was done using a model of Perkin Elmer Pyris-6 to investigate the thermal stabilities of the epoxy thin film composites. Note that only CCTO/epoxy thin film composites with the lowest and the highest filler loading were selected for the testing. Specimens were cut into small pieces, with a total weight of 10 to 30 mg. The temperature was set from 30 °C to 600 °C with the heating rate of 10 °C/min and conducted under nitrogen atmosphere. For this study, the change in mass or weight loss as a function of temperature was observed and analyzed which indicated the decomposition of the composite materials.

3.7.3 Dynamic Mechanical Analysis

The Dynamic Mechanical Analysis (DMA) provides information on the viscoelastic properties of materials. DMA was carried out for epoxy composites using Mettler Toledo DMA 861^{e} analyzer. Note that only CCTO/epoxy thin film composites with the lowest and the highest filler loading were selected for the testing. This is a technique in which the sample is subjected to an oscillating force and further monitored against time, temperature or frequency of oscillation while the temperature of the sample in a specified atmosphere is programmed. The measurements were done using tensile mode. All of the specimens were in the form of solid rectangular bar having a dimension of approximately 20 mm length, 3 mm width and 0.07 mm thickness. The temperature was increased from room temperature to 130 °C at a heating rate of 5 °C/min and frequency of 1 Hz. The force

amplitude was set at 1 N and the displacement amplitude was fixed at 10 μm followed by nitrogen gas being purged into the system environment. The storage modulus (*E'*) and loss tangent (*tan* δ) data were obtained from this test. Furthermore, the glass transition temperatures (T_g) of the epoxy composites were obtained from the peak of the loss tangent, *tan* δ curve.

3.7.4 Coefficient of Thermal Expansion Analysis

Thermo-Mechanical Analyzer (TMA) is a technique used in thermal analysis in which the change in the dimensions of a sample as a function of temperature is monitored. Note that only CCTO/epoxy thin film composites with the lowest and the highest filler loading were selected for the testing. The coefficient of thermal expansion (CTE) before the glass transition temperatures (T_g) was measured using a thermomechanical analyzer (model: Perkin Elmer TMA-7). The cured samples were cut into 5 mm diameter for CTE measurements and mounted on the TMA holder using compression mode with static force of 50 mN. The temperature range used was from 30 to 130 °C and the heating rate was 10 °C/min for both heating; first and second heating. The plot of probe position against temperature provides the value of CTE of the composites.

CHAPTER 4

RESULTS AND DISCUSSION

4.1 Introduction

The results of the experiment conducted as well as the discussion on the results are presented in this chapter. The division of the section will be based on the raw materials characterizations and objectives as stated in Chapter 1. The first section discusses on the raw materials characterizations from synthesized CCTO and pure $BaTiO_3$ powders, followed by the effect of different filler types and loading range on the dielectric, tensile and thermal properties of epoxy thin film composites. Next section is the effect of various fabrication methods on the dielectric and thermal properties of ceramic filler filled epoxy thin film composites and continued with the effect of hybrid fillers on the dielectric and thermal properties of epoxy thin film composites. The effect of silane coupling agent and effect of various epoxy resins on the properties of CCTO/epoxy thin film composites were discussed in the last part of the thesis. The discussion will be based on the results obtained and supported by the results reported by previous researchers.

4.2 Raw Materials Characterization

The raw materials that have been used as reinforcement fillers in this research are synthesized CCTO and pure $BaTiO_3$ powders. Characterizations based on Scanning Electron Microscopy (SEM) and X-ray Diffraction (XRD) were carried out to characterize the morphology and purity of the raw materials, respectively. Meanwhile particle size analyzer was used to measure the particle size of the ceramic fillers.

Figure 4.1 shows the XRD patterns of CCTO ceramic synthesized with a solid-state reaction and pure $BaTiO_3$ ceramic. There are nine peaks of CCTO and seven peaks of $BaTiO_3$ observed in XRD patterns. The synthesized CCTO and pure $BaTiO_3$ ceramics show a single phase which is highly crystalline in nature where the main peaks of the ceramics are comparable to those of the standard ceramic XRD patterns of CCTO (ICDD Data File Card No. 01-075-2188) and $BaTiO_3$ (ICDD Data File No. 00-005-0626).

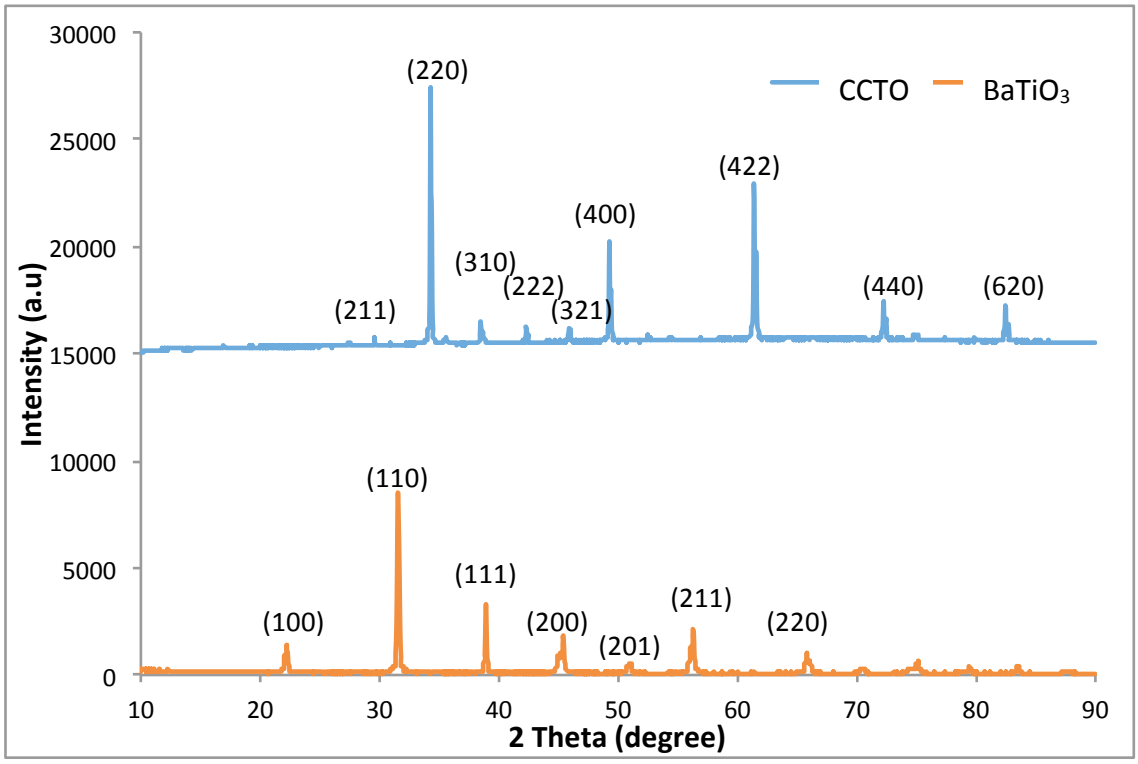

Figure 4.1: XRD patterns of synthesized CCTO and pure $BaTiO_3$ ceramics

SEM micrographs of synthesized CCTO pure $BaTiO_3$ powders are shown in Figure 4.2 (a – b). Based on the micrographs, it was observed that CCTO and $BaTiO_3$ powders are in irregular shape.

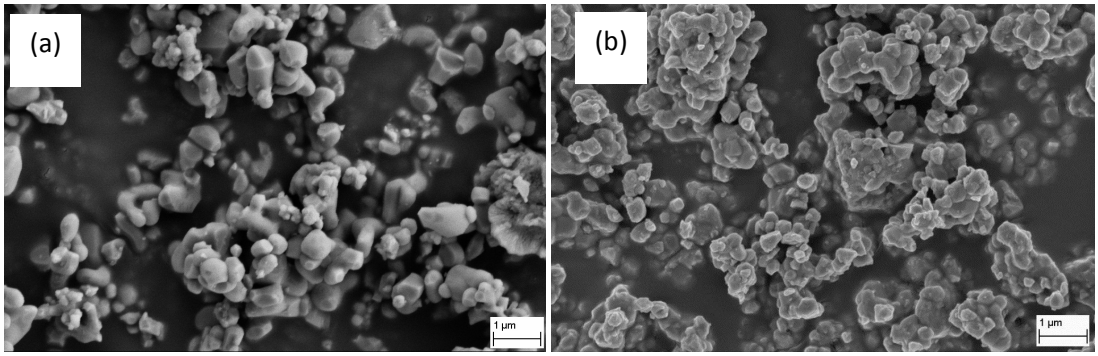

Figure 4.2: SEM micrographs of (a) synthesized CCTO and (b) pure $BaTiO_3$ powders [10000x magnification]

The average particles size (d_{50}) of CCTO and $BaTiO_3$ powders are 5.01 µm and 1.48 µm, respectively, as indicated in Figure 4.3. Moreover, the span factors of CCTO powder is 2.63 and $BaTiO_3$ powder is 1.12. Noted that, small span of $BaTiO_3$ powder indicates a narrow particle size distribution, whereby for CCTO powder, large span indicates the broad particle size distribution.

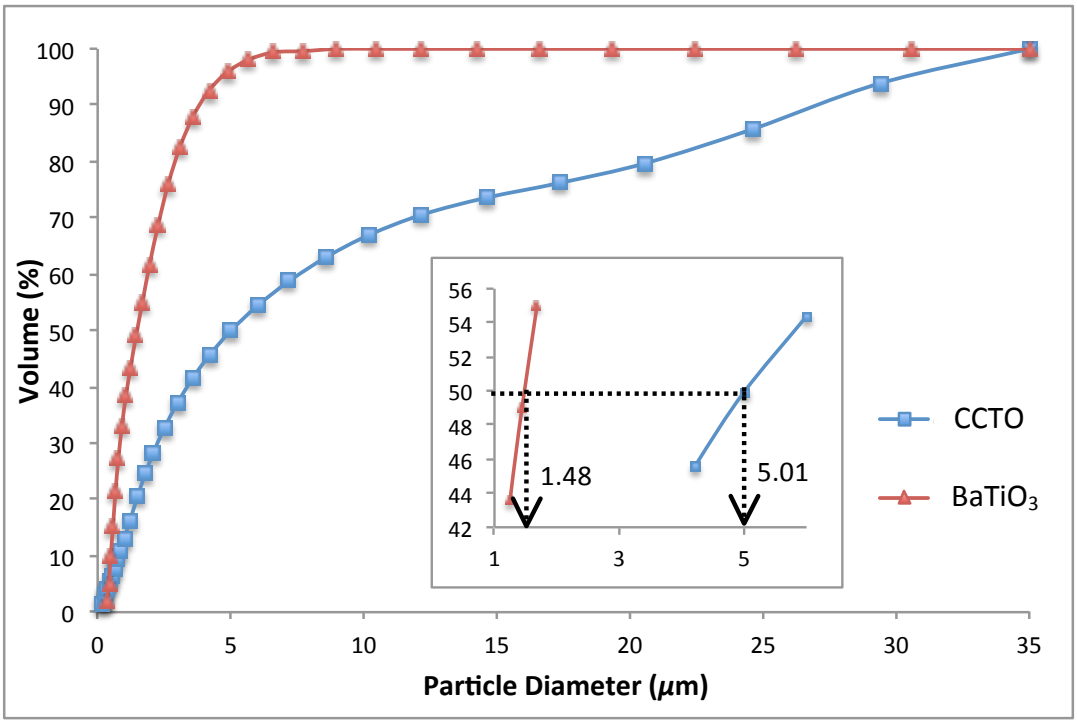

Figure 4.3: Particle size distribution for different raw materials, the inset shows the average particles size (d_{50}) of CCTO and $BaTiO_3$ powders

4.3 The Effect of Different Filler Types and Loading Range

The first objective of the present research is to study the effect of different filler types and loading range on the dielectric, tensile and thermal properties of CCTO/epoxy and $BaTiO_3$/epoxy thin film composites. Based on methodology in Section 3.3.2.1, the composites are prepared by spin coating method.

4.3.1 Dielectric Properties

Figure 4.4 shows the dielectric constant values of CCTO and $BaTiO_3$ composites at room temperature and 100 Hz, as a function of the filler loading (vol%). It can be seen that the dielectric constant of both composites increased evidently with increasing filler loadings. CCTO composites show slightly higher dielectric constant values as compared to $BaTiO_3$ composites for all filler loadings. By considering the dielectric constant of CCTO and $BaTiO_3$ which are 10^5 and 1000, respectively, it is found that the dielectric constant of both composites do not show a great differences at the same filler loading. There are many factors that might influence the dielectric constant of the composites such as filler-matrix adhesion, dispersion of filler in epoxy matrix, voids and etc. The same observation was reported by Ramajo et al. (2008) in their study on differences between the dielectric properties of ceramic filler filled polymer composites.

The dielectric loss of CCTO and $BaTiO_3$ composites are compared in Figure 4.5. It is observed that the dielectric loss of CCTO systems was higher than $BaTiO_3$ composites, throughout the volume fraction range. Nevertheless, these composites may still be potential candidates for charge storage applications as the value of dielectric loss is still within the acceptable limits. The trend is in accordance with the

previous work done by Prakash and Varma (2007) where the dielectric loss increased with increasing of CCTO filler loading in epoxy matrix but the values are still within the acceptable limit.

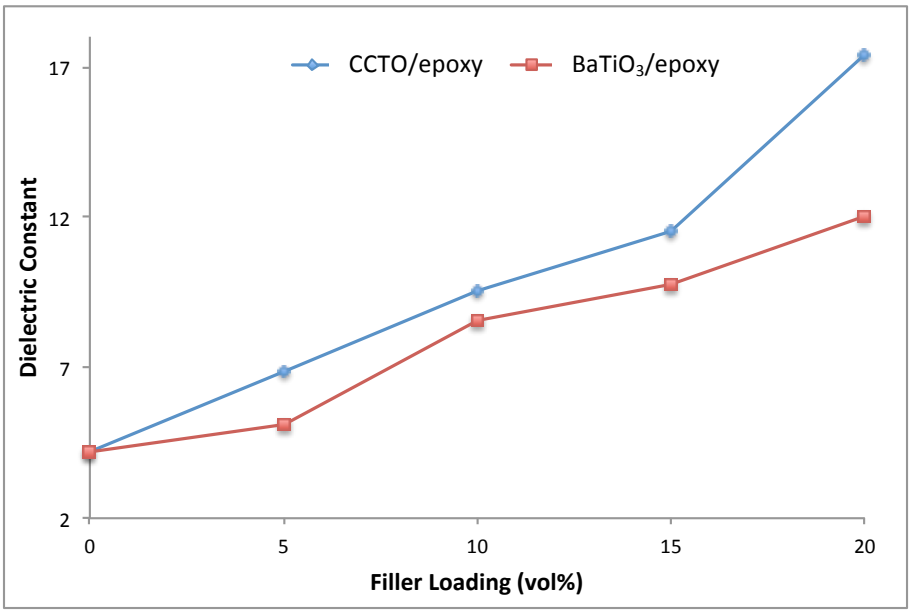

Figure 4.4: Dielectric constant of CCTO/epoxy and $BaTiO_3$/epoxy thin film composites as a function of filler loading at frequency of 100 Hz

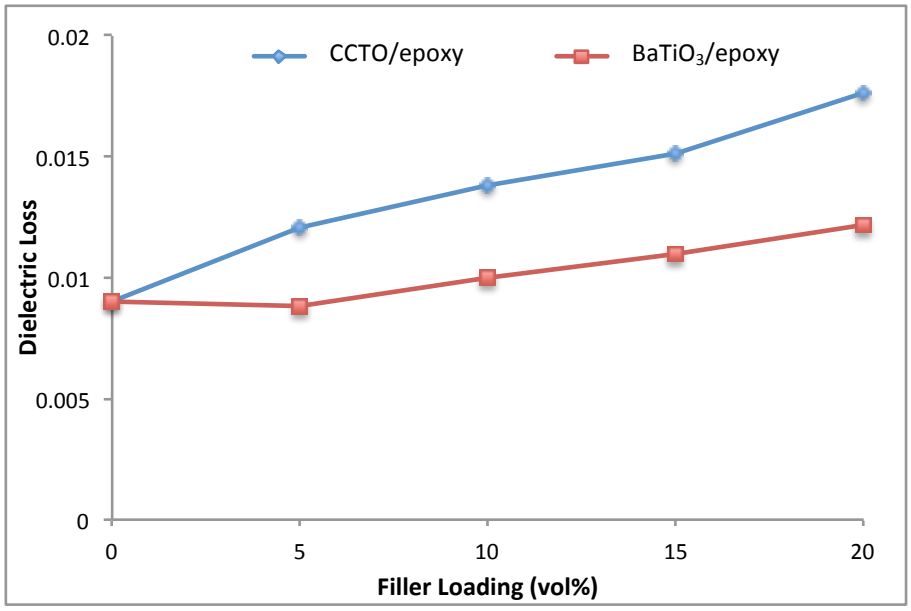

Figure 4.5: Dielectric loss of CCTO/epoxy and $BaTiO_3$/epoxy thin film composites as a function of filler loading at frequency of 100 Hz

Figure 4.6 illustrates the dielectric constant of the unfilled epoxy and epoxy thin film composites with 20 vol% of CCTO and $BaTiO_3$ fillers, the measurement is carried out at frequency of 100 Hz – 1 MHz. It is clearly indicated that the introduction of CCTO and $BaTiO_3$ filler in epoxy increased the dielectric constant of epoxy at 100 Hz from 4.2 to 17.4 for 20 vol% of CCTO and 12.1 for 20 vol% $BaTiO_3$ composites. However, the dielectric constant values of both composites decreased with increasing of frequency. As reported by Devaraju et al. (2005), this is because at high frequency, shorter time is required for the filler and epoxy dipole moments to polarize and keep up with the applied alternating current electric fields. However, it is observed that the dielectric constant of CCTO composite is still higher than $BaTiO_3$ composite, for all frequency ranges.

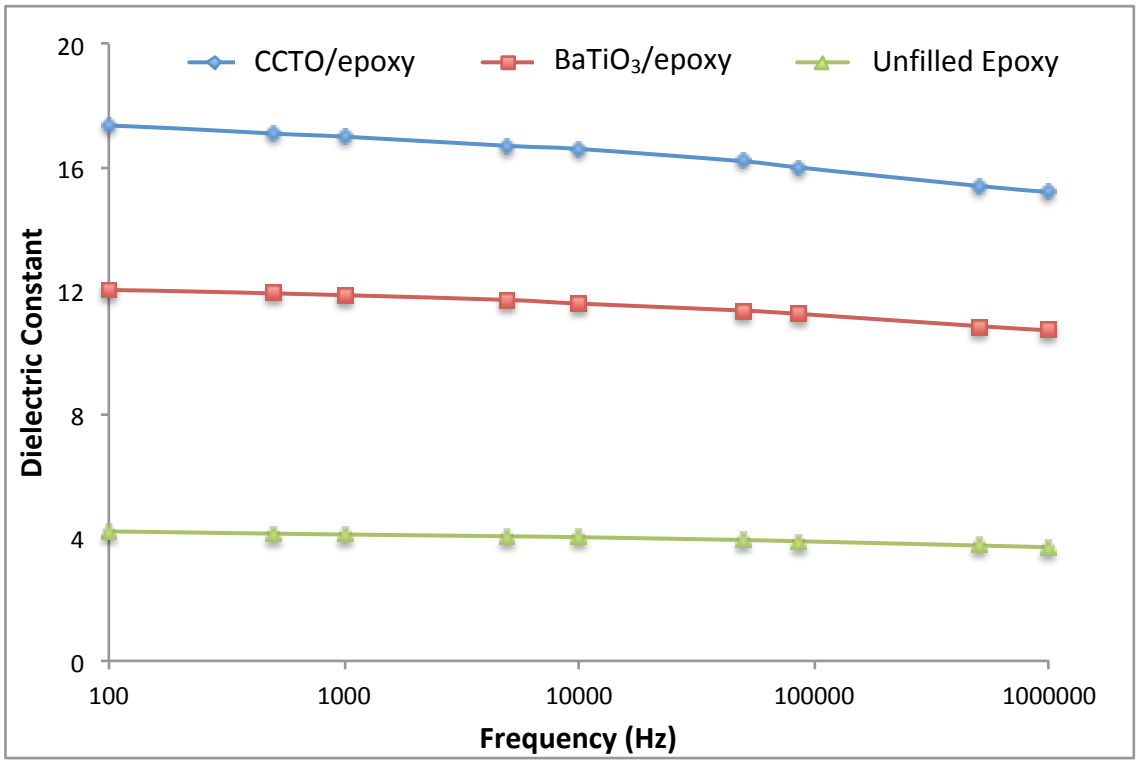

Figure 4.6: Dielectric constant of 20 vol% CCTO/epoxy and $BaTiO_3$/epoxy thin film composites as a function of frequency

The dielectric loss of unfilled epoxy and epoxy thin film composites with 20 vol% of CCTO and $BaTiO_3$ filler are shown in Figure 4.7. It can be seen that the dielectric loss values of unfilled epoxy and $BaTiO_3$ composite are slightly lower as compared to CCTO composite. Moreover, both composite systems show decreasing trend in the 100 Hz to ~ 1 kHz frequency range and rapidly increases at high frequency (>10^6 Hz), this trend is reported due to the dielectric relaxations. Epoxy resin generated relaxation process near its T_g in all composites. The relaxation was affected by the interfacial polarization process known as Maxwell-Wagner-Sillar which generated by CCTO particles. In the polarization process, it produced an accumulation of charges around the CCTO interfaces that displaced peaks to higher frequency (Ramajo et al., 2007).

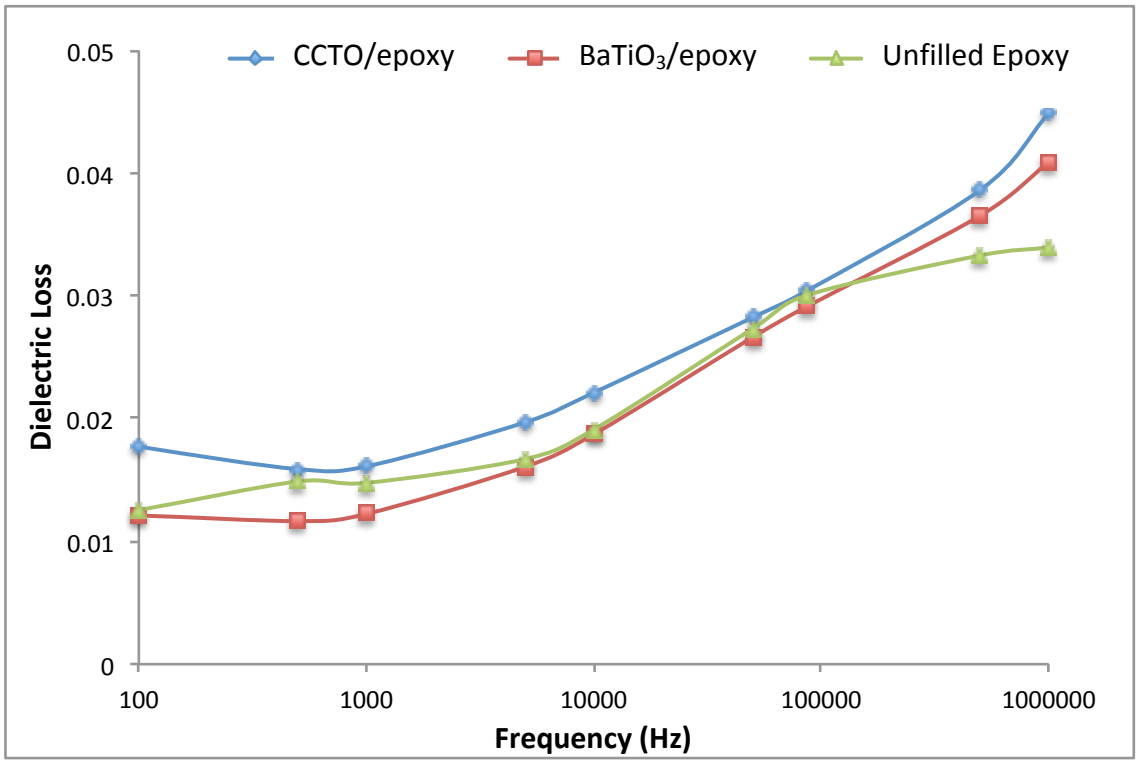

Figure 4.7: Dielectric loss of 20 vol% CCTO/epoxy and $BaTiO_3$/epoxy thin film composites as a function of frequency

4.3.2 Tensile Properties

The effect of filler loading on the tensile strength of the CCTO/epoxy and $BaTiO_3$/epoxy composites are shown in Figure 4.8. The experimental results showed that the addition of filler loading decreased the tensile strength of CCTO/epoxy composite. On the other hand, 20 vol% $BaTiO_3$/epoxy composite has increased 20% of tensile strength as compared to 5 vol% $BaTiO_3$/epoxy composite. Based on the error-bars, the tensile strength of both composites are comparable to that of unfilled epoxy. Previous work by Huang et al. (2011) presented similar result in their study on the effect of filler content to the tensile strength of micro-$BaTiO_3$/EVM composite where the tensile strength increased gradually with increasing of micro-$BaTiO_3$ filler content.

As known, epoxy resin is hydrophobic by nature, while the CCTO and $BaTiO_3$ fillers are hydrophilic (Owen, 1993; Gao et al., 2013). Hence, these two incompatible constituents weaken the interfacial interactions between the molecules as shown by the tensile strength of CCTO/epoxy composites. However, it did not gives significant effect on the tensile strength of $BaTiO_3$/epoxy composites. The greater strength of $BaTiO_3$/epoxy composite compared to CCTO/epoxy composite was mainly due to the small span factor of $BaTiO_3$ indicates a narrower particle size distribution, which means that $BaTiO_3$ shows a more uniform particle size distribution than CCTO. This results might be explained using morphology of $BaTiO_3$/epoxy composite shown in Figure 4.9, where the fillers dispersed well throughout the composite and less voids can be seen between epoxy resin and $BaTiO_3$ filler, if compared to CCTO/epoxy composites.

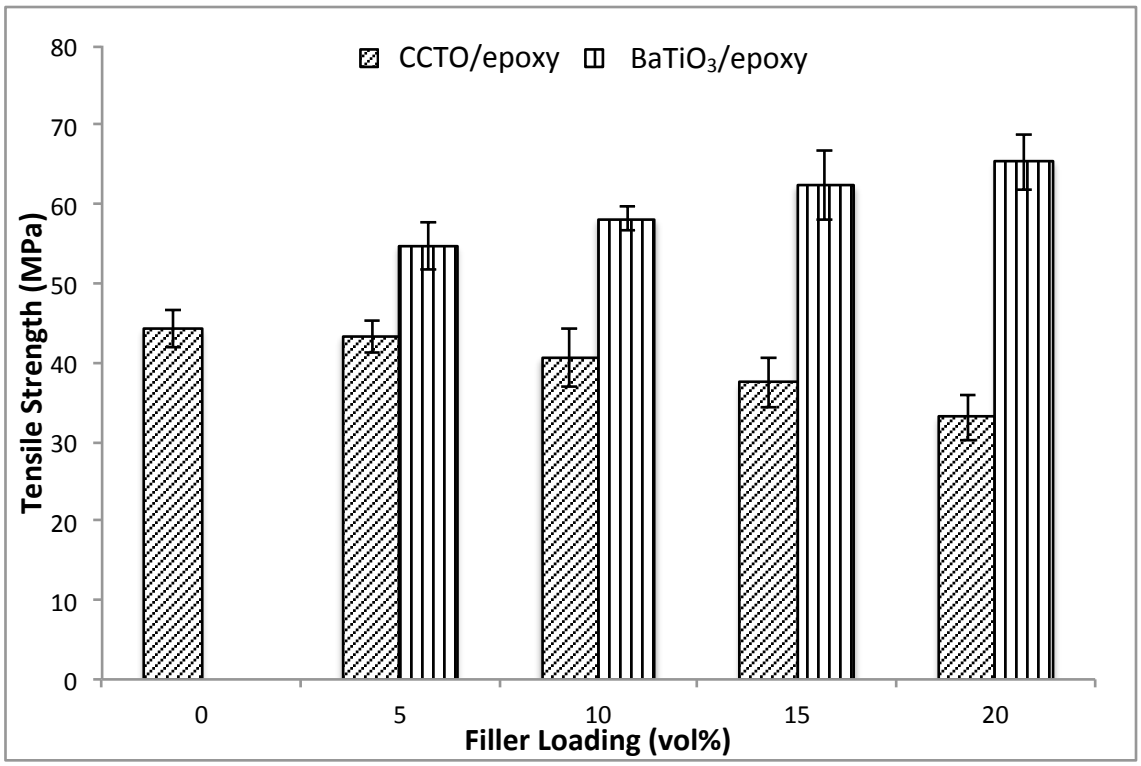

Figure 4.8: Comparison of tensile strength of unfilled epoxy and epoxy thin film composites

As shown in Figure 4.9 (a and b), the unfilled epoxy had a fairly smooth fracture surface, which is a typical brittle fracture for epoxy (Voo et al., 2012). This result proved that unfilled epoxy has low crack propagation resistance and can easily break upon the application of stress. As shown in Figure 4.9 (c, e, g, i), the fracture surfaces of the CCTO and $BaTiO_3$ thin film composites were rougher and had more waves than that of the unfilled epoxy. Rough fracture surface indicates high crack resistance causing the crack not to propagate as easily compared with unfilled epoxy. Thus, more energy is required to propagate the cracks (Wu et al., 2002; Poh et al., 2014). The epoxy composites had rougher surface make it harder to break than that of the unfilled epoxy. However, numerous cavities marked by red circles appeared on the fracture surface of the epoxy composites, as illustrated in Figure 4.9 (h, j). Schonhorn (1985) reported that the cavities or voids are due to the filler that been

pulled out during the stress application. This is caused by lack interactions of CCTO and $BaTiO_3$ with the epoxy matrix. The cavities or voids in Figure 4.9 (g-j) can also be caused by the formation of air bubbles during mixing. When the filler loading was increased, the viscosity of the mixture increased and produced voids that are difficult to be removed in the samples.

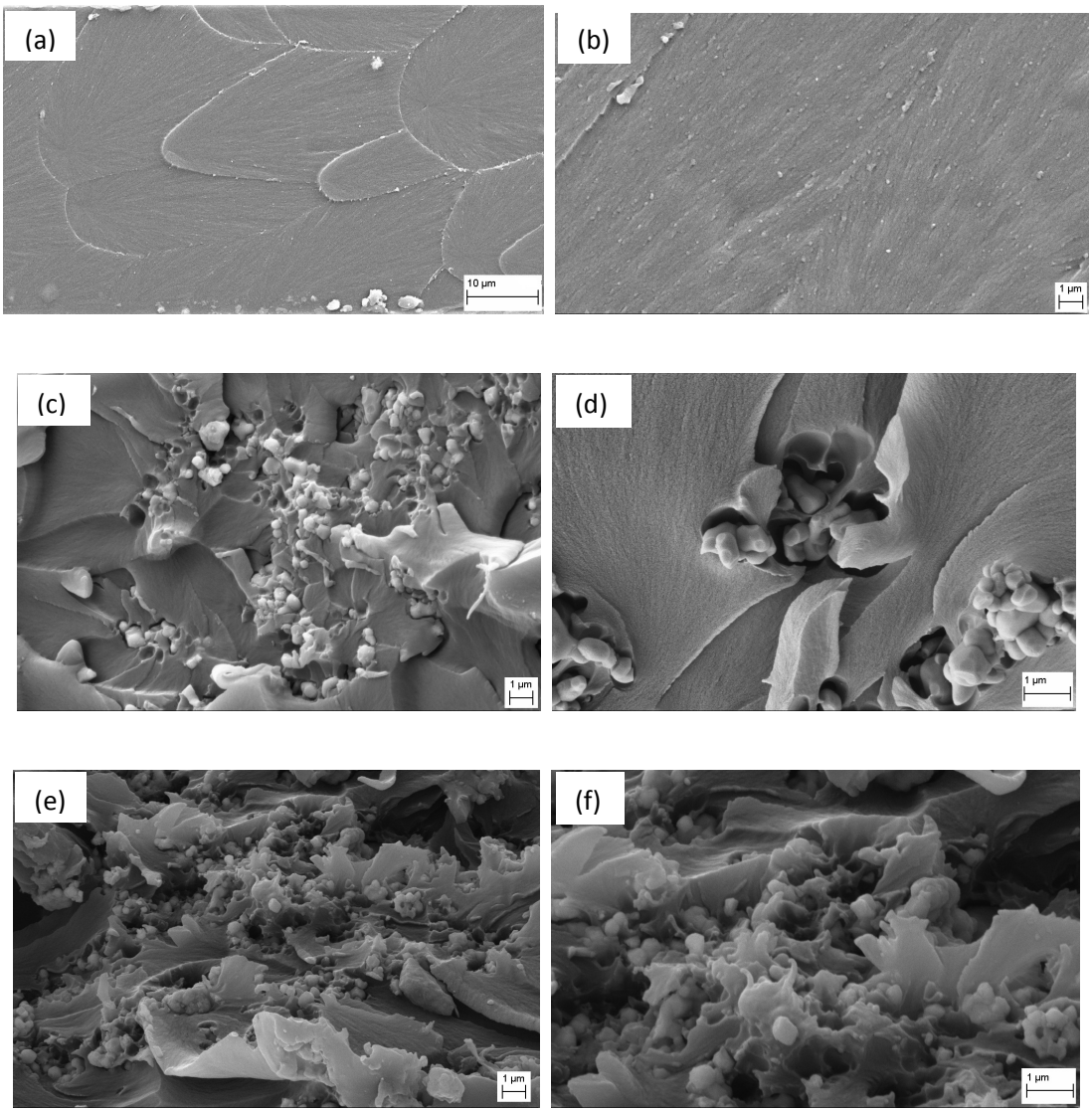

Figure 4.9: SEM micrograph of fracture surface of (**a**, **b**) unfilled epoxy, 5 vol% of fillers; (**c**, **d**) CCTO/epoxy, (**e**, **f**) $BaTiO_3$/epoxy, and 20 vol% of fillers; (**g**, **h**) CCTO/epoxy, (**i**, **j**) $BaTiO_3$/epoxy [magnifications of 5000x was used for (**a**, **c**, **e**, **g**, **i**), and 10000x for (**b**, **d**, **f**, **h**, **j**)]

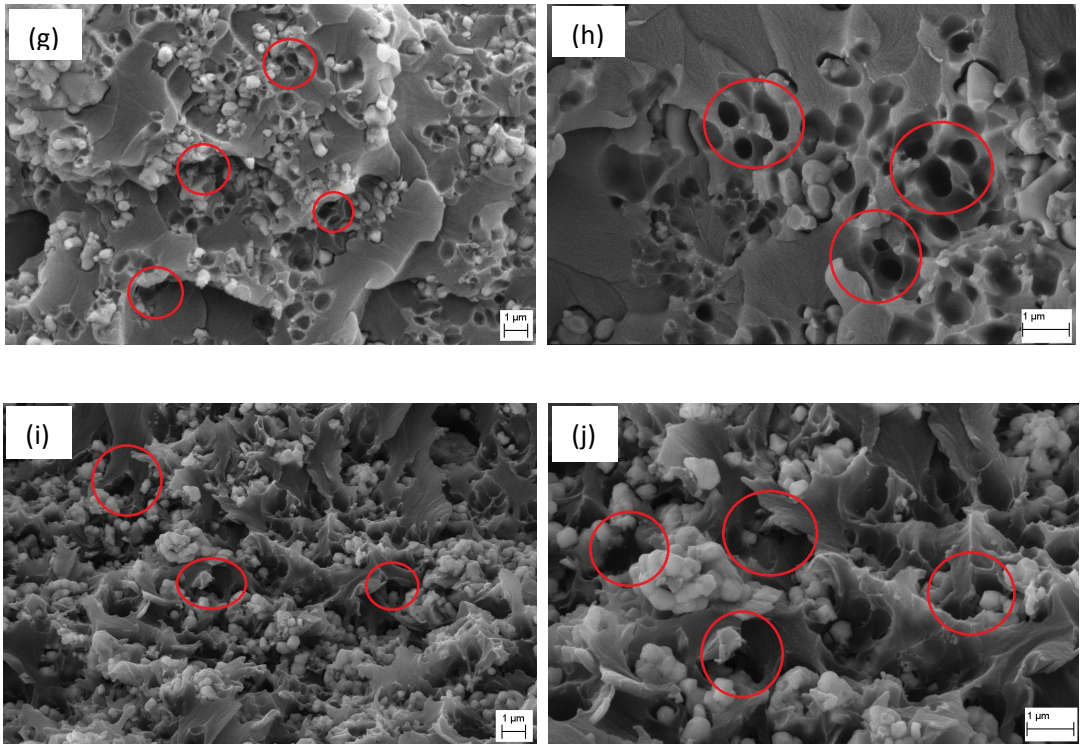

Figure 4.9: *Continued*

Elongation at break is an important parameter which describes the rupture behavior of composite materials. It was found that the elongation at break of pure epoxy resin was higher than the corresponding values for CCTO/epoxy and $BaTiO_3$/epoxy composites at any filler loading (vol%) as shown in Figure 4.10. This result might be influenced by the polymer matrix, with increasing of filler loadings, the amount of polymer matrix decreased, hence reduced the elongation at break of the composites. Besides that, high volumes of fillers can increase the viscosity of epoxy/filler mixtures. High mixture viscosity leads to filler agglomeration, causing increased filler-to-filler contact and thus create more voids which affect the elongation at break of the composites. The hypothesis is supported by observing the SEM micrographs in Figure 4.9 of both composites. It is observed that agglomeration is easily spotted on the fracture surface.

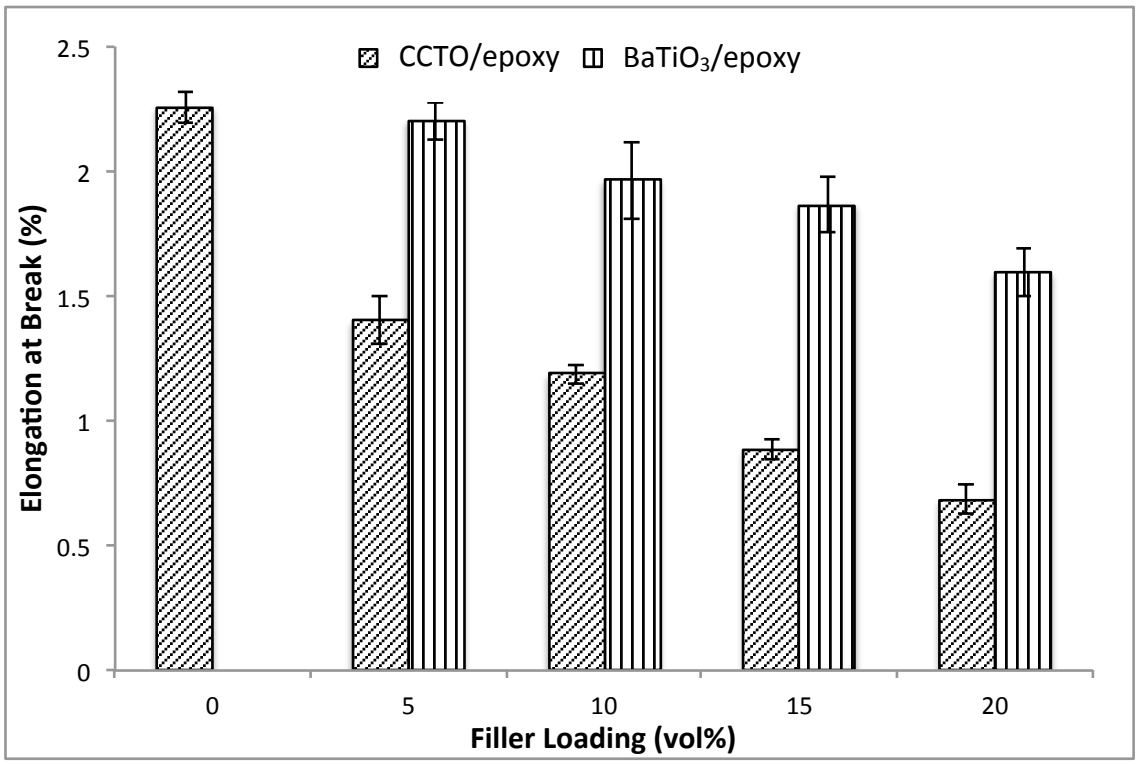

Figure 4.10: Comparison of elongation at break of unfilled epoxy and epoxy thin film composites

An overall improvement in the elastic modulus with increasing filler loading is shown in Figure 4.11. The increasing modulus trend with addition of filler is in accordance with the Rule of Mixture (equation (4.1)) where at high loading, the elastic modulus of polymer composite materials increased. This is because filler has higher elastic modulus than the polymer matrix.

$$E_c = E_f V_f + E_m V_m \quad (4.1)$$

where E_f is the filler modulus, V_f is the filler volume fraction, E_m is the matrix modulus, and V_m is the matrix volume fraction (Campbell, 2010). It is observed that $BaTiO_3$ composite exhibited the highest elastic modulus compared to CCTO composite and unfilled epoxy. This is largely attributed to the fact that the dispersion

of $BaTiO_3$ powder in epoxy matrix is better than CCTO powder (as shown in Figure 4.9) due to smaller particles size and narrow particle size distribution of $BaTiO_3$ powder. This subsequently contributes to the improvement in the mechanical properties of the composites.

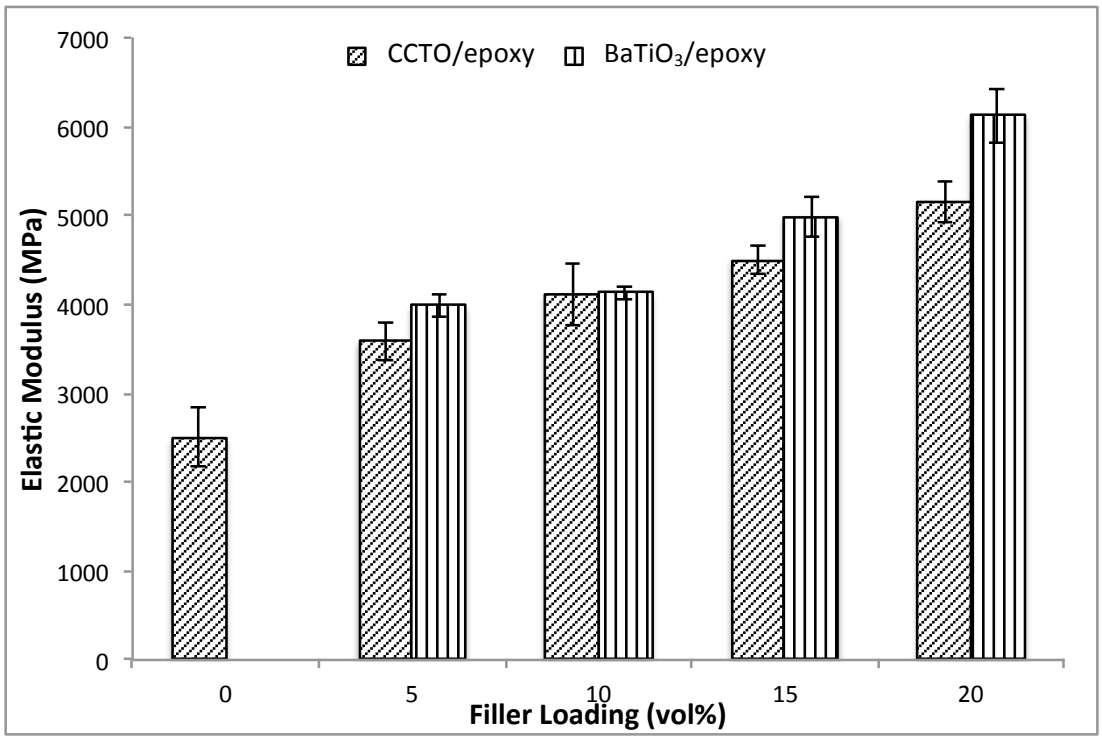

Figure 4.11: Comparison of elastic modulus of unfilled epoxy and epoxy thin film composites

4.3.3 Thermal Stability

Thermal stability of the composite is an important factor in processing and during application since it affects the performance of the materials. For electronic packaging application, thermogravimetric analysis (TGA) is important to determine the thermal stability of the materials at the application temperature of 150 - 200 °C (Voo et al., 2012). Figure 4.12 and Table 4.1 show the TGA curve and thermal analysis data of the unfilled epoxy and epoxy thin film composites, respectively.

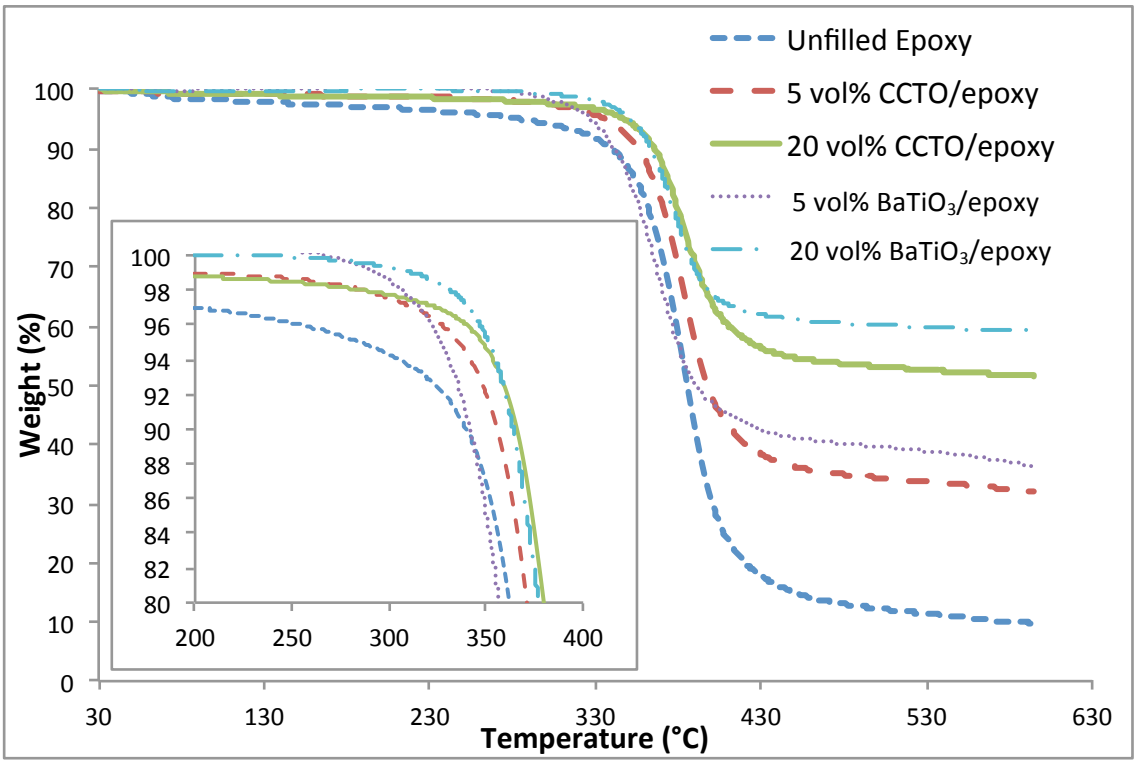

Figure 4.12: Comparison weight loss of unfilled epoxy and thin film composites with respect to temperature, the inset is an enlargement of weight-temperature curve

The initial degradation temperature, $T_{5\%}$ (°C) and onset degradation temperature, T_{onset} (°C) are reported in Table 4.1. The TGA results demonstrated that the incorporation of CCTO and $BaTiO_3$ fillers into epoxy improved the onset decomposition temperature (T_{onset}) of the thin film composites. This result can be attributed to the interaction of the filler particles with the epoxy matrix, as well as the good dispersion state of the filler in the polymer matrix which slowed down the diffusion of volatile degradation products. Hence, increase the movement restriction of the epoxy matrix because the composite system requires higher thermal energy to degrade (Xie et al., 2004; Leszczynska et al., 2007). Among all the composite systems in Table 4.1, 20 vol% $BaTiO_3$/epoxy composite shows the highest $T_{5\%}$ and T_{onset} compared to unfilled epoxy and other composites. Thus, this proved that ceramic fillers such as CCTO and $BaTiO_3$ improve the thermal stability of the epoxy,

hence indicate the stability of these materials to be used in electronic packaging applications.

Table 4.1: Decomposition temperature of various filler loading on epoxy thin film composites

Fillers loading on epoxy thin film	Initial degradation temperature, $T_{5\%}$ (°C)	Onset degradation temperature, T_{onset} (°C)
Unfilled Epoxy	285	331
5 vol% CCTO/epoxy	327	340
5 vol% $BaTiO_3$/epoxy	348	357
20 vol% CCTO/epoxy	335	348
20 vol% $BaTiO_3$/epoxy	351	360

4.3.4 Thermal Conductivity

Figure 4.13 depicts the thermal conductivity of CCTO/epoxy and $BaTiO_3$/epoxy thin film composites. As expected, the addition of inorganic fillers such as CCTO and $BaTiO_3$ increased the thermal conductivity of the polymer matrix with increasing filler content. This might be due to increased tendency to form continuous path as the filler content increased. According to Devaraju et al. (2005) and Kochetov et al. (2009), the continuous paths ease the phonon transfer and act as regions of heat conduction resulting in a rapid increase in thermal conductivity. It was observed, CCTO/epoxy thin film composite showed higher thermal conductivity than unfilled epoxy and $BaTiO_3$/epoxy thin film composite. When CCTO filler loading was at 20 vol%, the thermal conductivity of the thin film composites reached $2.3x10^{-1}$ W/mK. This indicates almost 360% and 90% increased as compared to the

unfilled epoxy and 20 vol% $BaTiO_3$/epoxy thin film composite. The agglomeration of CCTO fillers in epoxy matrix system (as seen in Figure 4.9) are potentially good for thermal conductivity as the filler-to-filler contact increased and created a path for the phonon transfer.

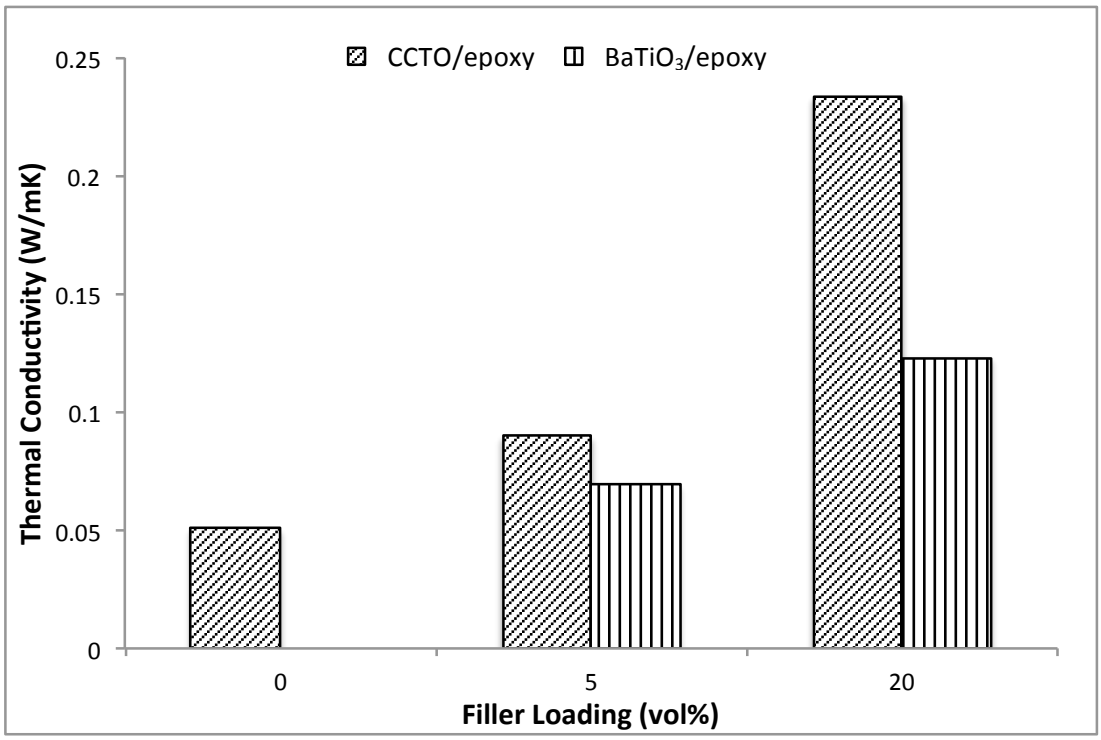

Figure 4.13: Thermal conductivity of CCTO/epoxy and $BaTiO_3$/epoxy thin film composites

4.3.5 Dynamic Mechanical and Thermal Mechanical Properties

Dynamic mechanical analysis (DMA) was used to evaluate the dynamic mechanical behavior of unfilled epoxy and epoxy thin film composites at the range of 30 to 120 °C. Figure 4.14 and 4.15 show the DMA curves; storage modulus, *E'* and loss tangent, *tan δ* spectrums recorded at 1 Hz for unfilled epoxy and epoxy thin film composites. Figure 4.14 indicates the effect of temperature on the storage modulus of unfilled epoxy and epoxy thin film composites. At temperature above T_g,

the matrix is in a rubbery state where modulus drops drastically (Goyanes et al., 2000). It can be observed, below T_g, the decrease of loss tangent maximum and the increase in *E'* with increasing volume fraction of filler by considering the reduction of matrix mobility in the vicinity of ceramic fillers due to the adsorption of polymer onto the filler surfaces. It is important to mention that the modulus in the glassy state is determined primarily by the strength of the intermolecular forces and the way the polymer chain is packed (Marcovich et al., 1999; Mandal et al., 2008).

Sample with 20 vol% $BaTiO_3$/epoxy thin film composite exhibited higher and slightly higher value of *E'* at 30 °C than that of unfilled epoxy and 20 vol% CCTO/epoxy thin film composite, respectively, as presented in Table 4.2. This is due to the reinforcement effect produced by the $BaTiO_3$ filler, which has high rigidity and stiffness. This trend is supported by Voo et al. (2012) in their study on the various nano-fillers filled epoxy thin film nanocomposites. They showed that the increment in *E'* is attributed to the addition of fillers on epoxy thin film composite.

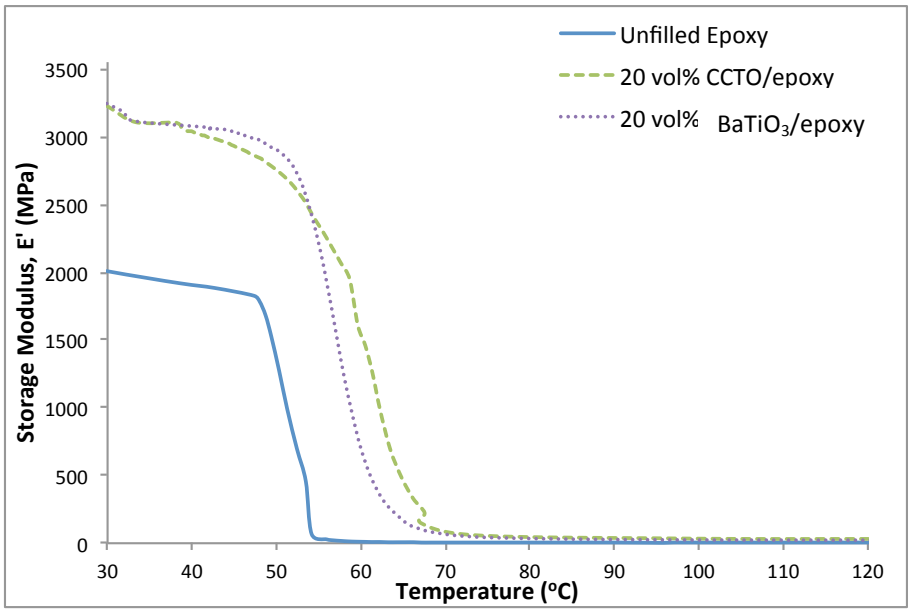

Figure 4.14: Storage Modulus, *E'* spectrums recorded at 1 Hz for unfilled epoxy and epoxy thin film composites

In the present study, T_g is more preferable to be obtained from *tan* δ curve (Figure 4.15), which is related to the occuring molecular chain relaxation (Park et al., 2003). It was observed, 20 vol% CCTO/epoxy thin film composite shows the highest value of T_g as compared to unfilled epoxy and 20 vol% $BaTiO_3$/epoxy thin film composite. In an unfilled epoxy system, the chain systems move freely. The increment in T_g can be associated with the decreased mobility of the chains due to the presence of fillers (Susumu et al., 1998). More interactions between ceramic fillers and epoxy matrix lead to a higher constraint of the polymer chains, hence increased the glass transition temperature.

Previous researchers reported that the T_g increases with filler loading, in which similar trend of *tan* δ peak position is observed in the present study (Jeefferie et al., 2010). This results might be explained using morphology of the composites in Figure 4.9, where fillers dispersed homogeneously throughout the epoxy system. However, the effect of sizes of fillers on the T_g of the thin film composites was not too significant. Although $BaTiO_3$ filler was found to have smaller particles size than CCTO, which means greater surface area, the difference observed in the T_g was not significant. McGrath et al. (2008) reported that the changes in T_g is dependent on the filler loading which influence the mobility of the polymer chains, rather than of average particle size and size distribution.

Table 4.2: Glass Transition Temperature, T_g and storage modulus, E' of unfilled epoxy and epoxy thin film composites

Composite	Glass Transition Temperature, T_g (°C)	Storage Modulus, E' at 30 °C (MPa)	Coefficient of Thermal Expansion, CTE (before T_g) (ppm/°C)
Unfilled Epoxy	55.3	1888	143
20 vol% CCTO/epoxy	67.5	3223	112
20 vol% $BaTiO_3$/epoxy	64.8	3244	38

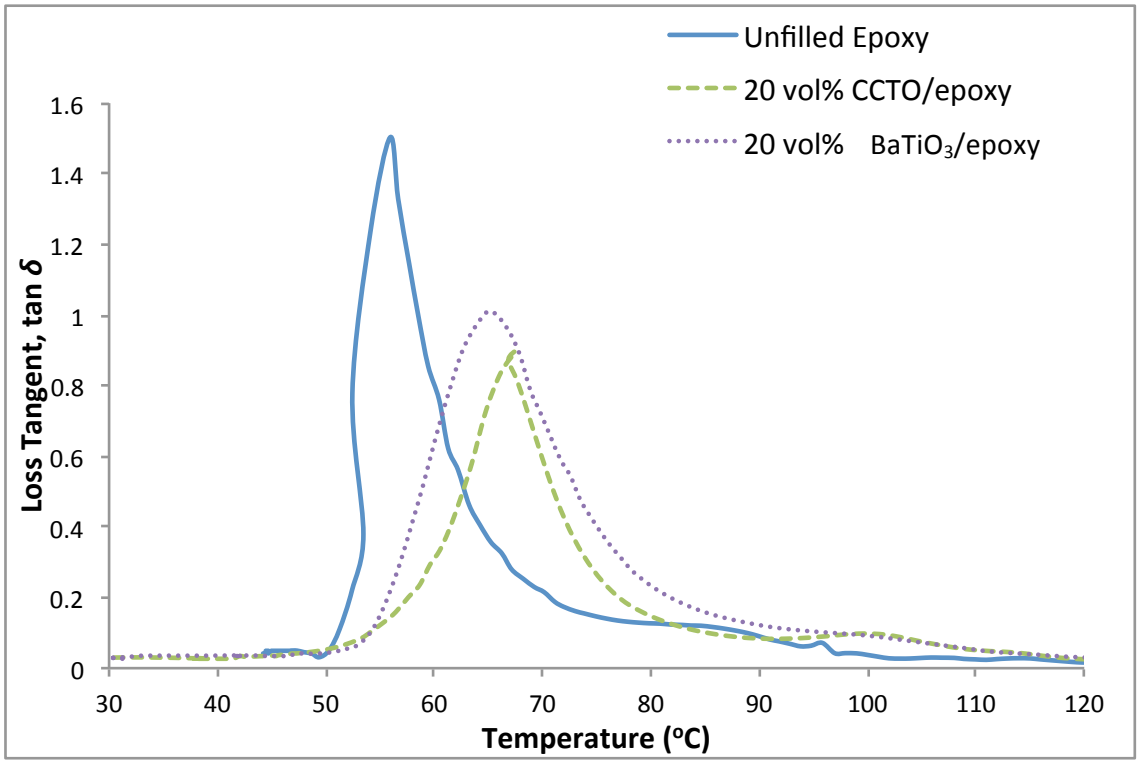

Figure 4.15: Loss Tangent, *tan δ* spectrums recorded at 1 Hz for unfilled epoxy and epoxy thin film composites

Common problem associated with the temperature different between components in the printed circuit board is the coefficient of thermal expansion (CTE) mismatch. Hence, thermal mechanical analysis graph is important. Table 4.2 shows

the CTE properties of unfilled epoxy and epoxy thin film composites, including 20 vol% CCTO/epoxy and 20 vol% $BaTiO_3$/epoxy thin film composites, respectively. It can be observed that CTEs before T_g was reduced with increasing filler loading. Sample with 20 vol% $BaTiO_3$/epoxy thin film composite shows the lowest CTE before T_g, ~38.1 ppm/°C as compared to unfilled epoxy and other composites. Low CTE value of $BaTiO_3$ filler (9.8 ppm/°C) is believed to be the main contributor to lower down the CTE of $BaTiO_3$-filled epoxy composites. However, despite the fact that CCTO has lower CTE (8.9 ppm/°C), it did not help in reducing the CTE of thin film composites. This can be explained by the CCTO/epoxy thin film composite having poor dispersion as compared to $BaTiO_3$/epoxy thin film composite. This is proven by the presence of cavities or voids as shown in the SEM micrographs of the fracture surface (Figure 4.9).

4.4 The Effect of Various Fabrication Methods

The second objective of the present research is to study the effect of various fabrication methods on the dielectric and thermal properties of CCTO/epoxy thin film composites. CCTO filler was chosen instead of $BaTiO_3$ due to better dielectric, tensile and thermal properties, as discussed in previous section. The fabrication methods used in the present study are spin coating (SC) method and hot press (HP) method.

4.4.1 Dielectric Properties

Figures 4.16 and 4.17 illustrate the dielectric constant and dielectric loss of CCTO/epoxy thin film composites at different fabrication methods, respectively. The measurement of dielectric properties is carried out at room temperature and

frequency range from 100 Hz to 1 MHz. Sample with 20 vol% CCTO/epoxy (SC) is chosen for comparison with HP samples due to better dielectric, tensile and thermal properties as compared to other composites as discussed previously in Section 4.3. This composite is compared with CCTO/epoxy (HP) at different filler loadings; 20 vol%, 30 vol% and 40 vol%, respectively. Based on the previous studies by Thomas et al. (2013), the CCTO filler loading can be added up to 38 vol% in Poly(methyl methacrylate) composite by using hot press method. One of the advantages of using hot press method over the spin coating method is the fabrication of epoxy thin film composite can be produced at high filler loading. It is reiterated that maximum filler loading up to 20 vol% can be prepared by spin coating method, however by using hot press, amount of filler used can be increased to 40 vol%.

From the figure, it can be seen that slightly higher dielectric constant is observed in 20 vol% CCTO/epoxy (SC) compared to that of 20 vol% CCTO/epoxy (HP), where the values are 17.4 and 15.3, respectively. This might be due to better dispersion and less clustering of CCTO filler in the epoxy matrix for composite produced by spin coating method as shown in Figure 4.18. Moreover, it was found that the dielectric constant continue to increase with increasing of CCTO content (up to 40 vol%) in the epoxy system for hot press method. However, the dielectric constant gradually decreases as the frequency increased for both fabrication methods (Shriprakash and Varma, 2007; Tuncer et al., 2007; Amaral et al., 2008). The result of dielectric constant obtained is paralled with the previous study reported by Thomas et al. (2013) in their study on PMMA/CCTO composite fabricated using hot press method where an increasing trend in dielectric constant is observed when the ceramic loading is increased to 38 vol% in PMMA. Yang et al. (2011) reported the same trend where the addition of CCTO (up to 52 vol%) in PVDF composite

fabricated using hot press method in general tend to increase the dielectric constant of the composites.

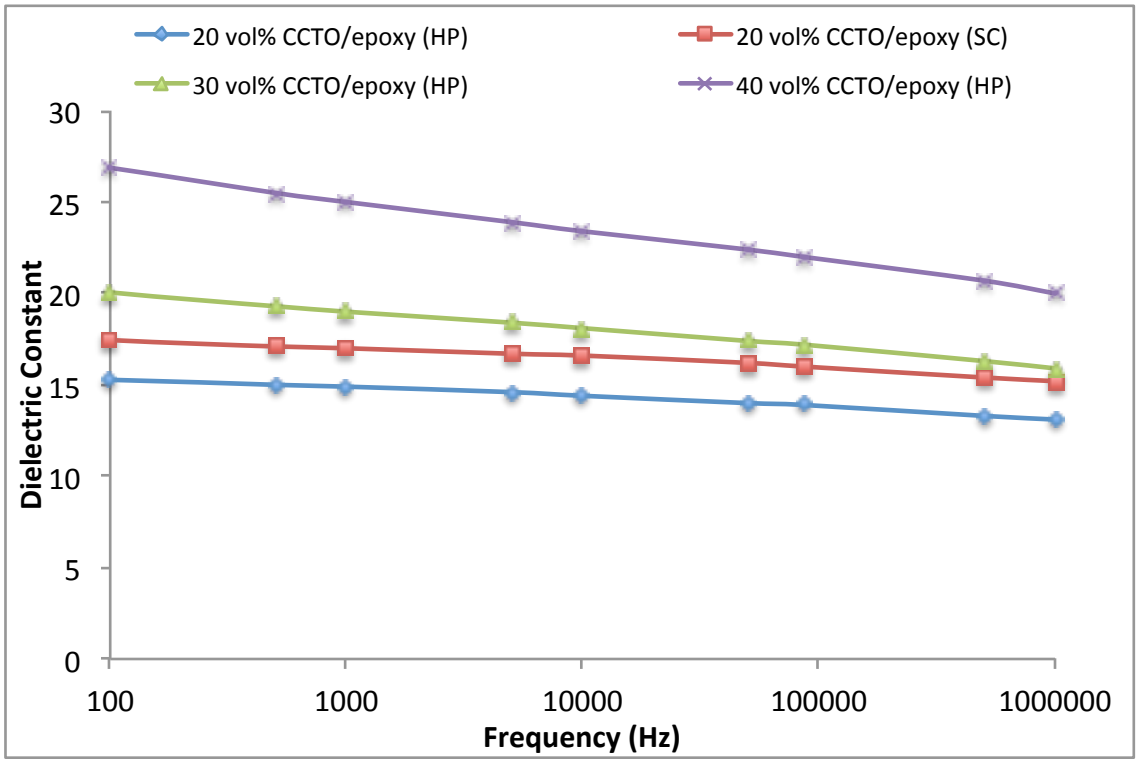

Figure 4.16: Dielectric constant of CCTO/epoxy thin film composites as a function of frequency using spin coating (SC) and hot press (HP) methods

The dielectric loss of CCTO/epoxy thin film composites fabricated using spin coating method and hot press method are shown in Figure 4.17. Low dielectric loss value is required for electronic packaging applications to minimize energy loss in the package (Chung, 1995). Sample with 20 vol% CCTO/epoxy (SC) exhibits the lowest dielectric loss (measured at 100 Hz) compared to 20 vol% CCTO/epoxy (HP), 30 vol% CCTO/epoxy (HP) and 40 vol% CCTO/epoxy (HP) with a value of 1.7×10^{-2}, 2.4×10^{-2}, 4.3×10^{-2} and 5.7×10^{-2}, respectively. However, it can be seen that the dielectric loss increased with increasing of CCTO filler in epoxy matrix. Moreover, there is a sudden drop of dielectric loss in the 100 Hz to ~ 1 kHz frequency range and

rapidly increases at high frequency (>10^6 Hz) for all composites due to dielectric relaxations. The same trend of increment in the dielectric loss was also observed with increasing of CCTO content in the epoxy matrix (Ramajo et al., 2007). Ibrhium et al. (2013) also indicated in their studies that the increase in dielectric loss of CCTO/epoxy composite at low frequency is due to increase in CCTO content and at high frequency is believed to be related to the relaxation process in the polymer matrix.

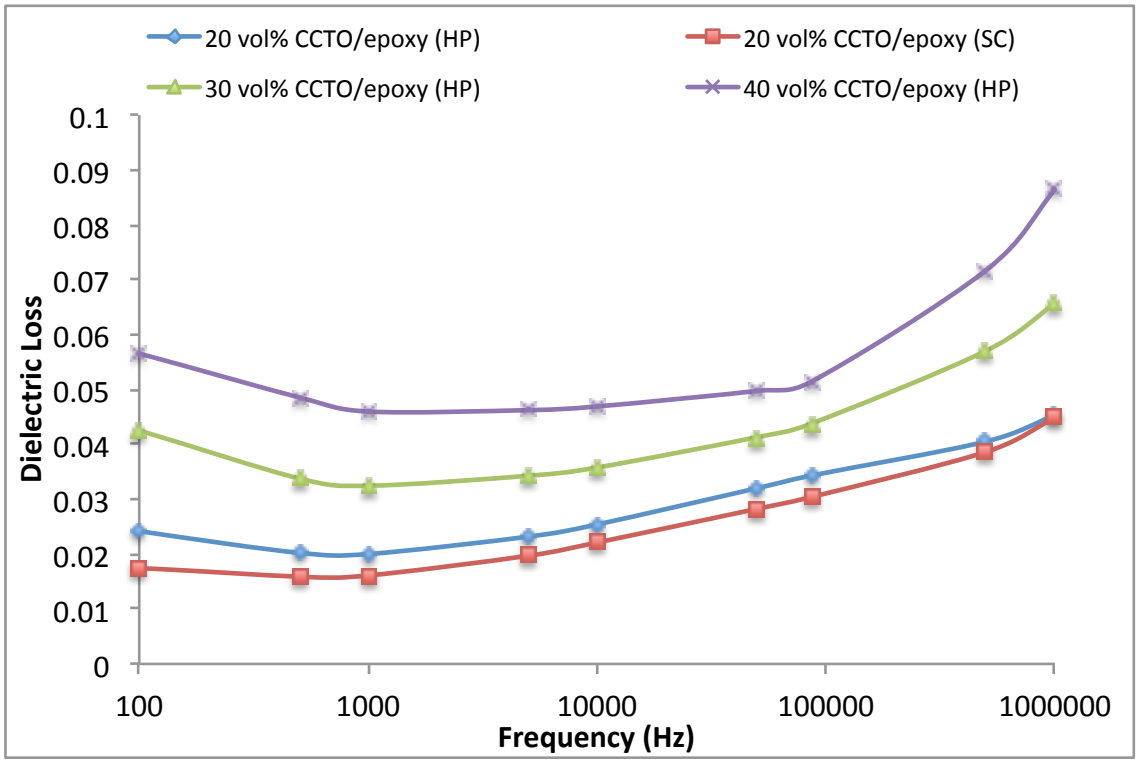

Figure 4.17: Dielectric loss of CCTO/epoxy thin film composites as a function of frequency using spin coating (SC) and hot press (HP) methods

Figure 4.18 (a – h) presents the fracture surfaces of the CCTO/epoxy thin film composites produced at different fabrication methods; spin coating (SC) method and hot press (HP) method. By comparing the fracture surface of 20 vol% CCTO/epoxy thin film composites at different fabrication methods, it can be seen

that the CCTO fillers are dispersed homogeneously and less clustering observed in the epoxy matrix for composite produced by spin coating method. Whereby for composite produced by hot press method, when the filler loading increases, slight agglomeration can be observed in the composites, i.e. 30 vol% and 40 vol% of fillers. The cavities or voids were seen in Figure 4.18 (c – h) due to lack of interaction between CCTO filler and epoxy matrix. Apparently, there is a tendency for the CCTO filler to be sedimented in epoxy matrix due to non-similarity in the density between CCTO filler and epoxy matrix. Nevertheless, as reported by Devaraju et al. (2005), slight non-uniformity of particle distribution would not affect the dielectric properties of the composite.

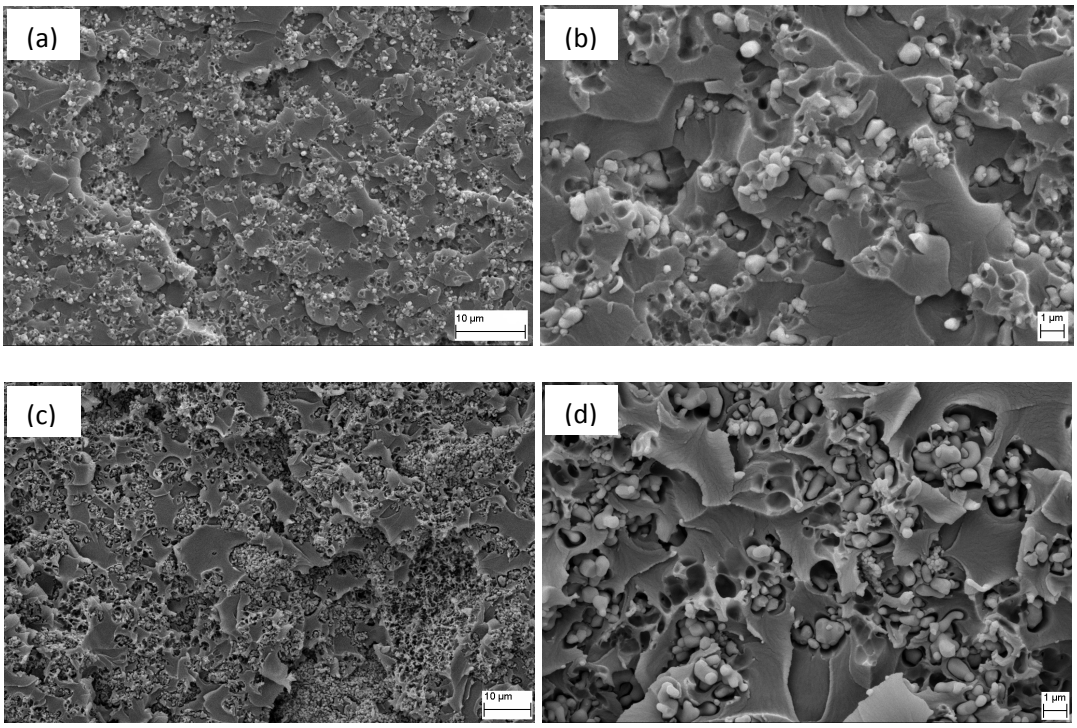

Figure 4.18: SEM micrograph of fracture surface of epoxy thin film composites (**a**, **b**) 20vol% CCTO/epoxy (SC), (**c**, **d**) 20vol% CCTO/epoxy (HP), (**e**, **f**) 30 vol% CCTO/epoxy (HP) (**g**, **h**) 40 vol% CCTO/epoxy (HP) [magnifications of 1000x was used for (**c**, **e**, **g**), 1500x for (**a**) and 5000x for (**b**, **d**, **f**, **h**)]

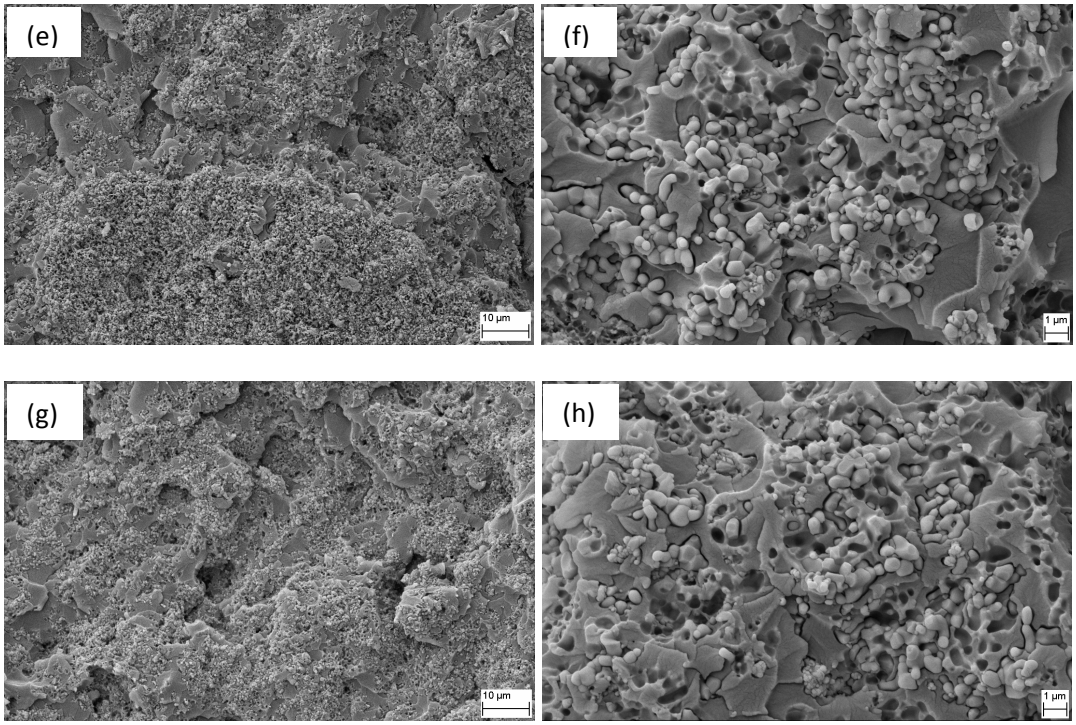

Figure 4.18: *Continued*

4.4.2 Thermal Stability

In order to examine the thermal stability, thermal analysis were carried out on CCTO/epoxy thin film composites produced using spin coating and hot press methods. The TGA curve obtained for the composites is illustrated in Figure 4.19. The detail information of thermal stability such as initial degradation temperature, $T_{5\%}$ (°C) and onset degradation temperature, T_{onset} (°C) are reported in Table 4.3.

The initial degradation temperature, $T_{5\%}$ and onset degradation temperature, T_{onset} have increased as the CCTO filler loading increased in epoxy matrix. By comparing 20 vol% CCTO/epoxy produced using spin coating and hot press methods, it can be seen that different fabrication methods did not significantly influence the thermal stability of the composites. Meanwhile for 40 vol% CCTO/epoxy (HP), it shows slightly higher $T_{5\%}$ and T_{onset} than other composites with

values of 362.5 °C and 363.3 °C, respectively. At higher filler loading, possibility of fillers to inhibit the segmental movement of epoxy are higher than that of low filler loading, hence slowing down the degradation process. This proved that composites produced at the same filler loading but using different fabrication methods do not influence the thermal stability of the composites. Based on experimental results, 40 vol% CCTO/epoxy (HP) promoted good thermal stability as compared to unfilled epoxy and other composites at low filler loading and produced by different fabrication methods.

Overall, the composites have better thermal stability since there is no weight loss up to 348 °C. The results obtained are parallel with work done by Thomas et al. (2013) in their study on PMMA/CCTO composite fabricated using hot press method where an increasing trend in the decomposition temperature is observed when the CCTO content is increased in the PMMA matrix.

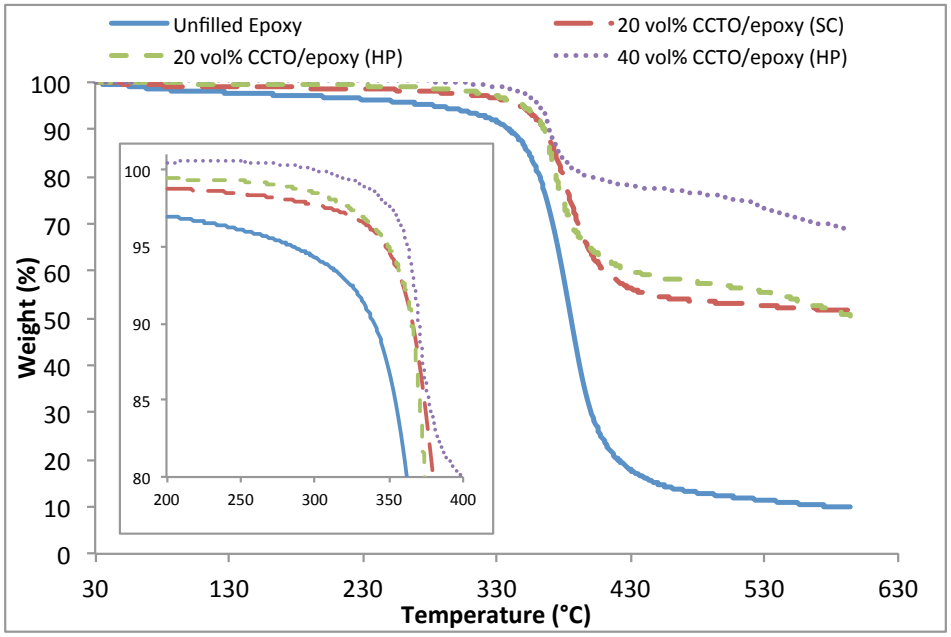

Figure 4.19: Comparison weight loss of unfilled epoxy and CCTO/epoxy thin film composites produced using different fabrication methods with respect to temperature, the inset is an enlargement of weight-temperature curve

Table 4.3: Decomposition temperature of unfilled epoxy and various filler loading on epoxy thin film composites produced using different fabrication methods

Fillers loading in epoxy thin film	Initial degradation temperature, $T_{5\%}$ (°C)	Onset degradation temperature, T_{onset} (°C)
Unfilled Epoxy	285	331
20 vol% CCTO/epoxy (SC)	335	348
20 vol% CCTO/epoxy (HP)	349.6	358.6
40 vol% CCTO/epoxy (HP)	362.5	363.3

4.4.3 Dynamic Mechanical and Thermal Mechanical Properties

Figures 4.20 and 4.21 show the temperature dependence of storage modulus (*E'*) and loss tangent (*tan δ*) for CCTO/epoxy thin film composites produced using different fabrication methods, respectively. Based on Figure 4.20, the storage modulus of the composite improved vastly with increasing of CCTO content in the epoxy matrix. Sample with 40 vol% CCTO/epoxy (HP) exhibits the highest storage modulus compared to those of unfilled epoxy and other composites with a value of 5882 MPa, as shown in Table 4.4. The improvement in storage modulus is attributed to the high stiffness and rigidity produced by CCTO particles. Meanwhile, 20 vol% CCTO/epoxy (SC) shows slightly higher storage modulus than that of 20 vol% CCTO/epoxy (HP) due to better filler distribution in epoxy system, as seen in Figure 4.18. This shows that the thin film fabrication method does not significantly influence the modulus of the composites.

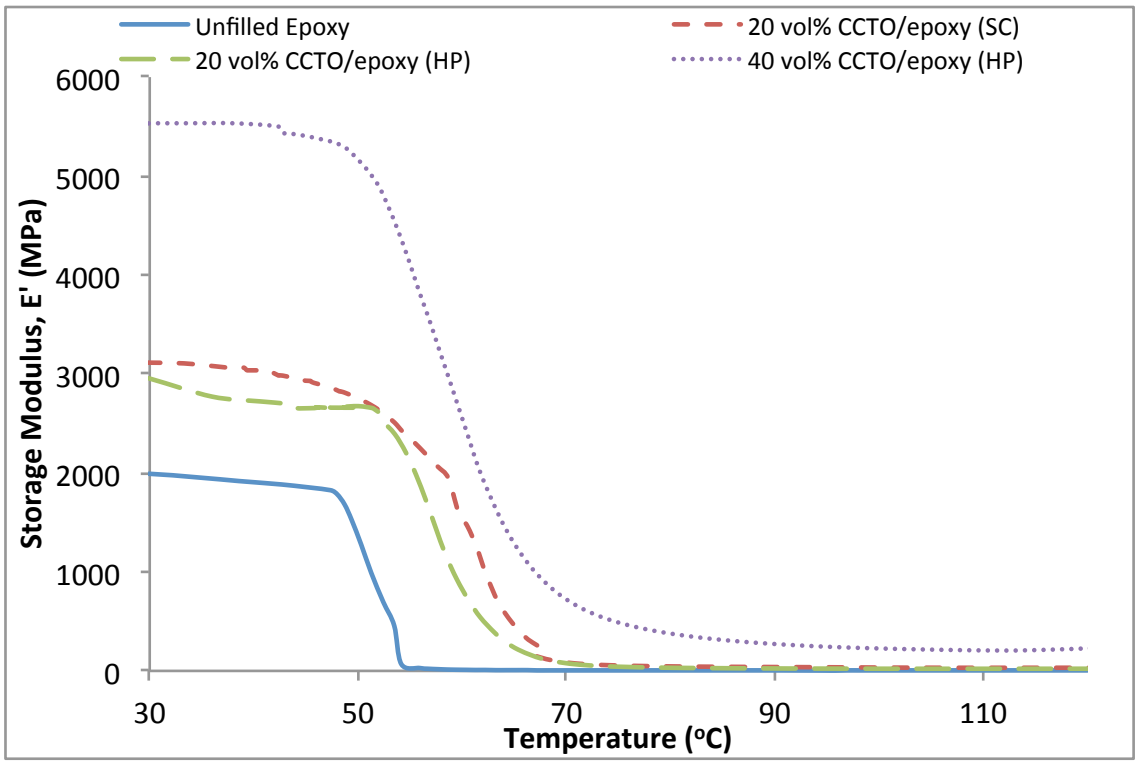

Figure 4.20: Storage Modulus (*E'*) spectrums recorded at 1 Hz for unfilled epoxy and CCTO/epoxy thin film composites produced using different fabrication methods

Glass transition temperature, T_g was measured at the maximum *tan* δ curve (Figure 4.21), which is related to the occuring molecular chain relaxation (Park et al., 2003). It was found that the T_g of composites at low filler loading were nearly constant with composite at high filler loading, as seen in Table 4.4. However, the T_g of 40 vol% CCTO/epoxy (HP) is slightly lower than other composites due to possibility of CCTO filler to agglomerate which then weaken the interfacial adhesion between CCTO filler and epoxy matrix yet higher than unfilled epoxy. According to Chisholm et al. (2004) and Suriati et al. (2012), the fillers agglomeration would significantly affect the Van der Waals interaction between polymer chains, hence reducing the cross-linking of epoxy matrix. A weak filler-to-matrix interaction could eventually increase the mobility of the polymer chain when subjected to load and this may lead to lower the T_g value of the composites.

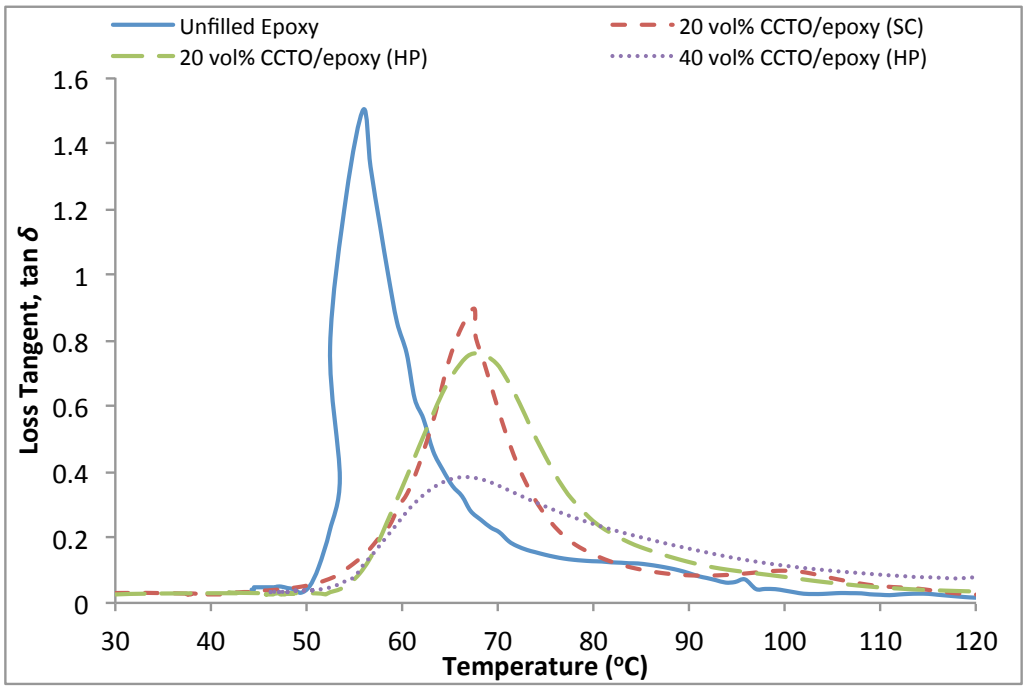

Figure 4.21: Loss tangent, *tan δ* spectrums recorded at 1 Hz for unfilled epoxy and CCTO/epoxy thin film composites produced using different fabrication methods

Table 4.4: Glass Transition Temperature, T_g and storage modulus, *E'* of unfilled epoxy and CCTO/epoxy thin film composites using different fabrication methods

Composite	**Glass Transition Temperature, T_g (°C)**	**Storage Modulus, *E'* at 30 °C (MPa)**	**Coefficient of Thermal Expansion, CTE (before T_g) (ppm/°C)**
Unfilled Epoxy	55.3	1888	143
20 vol% CCTO/epoxy (SC)	67.5	3223	112
20 vol% CCTO/epoxy (HP)	67.5	2957	147
40 vol% CCTO/epoxy (HP)	66.3	5882	35

Table 4.4 shows the CTE values of CCTO/epoxy thin film composites using different fabrication methods. Result shows that CTE before T_g was reduced with increasing filler loading. By comparing 20 vol% CCTO/epoxy produced using spin coating and hot press methods, it can be seen that composite produced using spin

coating method shows slightly lower CTE value than those of composites produced using hot press method due to better filler dispersion in epoxy matrix, as seen in Figure 4.18. Meanwhile, sample with 40 vol% CCTO/epoxy (HP) exhibits the lowest CTE value compared to other composites with a value of $35x10^{-6}$ ppm/°C. This can be explained where at high filler loading, more fillers with low CTE could significantly reduced the overall CTE value of the epoxy composite.

4.5 The Effect of Hybrid Fillers

The third objective of the present research is to study the effect of hybrid fillers on the dielectric and thermal properties of epoxy thin film composites. Investigation on the hybrid fillers were carried out due to significant effects produced by hybrid fillers composites which cannot be obtained from the single filler. Composites based on epoxy resin as matrix and 20 vol% of hybrid fillers (CCTO and $BaTiO_3$) as reinforcement were prepared with the ratio of hybrid fillers of CCTO: $BaTiO_3$ was varied from 30:70, 50:50 and, 70:30, respectively.

4.5.1 Dielectric Properties

Figure 4.22 illustrates the dielectric constant of 20 vol% CCTO/epoxy, 20 vol% $BaTiO_3$/epoxy and hybrid thin film composites according to the ratio of CCTO: $BaTiO_3$ at frequency of 100 Hz to 1 MHz. The additivity rule line represent the dielectric constant of the single filler; i.e. CCTO (at ratio 100:0) and $BaTiO_3$ (at ratio 0:100) filled epoxy thin film composites. Halimatudahliana et al. (2002) in their previous work have used this additivity rule line to show the positive and negative deviations of the polymer blend. It was observed that the dielectric constant of hybrid composites with the ratio of 30:70, 50:50 and 70:30 lie above the line, which

indicates the positive hybrid effect. The introduction of hybrid fillers in epoxy matrix show vastly improvement in the dielectric constant compared to single filler-epoxy thin film composites with a value of 19, 16.8 and 22.2 for Hybrid 30:70, Hybrid 50:50 and Hybrid 70:30, respectively. Hybrid 70:30 shows the highest dielectric constant amongst the hybrid composite systems, 20 vol% CCTO/epoxy and 20 vol% $BaTiO_3$/epoxy thin film composites with a value of 22.2.

Li et al. (2011) reported the same observations where the dielectric constant of hybrid $BaTiO_3$ and graphite nanosheet into polyvinylidene fluoride (PVDF) composite showed vastly improvement compared to $BaTiO_3$/PVDF composite. Besides that, the same trend of improvement in the dielectric constant of the hybrid composite was also observed in the addition of CCTO and Al powders into epoxy matrix, as reported in the article written by Prakash and Varma (2007).

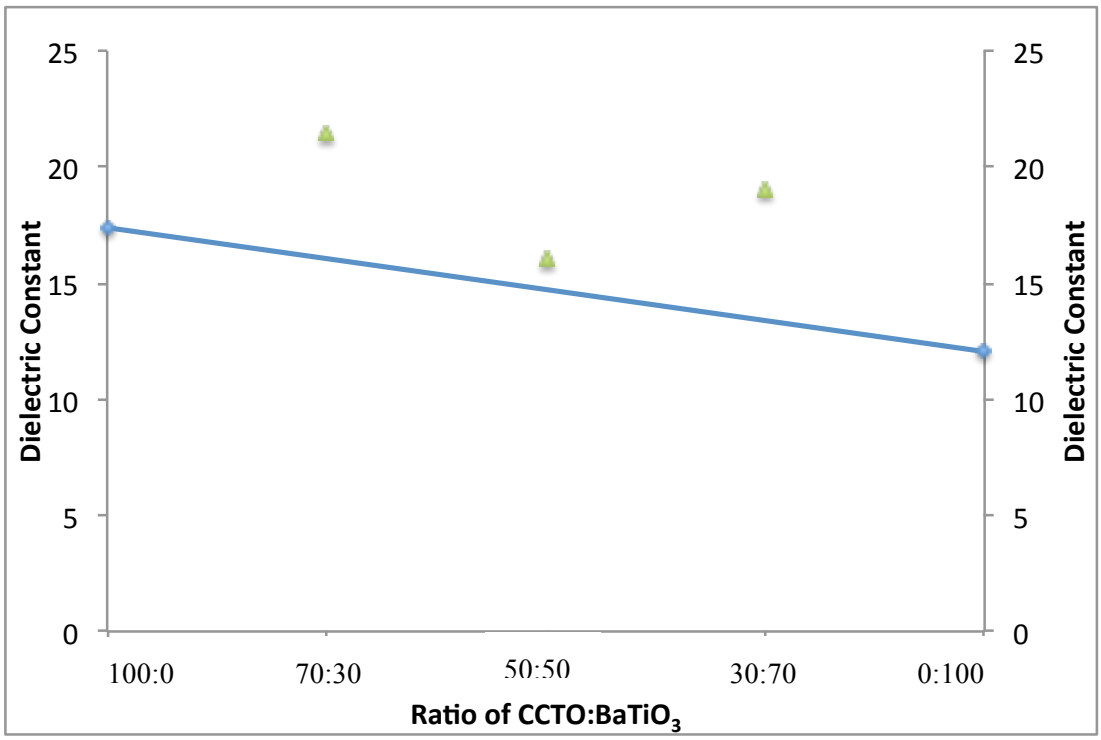

Figure 4.22: Dielectric constant of hybrid fillers and single filler filled epoxy thin film composites according to the ratio of CCTO:$BaTiO_3$ at frequency of 100 Hz

The dielectric loss of 20 vol% CCTO/epoxy, 20 vol% $BaTiO_3$/epoxy, and hybrid thin film composites is shown in Figure 4.23. It was found that Hybrid 50:50 with a value of $1.7x10^{-2}$ exhibits the lowest dielectric loss amongst the hybrid composite systems, 20 vol% CCTO/epoxy and 20 vol% $BaTiO_3$/epoxy. Nevertheless, all the composite systems still possessed dielectric loss less than 0.1.

It is interesting to note that based on Figure 4.22 and 4.23, it is apparent that positive hybrid effect exists in the dielectric constant and dielectric loss. Ioannou et al. (2011) also reported in their article that the hybrid-filler (containing micro size of ZnO and $BaTiO_3$ particles) filled epoxy composites showed higher dielectric constant compared to single-filler composites.

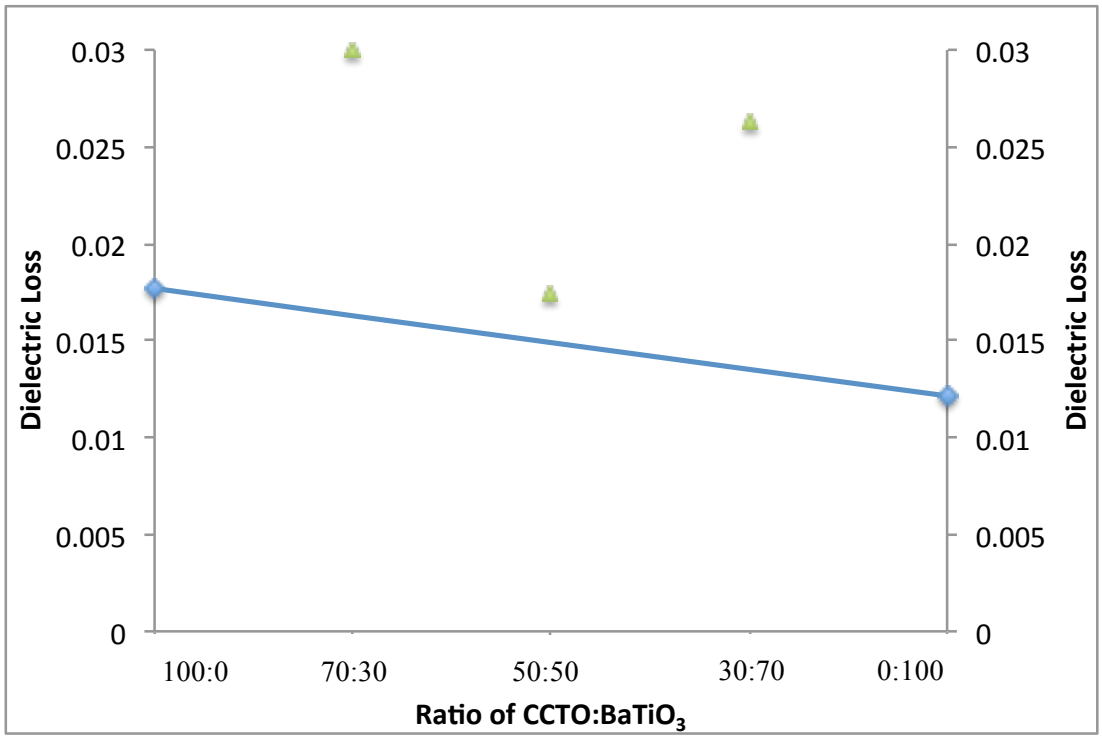

Figure 4.23: Dielectric loss of hybrid fillers and single filler filled epoxy thin film composites according to the ratio of CCTO:$BaTiO_3$ at frequency of 100 Hz

Figure 4.24 (a – j) shows SEM images of fractured surfaces of 20 vol% CCTO/epoxy, 20 vol% $BaTiO_3$/epoxy, and hybrid thin film composites. More voids (marked by circles) can be seen in the fracture surface of 20 vol% CCTO/epoxy and 20 vol% $BaTiO_3$/epoxy composites compared to those of hybrid composite. The voids are attributed to the fillers that have been pulled out when stress was applied. This is due to lack of interactions between CCTO and $BaTiO_3$ fillers with the epoxy matrix. Meanwhile Figure 4.24 (e – j) shows insignificant debonding and void at the particle-polymer matrix interphase. The fine dispersion of the hybrid fillers should be attributed to the possibility of $BaTiO_3$ fillers to fill the vacancies between CCTO fillers. As indicated in Section 4.2, $BaTiO_3$ fillers exhibit smaller particle sizes and lower span factor than that of CCTO fillers. This subsequently improved the dielectric and thermal properties of the hybrid composites.

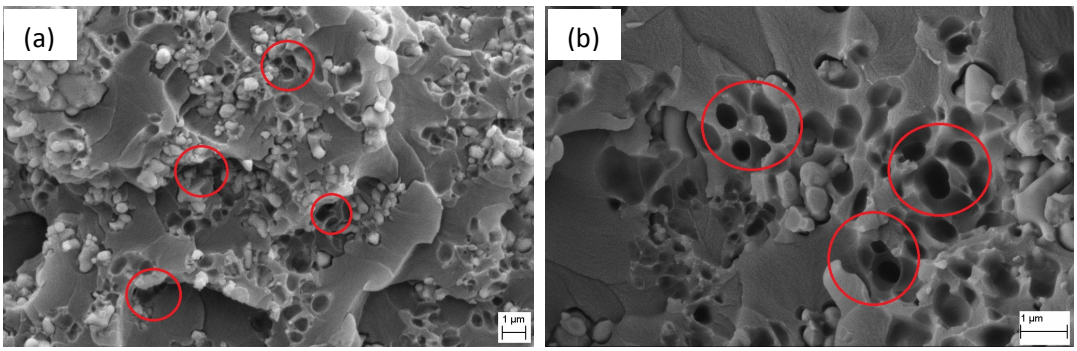

Figure 4.24: SEM micrograph of fracture surface of (**a**, **b**) 20 vol% CCTO/epoxy, (**c**, **d**) 20 vol% $BaTiO_3$/epoxy and hybrid fillers filled epoxy thin film composites according to the ratio of CCTO : $BaTiO_3$; (**e**, **f**) 30:70 ratio, (**g**, **h**) 50:50 ratio, and (**i**, **j**) 70:30 ratio [magnifications of 5000x was used for (**a**, **c**, **e**, **g, i**), and 10000x for (**b**, **d**, **f**, **h, j**)]

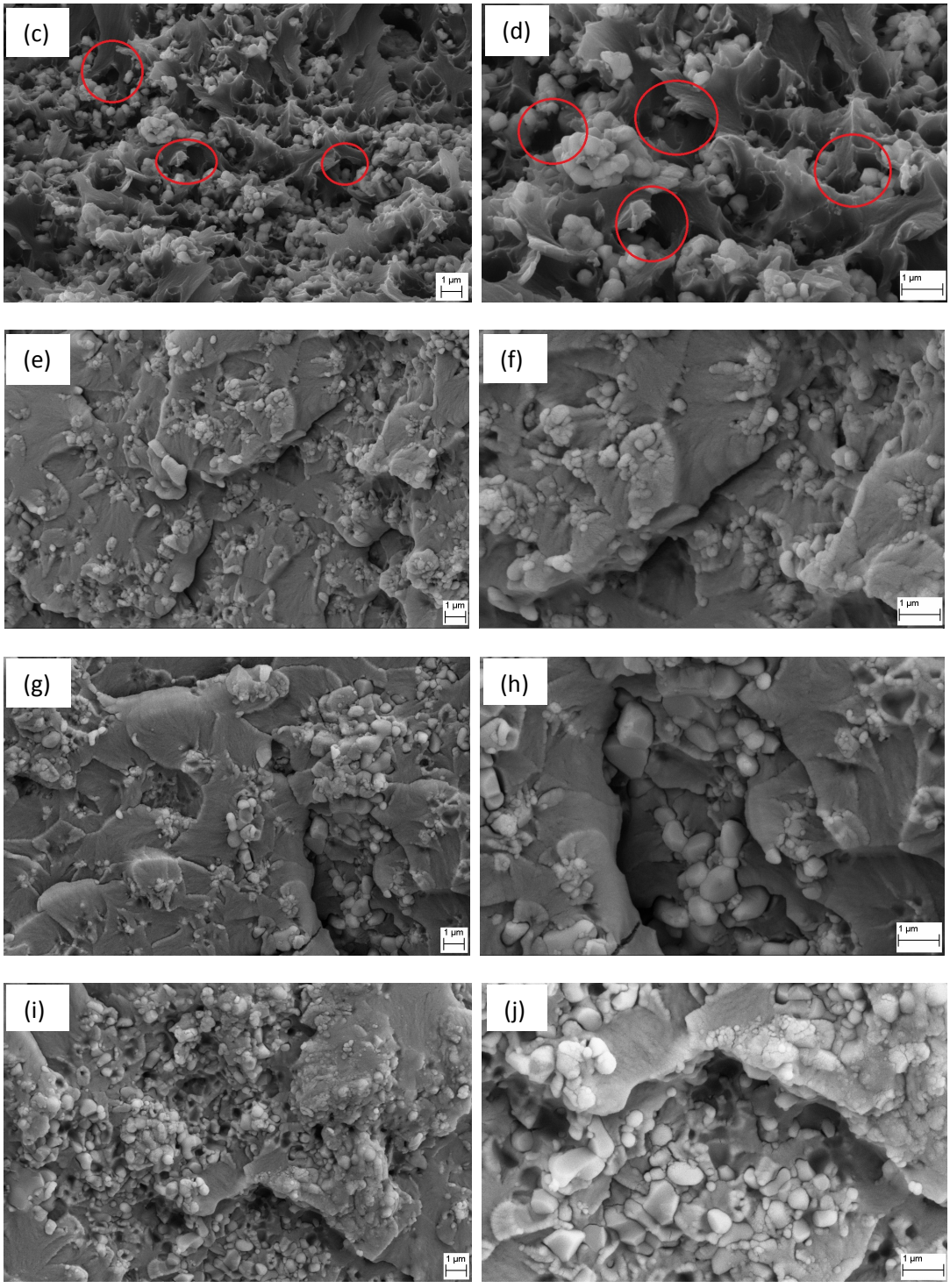

Figure 4.24: *Continued*

4.5.2 Thermal Stability

Table 4.5 and Figure 4.25 represent the TGA curve and thermal analysis data of single filler composites (20 vol% CCTO/epoxy and 20 vol% $BaTiO_3$/epoxy) and hybrid filler (20 vol%) at ratio of 70:30 thin film composites. In general (refering to $T_{5\%}$ and T_{onset}), hybrid 70:30 composite did not differ much compared to 20 vol% CCTO/epoxy and 20 vol% $BaTiO_3$/epoxy composites. Slightly similar thermal stability might be due to same amount of fillers being used in the epoxy composites.

It is apparent that all composite systems are thermally stable up to 330 °C which indicates the suitability of these materials to be used in electronic applications. The result is in parallel with work done by Oleksy et al. (2014) where it was reported that the thermal stability of epoxy resin composite improved with the addition of functional hybrid fillers. This indicates the composite is suitable to be used for higher temperature application.

Table 4.5: Decomposition temperature of CCTO/epoxy, $BaTiO_3$/epoxy, and hybrid thin film composites

Fillers loading on epoxy thin film	**Initial degradation temperature, $T_{5\%}$ (°C)**	**Onset degradation temperature, T_{onset} (°C)**
20 vol% CCTO/epoxy	348	361.7
20 vol% $BaTiO_3$/epoxy	351.4	356.7
Hybrid 70:30	332.2	340

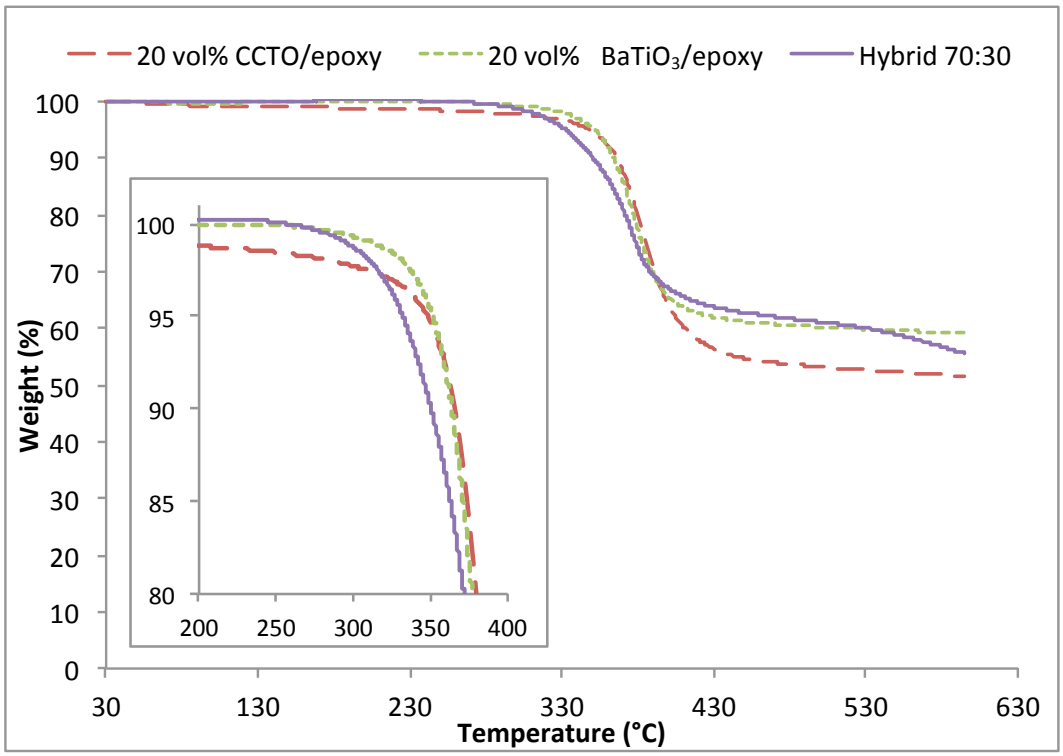

Figure 4.25: Comparison weight loss of CCTO/epoxy, $BaTiO_3$/epoxy, and hybrid thin film composites with respect to temperature, the inset is an enlargement of weight loss-temperature curve

4.5.3 Dynamic Mechanical and Thermal Mechanical Properties

The temperature dependence at the range of 30 to 130 °C of storage modulus (*E'*) and loss tangent (*tan δ*) for hybrid fillers filled epoxy thin film composites are shown in Figure 4.26 and 4.27. It was found that CCTO/epoxy composite and $BaTiO_3$/epoxy composite showed higher *E'* at the glassy region (30 °C) compared to that of hybrid composite, as in Table 4.6. It can be deduced that the incorporation of the single filler (CCTO and $BaTiO_3$) gives higher resistance towards any molecular movement in the epoxy composite, hence contributing to higher *E'*. This could possibly due to closed-packed structure between CCTO and $BaTiO_3$ in epoxy matrix as less voids can be seen which inhibit the movement of the polymer chains.

The *E'* for all composites decreased with increasing of temperature until stabilization can be achieved in the rubbery region. It is observed that the hybrid composite exhibits lower storage modulus compared to CCTO/epoxy composite and $BaTiO_3$/epoxy composite, but the *E'* of hybrid composite is still higher when compared to unfilled epoxy. This observation is in accordance with the previous work by Mandal and Alam (2011) where the storage modulus of the single fiber (glass fiber) reinforced unsaturated polyester (USP) composite is higher than the hybrid fibers (glass fibers and bamboo fibers) reinforced USP composite.

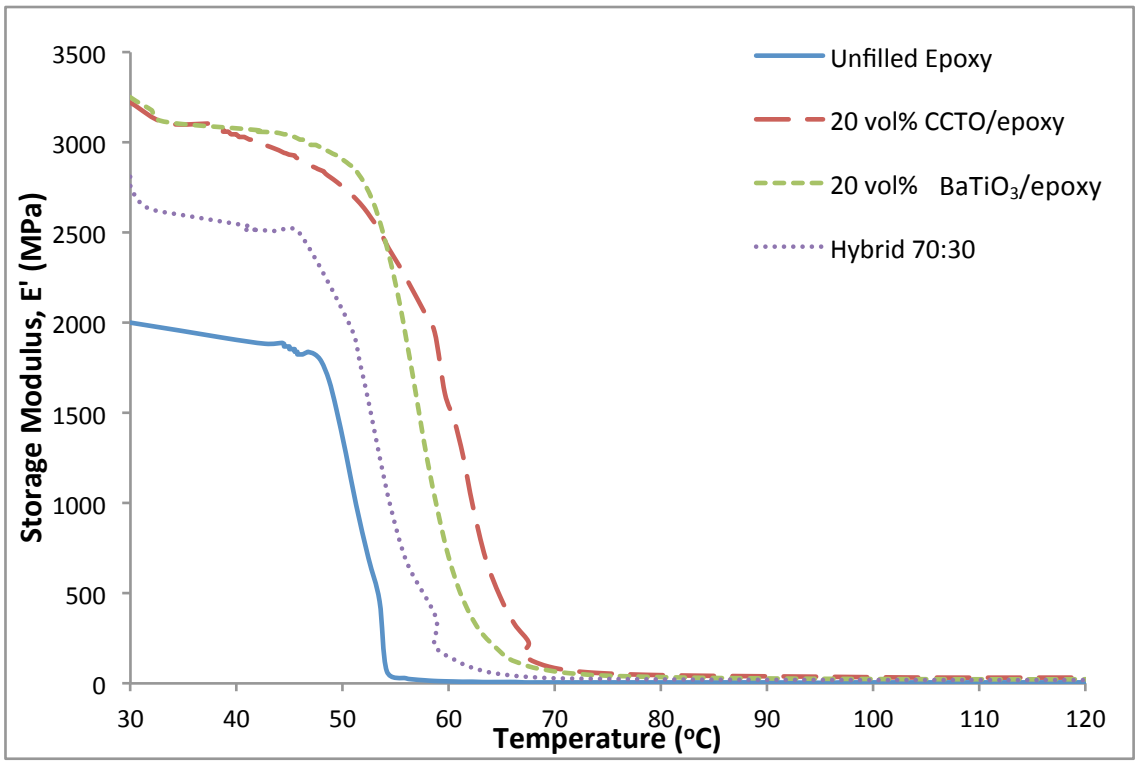

Figure 4.26: Storage Modulus, *E'* spectrums recorded at 1 Hz for unfilled epoxy, CCTO/epoxy, $BaTiO_3$/epoxy, and hybrid thin film composites

Figure 4.27 displayed the dumping spectrum (*tan δ*) of the single filler composite and hybrid filler composite. The glass transition temperature, T_g was derived from the peak of the *tan δ*. Expectedly, hybrid composite did not alter much on the T_g of the composites, with a variation of $\pm$ 3 °C. It was observed that the T_g of the hybrid composite is slightly similar with those of CCTO/epoxy composite and $BaTiO_3$/epoxy composite. This finding is in agreement with Nurdina (2010) findings where the T_g is governed by the amount of fillers that been loaded in the composites, slightly similar filler loading results in insignificant in T_g.

Table 4.6: Glass Transition Temperature, T_g and storage modulus, *E'* of CCTO/epoxy, $BaTiO_3$/epoxy, and hybrid thin film composites

Composite	**Glass Transition Temperature, T_g (°C)**	**Storage Modulus, *E'* at 30 °C (MPa)**	**Coefficient of Thermal Expansion, CTE (before T_g) (ppm/°C)**
20 vol% CCTO/epoxy	67.5	3223	112
20 vol% $BaTiO_3$/epoxy	64.8	3244	38
Hybrid 70:30	61	2956	16

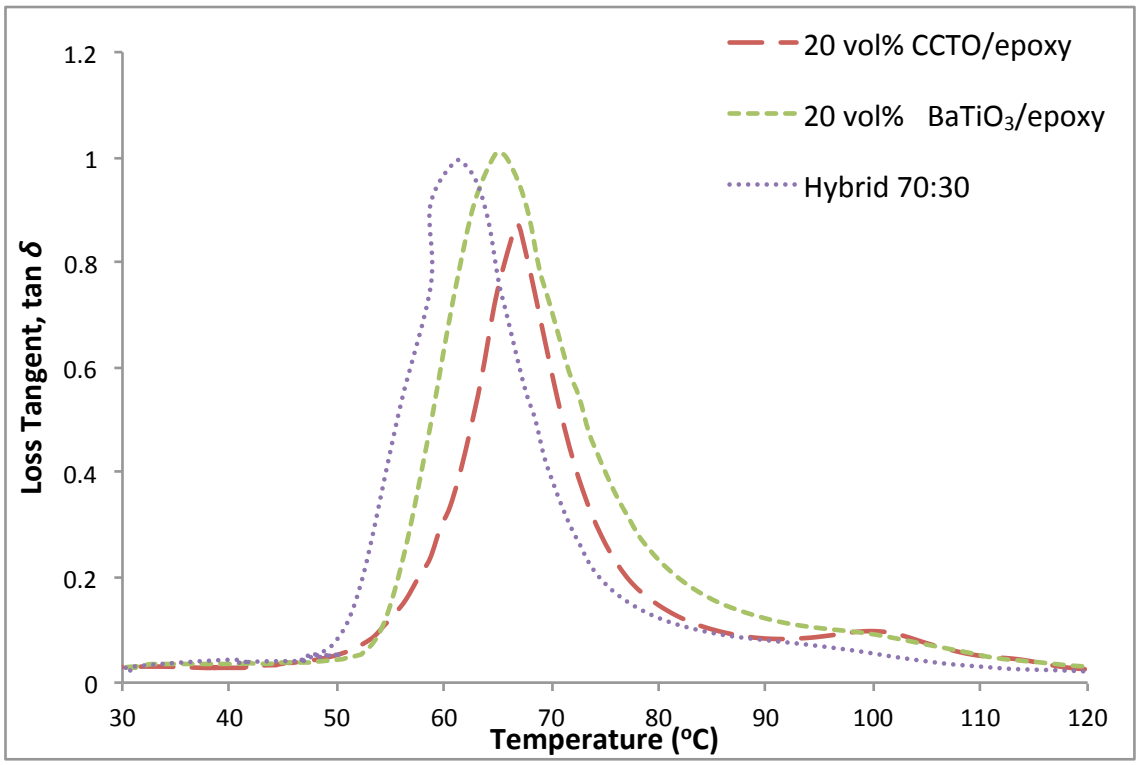

Figure 4.27: Loss Tangent, *tan δ* spectrums recorded at 1 Hz for CCTO/epoxy, $BaTiO_3$/epoxy, and hybrid thin film composites

Table 4.6 displayed the CTE of the single filler composite and hybrid filler composite. Hybrid 70:30 showed the lowest CTE, with a value of ~16 ppm/°C compared to CCTO/epoxy and $BaTiO_3$/epoxy composites. The combination of low intrinsic CTE of $BaTiO_3$ filler (9.8 ppm/°C) and CCTO filler (8.9 ppm/°C) is believed to be the main contributor to the low CTE of hybrid composite systems. It was also noticed that the hybrid composite showing better filler distribution in epoxy system compared to the single filler composite. This is due to the difference in particles size and span factor of both fillers. The smaller size of $BaTiO_3$ particles acted to improve the dispersion of the composites by filling the vacancies between CCTO filler and epoxy matrix.

4.6 The Effect of Silane Coupling Agent

In this study, the effect of silane coupling agent on the dielectric properties of CCTO/epoxy thin film composite were investigated. The silane-based coupling agent was introduced on the surface of CCTO filler in order to enhance the surface interaction between CCTO filler and epoxy matrix. The concentration of CCTO ceramic was fixed at 20 vol% because these fillers have displayed a reasonably good balance of dielectric and thermal properties, as discussed in Section 4.3. The concentration of silane coupling agent (GPTMS) was varied at 1%, 5% and 10%.

4.6.1 Elemental Analysis by Energy Dispersive Spectroscopy (EDS)

EDS analysis is carried out to investigate the presence of silicon (Si) element on the surface of CCTO particles after chemically treated by GPTMS silane coupling agent. The CCTO particles are believed to be coated with a thin layer of Si-based compound after the incorporation with silane-based coupling agent.

Figures 4.28 and 4.29 are the EDS spectrums obtained after analyzing untreated and treated systems, respectively. It is confirmed that the treated system using 10% of silane coupling agent shows the presence of Si element on the CCTO particles by the small peak at around 1.8 keV, as shown in Figure 4.29. The peak is detected at much lower concentration as compared to peak of Ca, Cu, Ti and O elements obtained from CCTO particles. It is reasonable due to lower concentration of GPTMS silane coupling agent being introduced into the surface of CCTO particles. The EDS analysis confirms the presence of Si-based compound on the surface of CCTO particles.

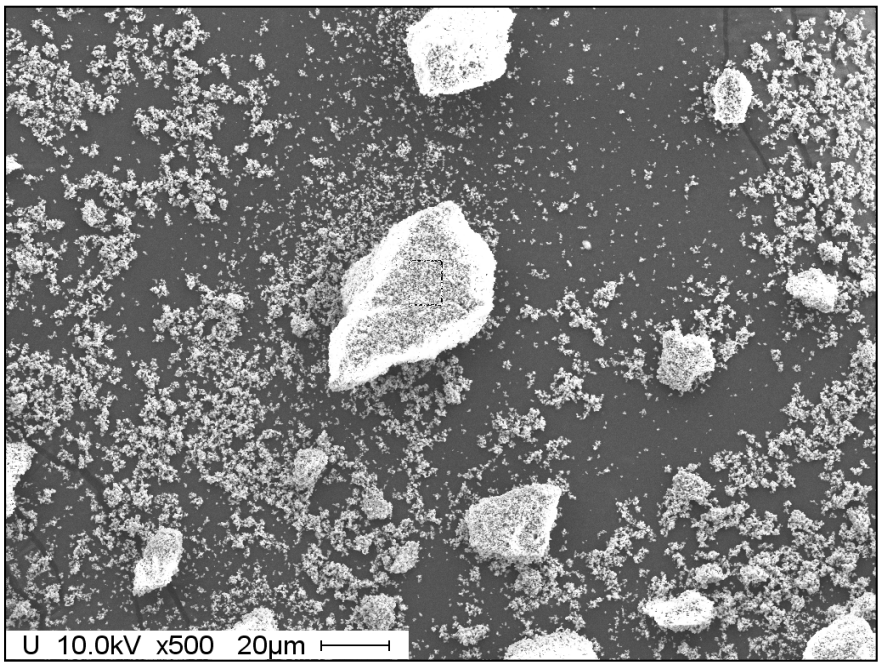

(a)

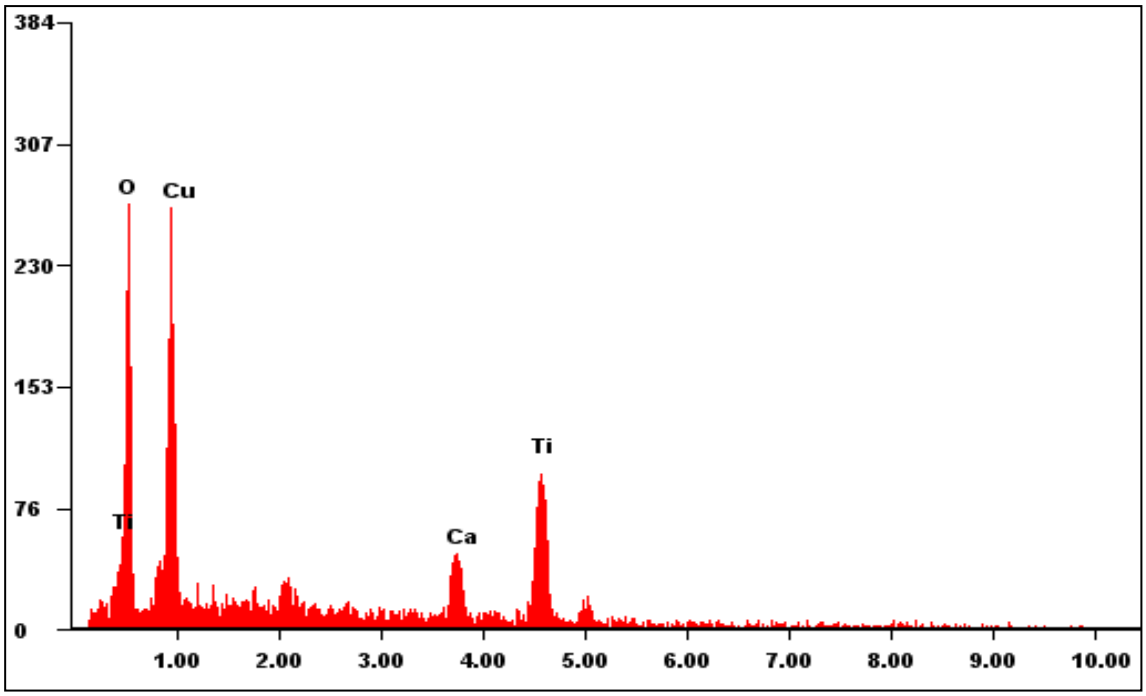

(b)

Figure 4.28: EDS analysis on untreated CCTO filler; (a) Spot taken for EDS analysis and (b) EDS spectrum shows the absence of Si element on the surface of CCTO particles

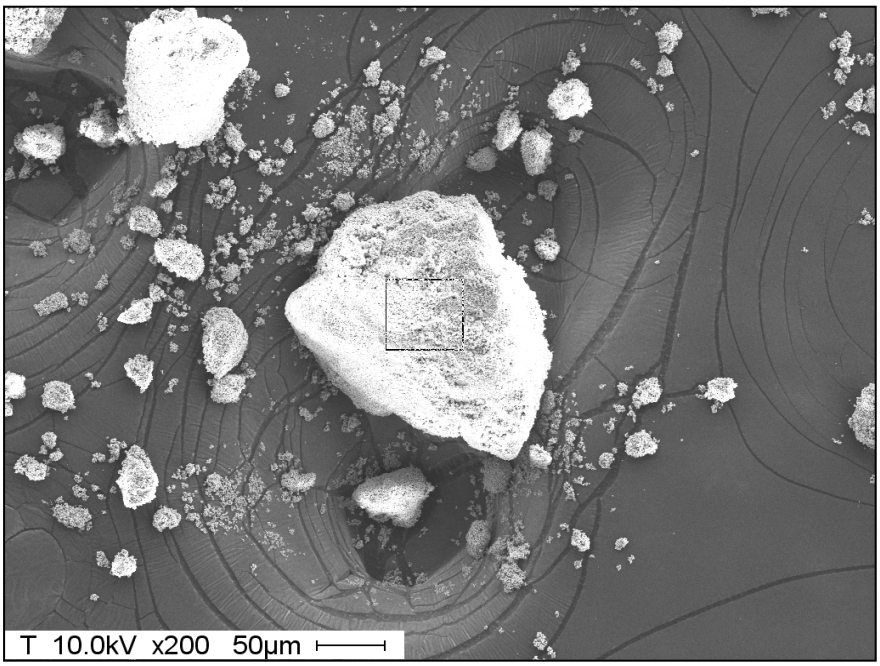

(a)

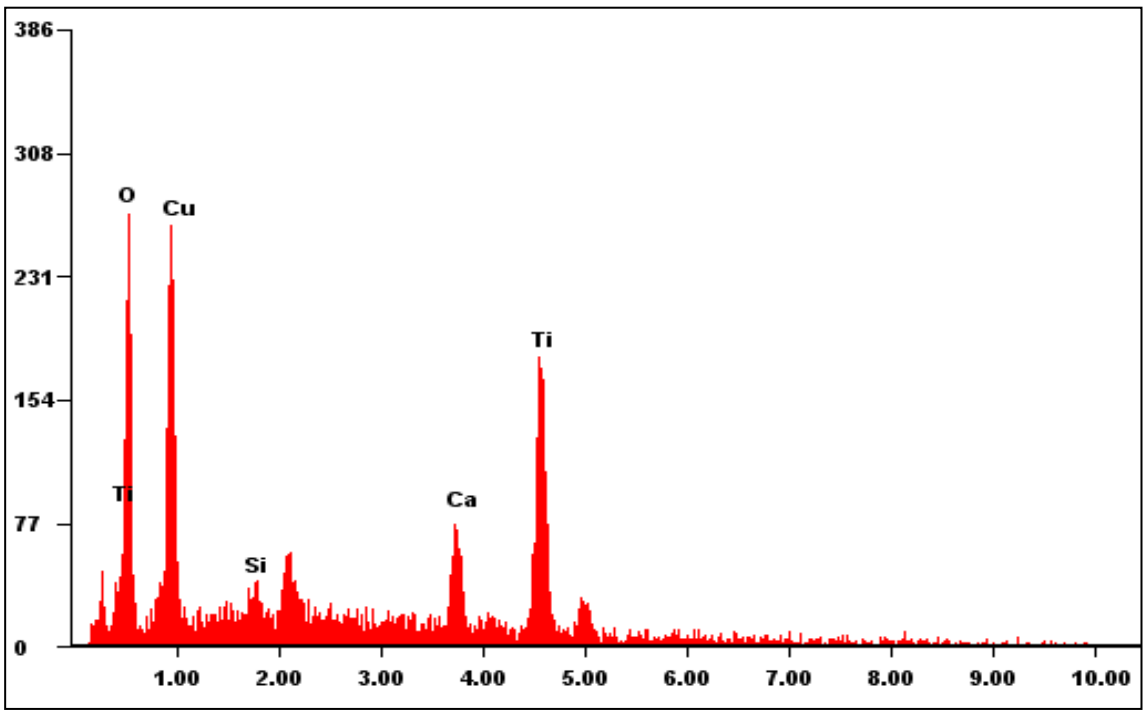

(b)

Figure 4.29: EDS analysis on treated CCTO filler; (a) Spot taken for EDS analysis and (b) EDS spectrum shows the presence of Si trace on the surface of CCTO particles

4.6.2 Fourier-Transform Infrared (FTIR) Analysis

Fourier transform infrared (FTIR) spectroscopy is useful for studying type of possible chemical bonding formed between ceramic filler and epoxy matrix. Analysis of the FTIR spectra of the composites enabled the identification of interactions before and after surface treatment of CCTO fillers.

Figure 4.30 presents the FTIR spectra of untreated and treated CCTO/epoxy thin film composites. In untreated system, the detection of characteristics absorption band at around 963, 1249 and 1301 cm^{-1} may be attributed to the epoxy group. The broad and medium peaks at 2910 – 2972 cm^{-1} are related to CH stretch in C-CH_3 compounds which could possibly due to several bands defects. The absorption bands indicating the presence of the hydroxyl hydrogen (O-H) and CH_3 deformation were observed at around 3428 and 1510 cm^{-1}, respectively. The appearance of a sharp and strong peak at 1184 cm^{-1} reveals the formation of C-N stretch bond which most probably contributed by the reaction between amine groups (N-H) from curing agent and C from epoxy matrix.

On the other hand, in the case of treated CCTO/epoxy thin film composite, the silane bonding which was indicated by absorption bands at around 2209 and 2000 cm^{-1} can be due to the interaction of siloxane with the amine type hardener. It is noteworthy that the appearance of peak 1106 and 1036 cm^{-1} can be referred to the formation of Si-O-C stretch bond in the treated system. The role of surface treatment of CCTO filler using silane-based coupling agent GPTMS is inferred to be success via the formation of chemically bonded silane coating on the surface of CCTO filler.

Based on the analysis (according to Figure 4.29 and Figure 4.30), the mechanism of silane-based coupling agent GPTMS during formation of interface between CCTO filler and epoxy matrix is illustrated in Figure 4.31. The chemical bonding of –C–O–Si–O–CCTO and –Si … O–C–C–C–C– might be formed between filler, silane compound and epoxy. It is noteworthy that these bondings can offer better adhesion between filler and matrix which then promote better filler to matrix interaction at higher volume fraction of resin.

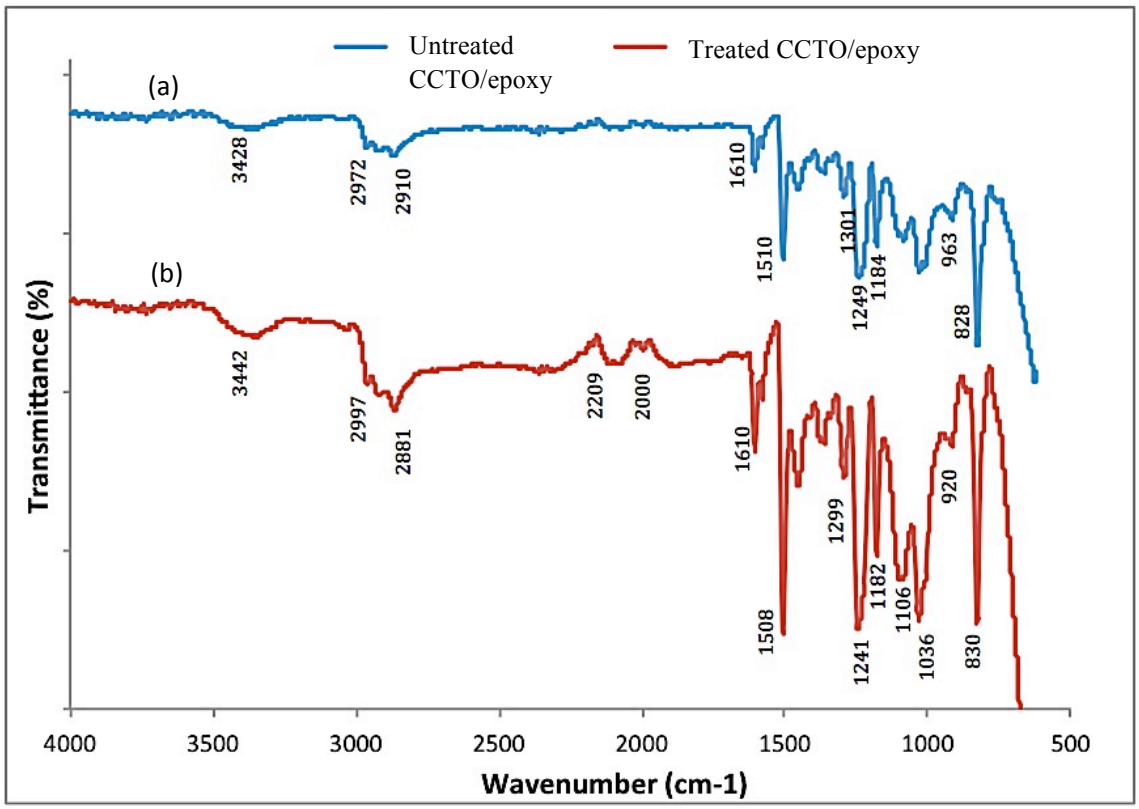

Figure 4.30: FTIR spectra of (a) untreated CCTO/epoxy and (b) treated CCTO/epoxy

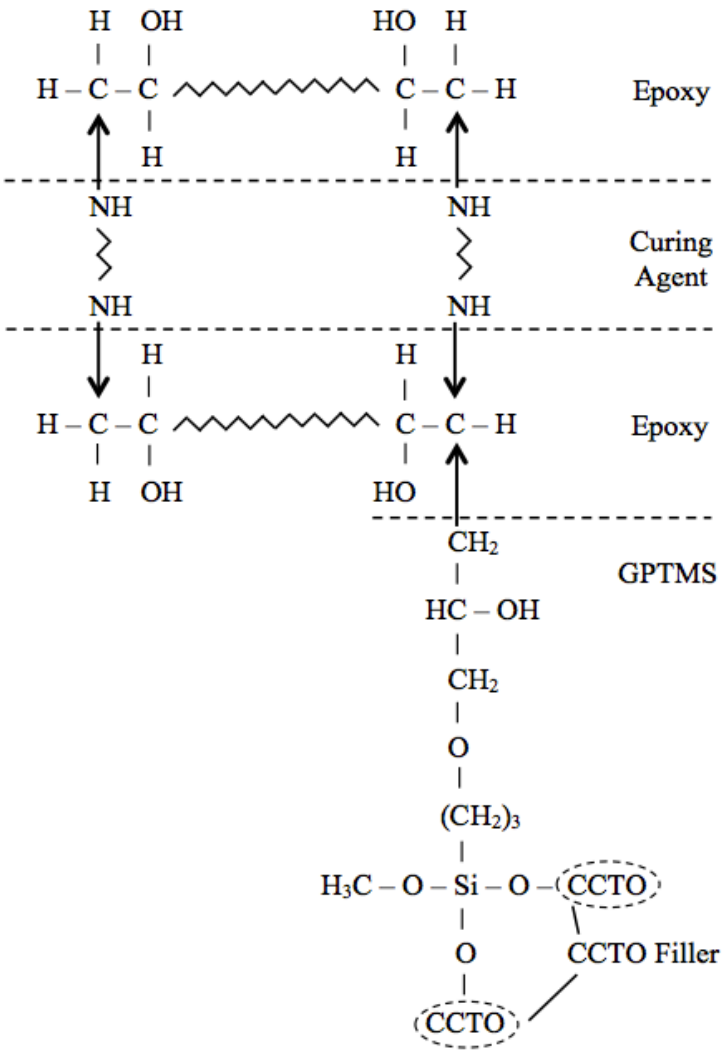

Figure 4.31: Schematic illustration of the action mechanism of silane coupling agent during the formation of interface between CCTO fillers and epoxy matrix

4.6.3 Dielectric Properties

Figure 4.32 illustrates the dielectric constant of the untreated and treated CCTO/epoxy thin film composites, the measurement is carried out at frequency of 100 Hz – 1 MHz. It can be seen that the dielectric constant of the composite increased evidently with increasing concentration of silane-based coupling agent GPTMS. The largest dielectric constant was 27.8, at 1 kHz when 10% of silane-based coupling agent GPTMS was used in treated CCTO/epoxy thin film composite.

If compared to the dielectric constant of the untreated CCTO/epoxy thin film composite, the dielectric constant of the treated CCTO/epoxy thin film composite at 10% of silane-based coupling agent increased by 60%.

According to Ramajo et al. (2007), the silane coupling agent act as molecular bridges between the ceramic filler and polymer matrix, resulting in the formation of covalent bonds across the interface, which improve significantly the dielectric properties. The increase in dielectric constant of the treated composite is attributed to the interfacial polarization of the chemical bonds formed between GPTMS and CCTO. This is in accordance with the previous work done by Yang et al. (2013) where the dielectric constant of treated CCTO/PVDF composite increased significantly after the addition of silane coupling agent on the surface of CCTO filler.

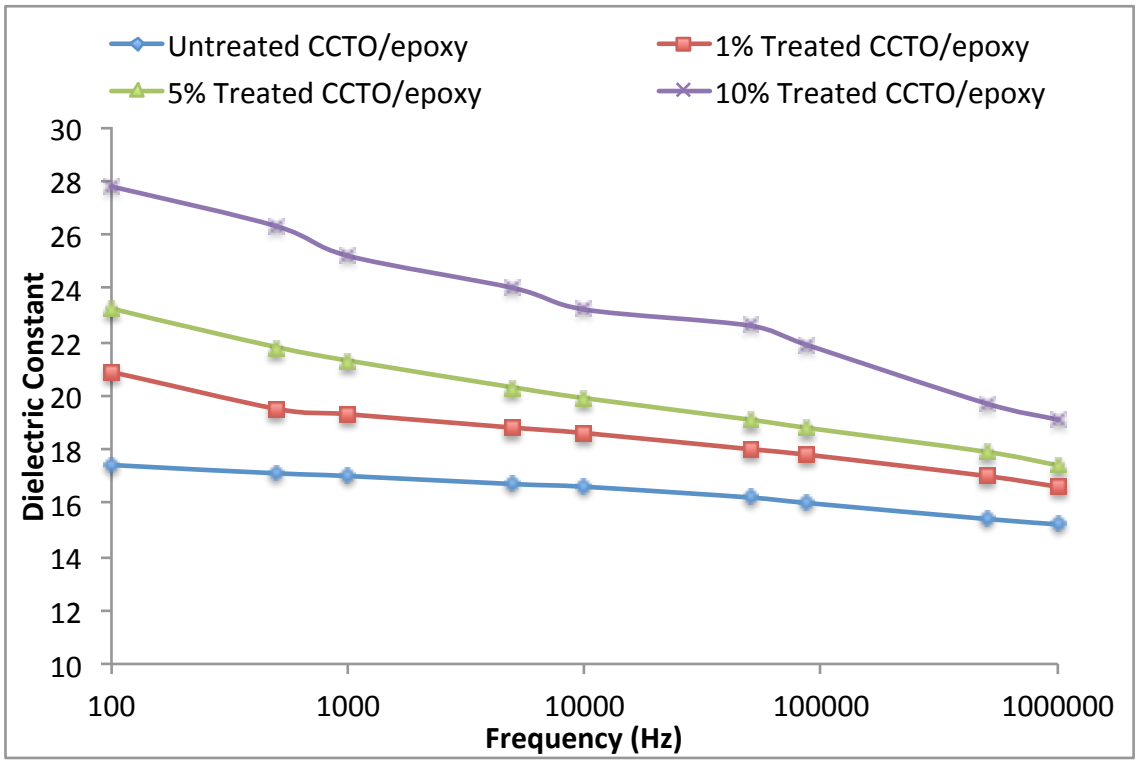

Figure 4.32: Dielectric constant of untreated and treated CCTO/epoxy thin film composites as a function of frequency

The dielectric loss of the untreated and treated CCTO/epoxy thin film composites is shown in Figure 4.33. It was observed that the dielectric loss of the composite increased gradually with increasing concentration of silane-based coupling agent GPTMS. If compared to the dielectric loss of the untreated CCTO/epoxy thin film composite ($1.8x10^{-2}$) which is measured at 100 Hz, the dielectric loss of the treated CCTO/epoxy thin film composite at 10% of silane-based coupling agent is about 4 times higher than the untreated CCTO/epoxy thin film composites, with a value of $9.8x10^{-2}$. This might be due to small amount of silane coupling agent that possibly caused an interfacial polarization loss occurred at bridging of GPTMS between the CCTO filler and epoxy matrix. The same finding was also reported by Yang et al. (2013) where the treated CCTO filled PVDF composite showed increment in the dielectric loss due to polarization effect.

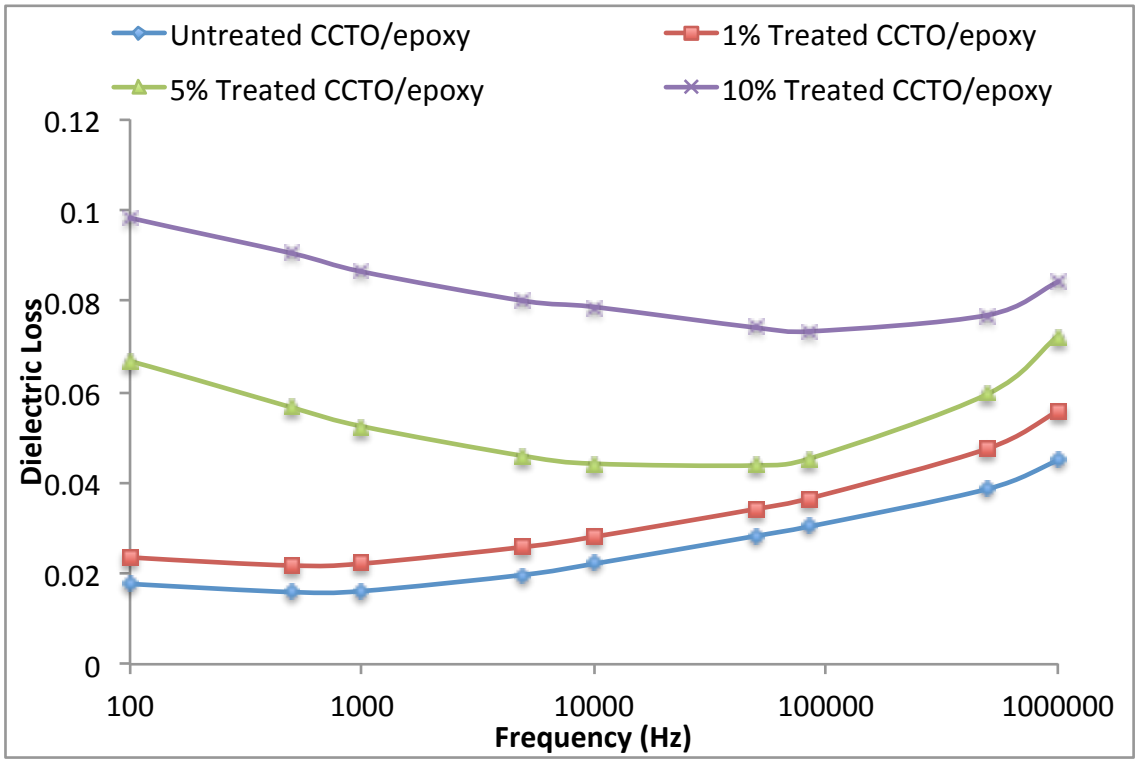

Figure 4.33: Dielectric loss of untreated and treated CCTO/epoxy thin film composites as a function of frequency

Figure 4.34 shows the SEM micrographs of treated 20 vol% CCTO/epoxy thin film composites at different concentration of silane coupling agent varied from 1%, 5% and 10%, respectively. The fractured surfaces of treated composites differ sharply compared to that of untreated composites (refer to Figure 4.9 (g) and (h)). It was observed that treated composites showed coarser fractured surfaces as compared to the untreated composites. This indicates a stronger adhesion and compatibility between CCTO fillers and epoxy matrix can be found in the treated composite which contributed to the vast improvement in dielectric properties. It was also observed that the treated surface CCTO fillers are embedded well in the epoxy matrix, one can observe the presence of large voids was reduced upon surface modification of the CCTO particles. Compared with the treated CCTO/epoxy thin film composite, the interfacial adhesion and filler distribution of the untreated CCTO/epoxy thin film composite are obviously poor and weak, as discussed in Section 4.3.2.

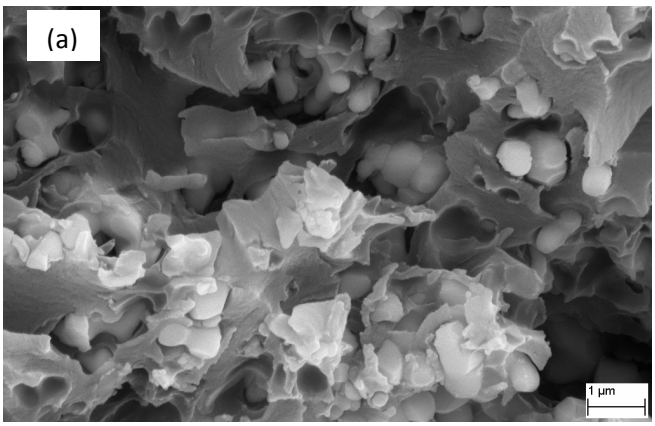

Figure 4.34: SEM micrograph of fracture surface of treated 20 vol% CCTO/epoxy thin film composites at different concentration of silane coupling agent (**a**) 1%, (**b**) 5% and (**c**) 10% [magnifications of 10000x]

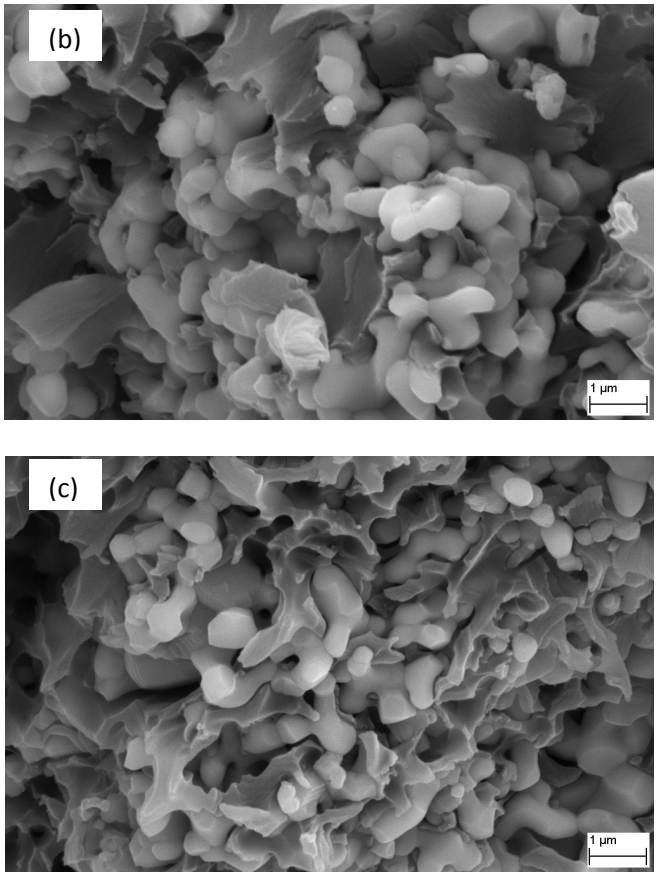

Figure 4.34: *Continued*

4.7 The Effect of Various Epoxy Resins

The final objective of the present research is to study the effect of various epoxy resins on the dielectric and thermal properties of treated CCTO/epoxy thin film composites. The properties of treated DER 332 epoxy thin film composite which has been discussed in Section 4.6 was compared with treated Epolam 2015 and OP 392 epoxy thin film composites. Epolam 2015 and OP 392 epoxies have been chosen due to its superior T_g compared to that of DER 332 epoxy. Epoxy resin with high T_g is required in electronic packaging applications. In this study, 10% Treated CCTO/epoxy was used for the comparison purpose due to the highest dielectric constant value, as mentioned in Section 4.6.3.

4.7.1 Dielectric Properties

Figure 4.35 illustrated the comparison of treated CCTO filled DER 332, Epolam 2015 and OP 392 epoxy thin film composites at frequency range of 100 Hz – 1 Mhz. The dielectric constant of treated CCTO filled DER 332, Epolam 2015 and OP 392 epoxy thin film composites are 27.8, 17.6 and 23.5, respectively. It is observed that the dielectric constant values for Epolam 2015 and OP 392 epoxy thin composites were not differed much with that of DER 332 epoxy thin film composite. This could possibly be attributed to the similar amount of CCTO filler used to fabricate DER 332, Epolam 2015 and OP 392 epoxy thin film composites. Therefore, similar amount of CCTO filler with various types of epoxy resins did not give significant effect on the dielectric constant of the composites.

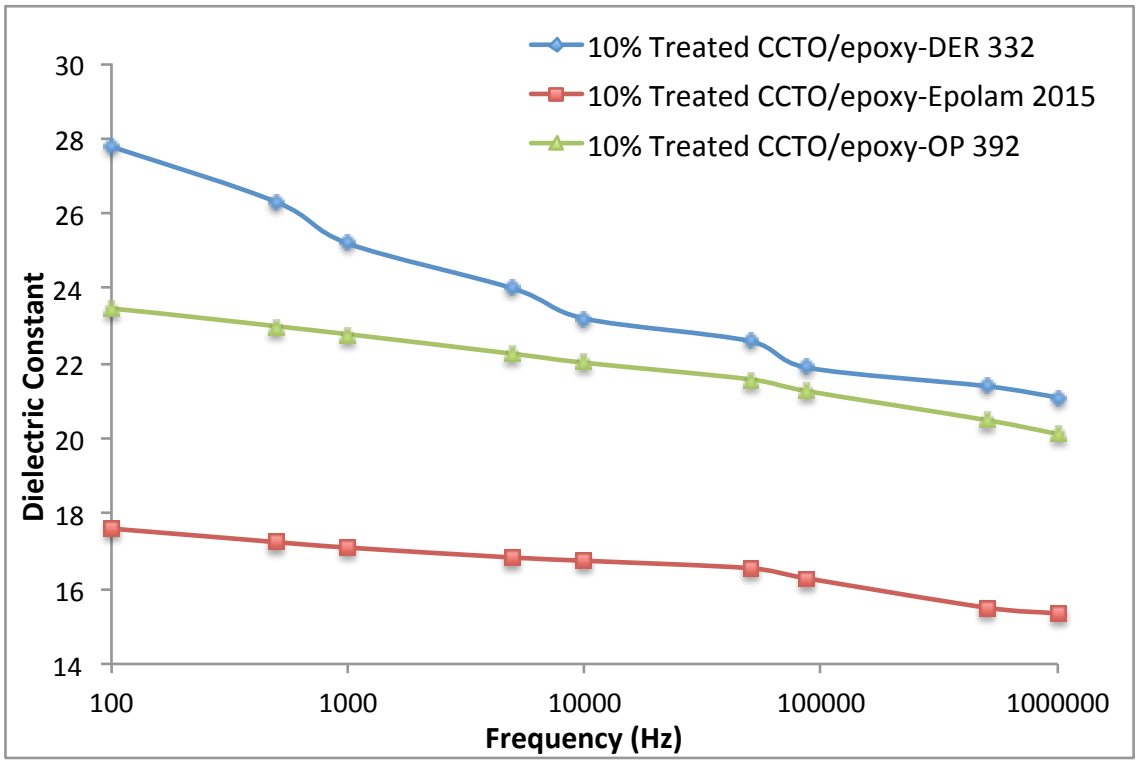

Figure 4.35: Dielectric constant of treated CCTO filled DER 332, Epolam 2015 and OP 392 epoxy thin film composites

The comparison of dielectric loss of treated CCTO filled DER 332, Epolam 2015 and OP 392 epoxy thin film composites is shown in Figure 4.36. It is observed that the dielectric loss of treated CCTO filled DER 332, Epolam 2015 and OP 392 epoxy thin film composites are $9.8x10^{-2}$, $2.1x10^{-2}$ and $2.1x10^{-2}$, respectively. The dielectric loss of Epolam 2015 and OP 392 epoxy thin film composites were slightly lower than DER 332 epoxy thin film composite. The low dielectric loss value is required for electronic packaging applications. Nevertheless, due to the similar amount of CCTO filler used to fabricate DER 332, Epolam 2015 and OP 392 epoxy thin film composites, the slight difference in dielectric loss values were observed.

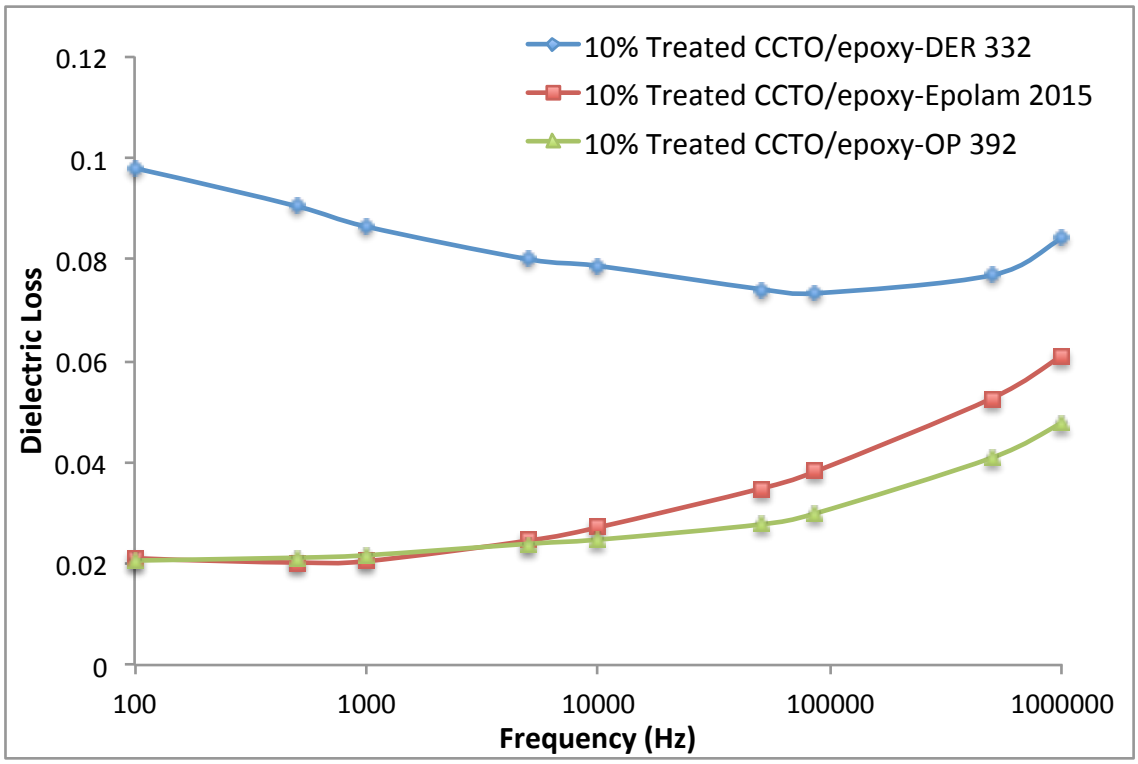

Figure 4.36: Dielectric loss of treated CCTO filled DER 332, Epolam 2015 and OP 392 epoxy thin film composites

SEM images of the fractured surface of treated CCTO/epoxy thin film composites using epoxy resins Epolam 2015 and OP 392 are shown in Figure 4.37. It was observed that the incorporation of treated CCTO in epoxy EPOLAM 2015 and OP 392 were similar with treated CCTO in epoxy DER 332 from Figure 4.34, as discussed in Section 4.6.3. Both types of epoxy resins show good interaction with treated CCTO and less voids can be seen in Figure 4.37 (a) and (c) due to better surface adhesion and compatibility between treated CCTO filler and epoxy matrix. According to Salmah et al. (2012), the improvement of surface adhesion between filler and matrix show decreased in the hydrophilicity of the fillers via surface treatment which then increased the compatibility of the fillers with the hydrophobic polylactic matrix.

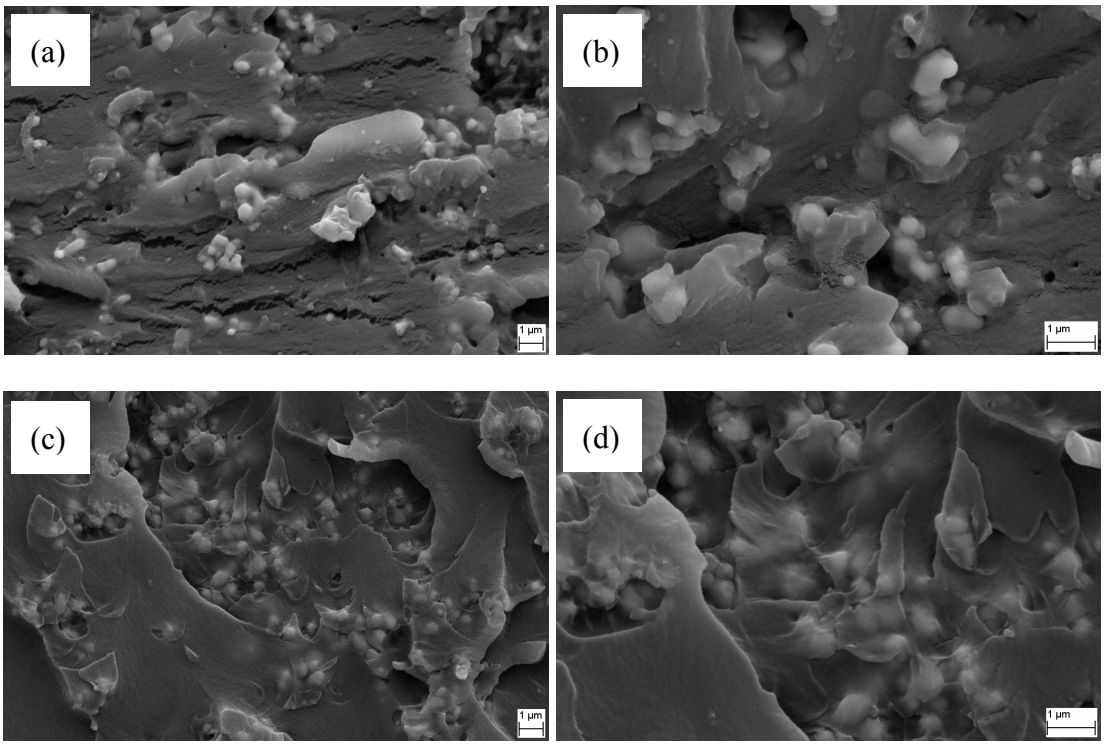

Figure 4.37: SEM micrograph of fracture surface of treated CCTO/epoxy thin film composites at different types of epoxy resins; (**a**, **b**) Epolam 2015, (**c**, **d**) OP 392 [magnifications of 5000x was used for (**a**, **c**) and 10000x for (**b**, **d**)]

4.7.2 Thermal Stability

Figure 4.38 and Table 4.7 present the TGA curve and thermal analysis data of treated CCTO filled DER 332-, Epolam 2015- and OP 392- epoxy thin film composites. It was found that degradation temperature of OP 392 epoxy thin composite was higher than DER 332 and Epolam 2015 epoxy thin film composites. From Table 4.7, $T_{5\%}$ of OP 392 epoxy thin film composite has increased 12% and 2% than the treated DER 332- and Epolam 2015- epoxy thin film composites. Meanwhile for T_{onset}, OP 392 epoxy thin film composite has increased 17% and 5% compared to those of DER 332- and Epolam 2015- epoxy thin film composites.

Besides that, the TGA curve of OP 392 epoxy composites tend to shift to right than that of DER 332- and Epolam 2015- epoxy thin film composites. This could be due to OP 392 epoxy has higher T_g compared to DER 332 and Epolam 2015, respectively. Epoxy with high T_g offers superior performance at high temperature.

According to Arends and Hudgin (1996), a thermoset resin with very high cross-link density such as OP 392 epoxy requires higher thermal energy to break the cross-link structure of the epoxy composite as the mobility of the polymer chain reduced. This proved that OP 392 epoxy thin film composite had better thermal stability compared to DER 332- and Epolam 2015- epoxy thin film composites.

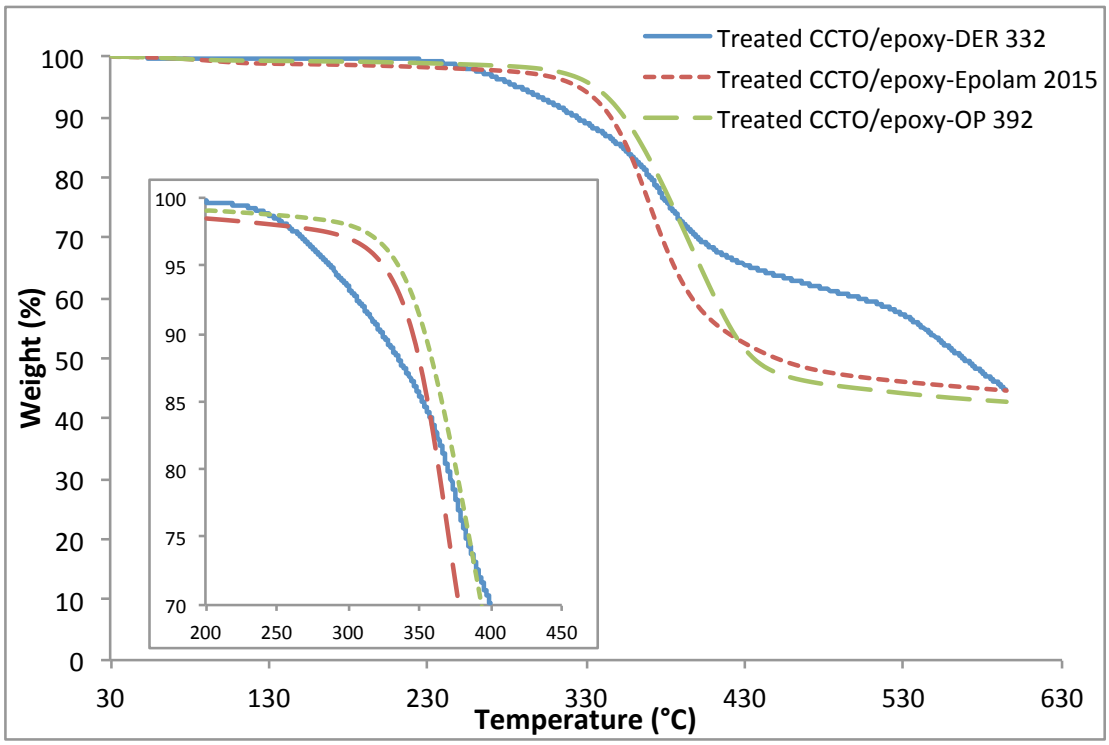

Figure 4.38: Comparison weight loss of treated CCTO/epoxy thin film composites using various epoxy resins with respect to temperature, the inset is an enlargement of weight loss-temperature curve

Table 4.7: Decomposition temperature of treated CCTO filled DER 332-, Epolam 2015- and OP 392- epoxy thin film composites

Fillers loading on epoxy thin film	**Initial degradation temperature, $T_{5\%}$ (°C)**	**Onset degradation temperature, T_{onset} (°C)**
Treated CCTO/epoxy-DER 332	287.1	311
Treated CCTO/epoxy-Epolam 2015	320	339.8
Treated CCTO/epoxy-OP 392	335	347.8

4.7.3 Dynamic Mechanical and Thermal Mechanical Properties

Figure 4.39 and 4.40 present storage modulus (*E'*) and loss tangent (*tan δ*) of treated CCTO/epoxy thin film composites fabricated using various epoxy resins, i.e. DER 332, EPOLAM 2015 and OP 392. As seen in Table 4.8, the storage modulus at 30 °C of treated CCTO/epoxy thin film composites using epoxy resins DER 332, EPOLAM 2015 and OP 392 are 2254 MPa, 1588 MPa and 773 MPa, respectively. Sample with treated OP 392 epoxy thin film composite shows the lowest storage modulus compared to DER 332 and EPOLAM 2015. In this point of view, this could possibly due to the crack that easily formed during operation as the sample of treated OP 392 epoxy thin film composite were too thin and brittle. The DMA test might be difficult to be handled and therefore, affects the storage modulus of OP 392 epoxy thin film composite (Prall, 2000).

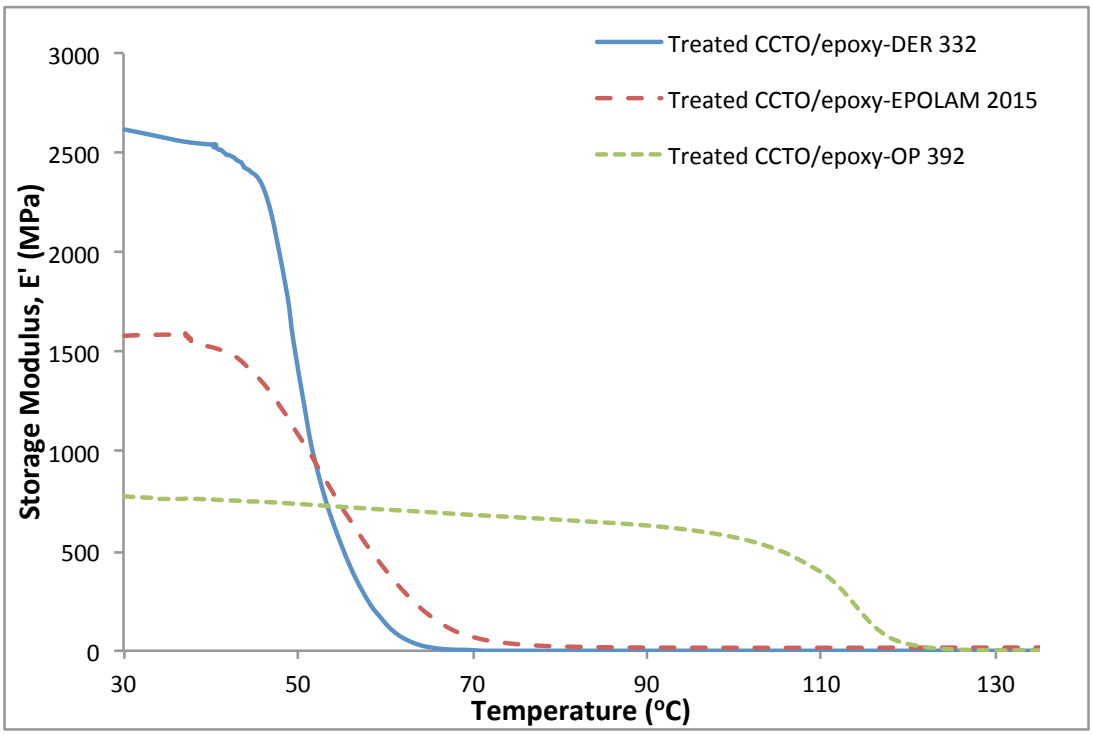

Figure 4.39: Storage Modulus, *E'* spectrums recorded at 1 Hz for treated CCTO/epoxy thin film composites at different types of epoxy resins

Table 4.8: Glass Transition Temperature, T_g and storage modulus, *E'* of treated CCTO/epoxy thin film composites using various epoxy resins

Composite	Glass Transition Temperature, T_g (°C)	Storage Modulus, *E'* at 30 °C (MPa)	Coefficient of Thermal Expansion, CTE before T_g (ppm/°C)
Treated CCTO/epoxy-DER 332	57.3	2254	15
Treated CCTO/epoxy-Epolam 2015	70.5	1588	25
Treated CCTO/epoxy-OP 392	117.7	773	20

Figure 4.40 shows the loss tangent, *tan* δ spectrums of treated CCTO/epoxy thin film composites produced using different types of epoxy resins. The glass transition temperature, T_g of epoxy thin film composites were obtained from the maximum curve of *tan* δ spectrums. From the figure, the T_g of treated DER 332-, EPOLAM 2015- and OP 392- epoxy thin film composites are 57.3 °C, 70.5 °C and 117.7 °C. OP 392 epoxy thin film composite exhibits the highest T_g compared to DER 332- and EPOLAM 2015- epoxy thin film composites.

According to Urbaniak (2011), this is because of the high crosslinked structure of OP 392 epoxy which inhibit the mobility of polymer chain and therefore, require higher temperature to soften the polymer chain from glassy state to rubbery state.

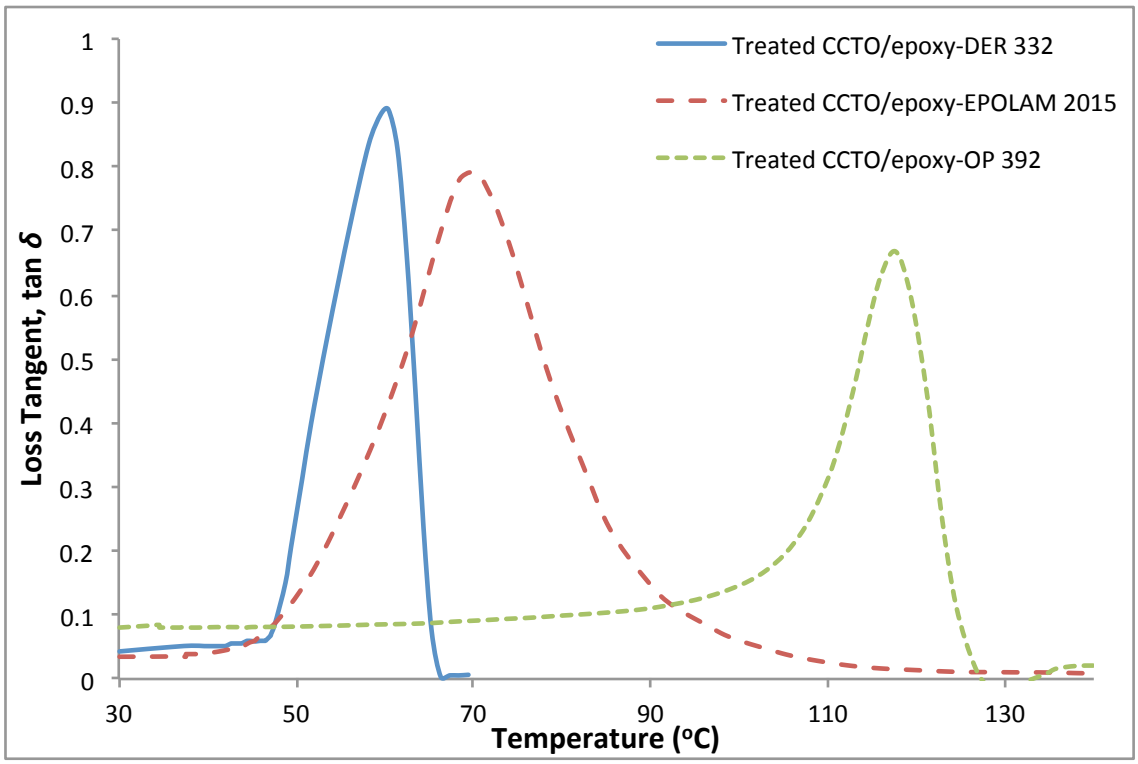

Figure 4.40: Loss Tangent, *tan δ* spectrums recorded at 1 Hz for treated CCTO/epoxy thin film composites at different types of epoxy resins

Table 4.8 presents the CTE values of treated DER 332-, Epolam 2015- and OP 392- epoxy thin film composites. The CTE value is obtained from the temperature below T_g due to polymers or composites lost most of their thermal properties above T_g. Result shows that CTE before T_g of treated DER 332-, Epolam 2015- and OP 392- epoxy thin film composites were nearly constant with a value of 15 ppm/°C, 25 ppm/°C and 20 ppm/°C, respectively. Therefore, similar amount of treated CCTO filler with various epoxy resins did not have significant effect on the CTE properties.

4.7.4 Comparison of Properties of the Commercial Dielectric Material and the Present Study

The comparison of selected properties between commercial dielectric material, i.e. 3M Embedded capacitance material with present study; i.e. treated CCTO/epoxy-DER 332, treated CCTO/epoxy-Epolam 2015 and treated CCTO/epoxy-OP 392, respectively are shown in Table 4.9. From the table, the dielectric materials used in the present study show higher dielectric constant, T_g and degradation temperature as compared to 3M Embedded capacitance material. Among these dielectric materials used in the present study, treated CCTO/epoxy-OP 392 exhibits good dielectric properties, excellent T_g and degradation temperature compared to those of treated DER 332- and Epolam 2015- epoxy thin film composites. However the dielectric loss of the present dielectric materials were slightly higher than commercial 3M embedded capacitance material but the dielectric loss values still lie in the acceptable limit which is less than 0.1. Besides that, the CTE values of the present study such as treated DER 332-, Epolam 2015- and OP 392- epoxy thin film composites were lower than the commercial 3M Embedded capacitance material. Low CTE value is required to minimize the CTE mismatch between components in the printed circuit board. Therefore, treated CCTO/epoxy thin film composite produced using OP 392 epoxy is suitable and can be consider to be used in order to fabricate dielectric materials for embedded capacitor application.

Table 4.9: Comparison properties of the commercial dielectric material (3M Embedded Capacitor) and the present study

	***Commercial**	**Experiment**		
	3M Embedded Capacitor	Treated CCTO/epoxy-DER 332	Treated CCTO/epoxy-Epolam 2015	Treated CCTO/epoxy-OP 392
Dielectric Materials	$BaTiO_3$/epoxy	CCTO/epoxy	CCTO/epoxy	CCTO/epoxy
Thickness	0.014 mm	0.0825 mm	0.13 mm	0.12 mm
Capacitance/ Unit Area (1 kHz)	1.0 nF/cm^2	0.3 nF/cm^2	0.2 nF/cm^2	0.1 nF/cm^2
Dielectric Constant (1 kHz)	16	27.8	23.5	17.6
Dielectric Loss (1 kHz)	0.005	0.098	0.021	0.021
Glass Transition Temp, T_g (°C)	115	57.3	70.5	117.7
CTE (ppm/°C) (below T_g)	32	15	25	20
Degradation Temperature (°C)	345	311	339.8	348

* Data based on the 3M Embedded capacitance material

CHAPTER 5

CONCLUSIONS & RECOMMENDATIONS

5.1 Conclusions

Based on the findings reported from the investigation done in the present research, the following conclusions can be summarized as follows:

1. $BaTiO_3$/epoxy thin film composite showed better tensile properties, thermal stability, *E'* and CTE compared to those of unfilled epoxy and CCTO/epoxy thin film composite. Meanwhile, sample with 20 vol% of CCTO/epoxy thin film composite showed the highest dielectric constant, T_g and thermal conductivity than unfilled epoxy and 20 vol% $BaTiO_3$/epoxy thin film composite with a value of 17.4, $1.7x10^{-2}$, 67.5 °C and $2.3x10^{-1}$, respectively. In short, 20 vol% CCTO/epoxy thin film composite is suitable to be used as dielectric materials than 20 vol% of $BaTiO_3$/epoxy thin film composite.

2. Sample with 20 vol% CCTO/epoxy composite fabricated using spin coating method showed slightly higher dielectric constant, $T_{5\%}$, T_{onset}, T_g and *E'* compared to 20 vol% CCTO/epoxy composite fabricated using hot press method. Nevertheless, 40 vol% CCTO/epoxy thin film composite showed increment vastly in dielectric constant, thermal stability, dynamic mechanical properties and thermal mechanical properties compared to other composites. In short, composite produced using spin coating method is suitable to be used to produce thin film for embedded capacitor.

3. Combination of CCTO and $BaTiO_3$ as hybrid fillers with the ratio of CCTO: $BaTiO_3$ was varied from 30:70, 50:50 and, 70:30 vastly improved the dielectric properties of the composite as compared to single filler composite. The highest dielectric constant and significantly lower dielectric loss at 100 Hz was observed in 70:30 ratio of CCTO : $BaTiO_3$ hybrid fillers. However, hybrid 70:30 thin film composite showed slightly lower thermal properties than single filler composite but did not differ much.

4. The dielectric constant of the treated CCTO/DER 332- epoxy composite at 10% of silane-based coupling agent increased by 60% to 27.8 compared to untreated CCTO/epoxy composite. Meanwhile, OP 392 epoxy thin film composite exhibits excellent thermal stability and T_g compared to those of DER 332- and Epolam 2015- epoxy thin film composites.

5. OP 392 epoxy thin film composite is suitable to be used as dielectric materials for embedded capacitor application due to its excellent T_g and thermal stability and also, good dielectric properties as compared to the commercial dielectric material, i.e. 3M Embedded capacitance material.

5.2 Recommendations for Future Research

Many efforts have been made in this research to fulfill the objectives of the study on epoxy thin film composites. However, there are still much more room for improvement to further understand the behavior of epoxy thin film composites. The following litst are the recommendation works to be done for the improvement in further studies:

1. Ceramic fillers such as CCTO and $BaTiO_3$ were mixed with epoxy resin and hardener by using ultrasonication technique. From the observation on the fracture surface of the composites by using SEM micrographs, it was found that the fillers were not well dispersed in the epoxy matrix. Therefore, other mixing techniques such as ball milling and mini twin-screw extruder could be possibly used to improve the filler distribution in the epoxy matrix. These techniques have been reported to produce more homogeneous composites.

2. Investigation on the different type of polymer matrices which offer higher dielectric properties and thermal properties could also carry out. This could be helpful in improving the dielectric and thermal properties of the composites.

3. The void content does play an essential role in controlling the dielectric, tensile and thermal properties of the resulting composites. Accordingly, this variable should be studied in the future work by considering several processing parameters such as duration of ultrasonic agitation and vacuum efficiency in air removal.

4. The properties of potential hybrid filler filled epoxy thin film composites should be further investigated. The hybrid filler could produce novel structure which if successfully incorporated into epoxy matrix could produce epoxy thin film composites with extraordinary properties compared to single filler composites.

5. The use nanosized CCTO and $BaTiO_3$ in either single filler or hybrid filler composite system should be considered as a part of the study, in order to compare the effect of these nanosized fillers on the properties of composites relative to micron-sized ceramic fillers.

REFERENCES

Ade, H., Winesett, D.A. & Smith, A.P. (1998). Bulk and Surface Characteriation of a Dewetting Thin Film Polymer Bilayer. *Applied Physics Letters*. Vol. 73, pp. 3775.

Adhami, R., Meenen, P.M.III. & Hite, D. (2007). Fundamentals Concepts in Electrical and Computer Engineering with Practical Design Problems, Second Edition. Universal Publishers. pp. 175.

Alam, M.A., Azarian, M.H., Osterman, M. & Pecht, M. (2011). Temperature and Voltage Aging Effects on Electrical Conduction Mechanism in Epoxy-$BaTiO_3$ Composite Dielectric Used in Embedded Capacitors. *Microelectronics Reliability*. Vol. 51, pp. 946-952.

Amaral, F., Rubinger, C.P.L., Henry, F., Costa, L.C., Valente, M.A. & Timmons, A.B. (2008). Dielectric Properties of Polystyrene–CCTO Composite. *Journal of Non-Crystalline Solids*. Vol. 354, pp. 5321- 5322.

Argawal, G., Patnaik, A. & Sharma, R.K. (2013). Parametric Optimisation of Three-Body Abrasive Wear Behavior of Long and Short Carbon Fibre Reinforced Epoxy Composites. *Tribology- Materials, Surfaces and Interfaces*. Vol. 7, pp. 150-160.

Arkles, B. (1977). Tailoring Surfaces with Silanes. Chemtech. Vol. 7, pp. 766-778.

Arends, C.B. & Hudgin, D.E. (1996). Polymer Toughening. Marcel Dekker, Inc., New York, N.Y. pp. 15.

Augustsson, C. (2004). NM Epoxy Handbook, Third Edition. Nils Malmgren AB. pp. 111.

Bai, Y., Cheng, Z.Y., Bharti, V., Xu, H.S. & Zhang, Q.M. (2000). High-Dielectric-Constant Ceramic-Powder Polymer Composites. *Applied Physics Letters*. Vol. 76, pp. 3804–3806.

Benlahrache, M.T., Benhamla, N. & Achour, S. (2004). Dielectric Properties of $BaTiO_3$-$NaNbO_3$ Composites. *Journal of the European Ceramic Society*. Vol. 24, pp. 1493-1496.

Bhalerao, V. (2004). Process Development and Reliability Study for 01005 Components in a Lead-Free Assembly Environment. MSc Thesis. Mumbai University.

Bhatnagar, M.S. (1996). Epoxy Resins (Overview). The Polymeric Materials Encyclopedia. CRC Press, Inc.

Bhattacharya, S.K. & Tummala, R.R. (2000). Next Generation Integral Passives: Materials, Processes, and Integration of Resistors and Capacitors on PWB Substrates. *Journal of Materials Science: Materials in Electronics*. Vol. 11, pp. 253-268.

Bhattacharya, S.K. & Tummala, R.R. (2001). Integral Passives For Next Generation of Electronic Packaging: Application of Epoxy/Ceramic Nanocomposites As Integral Capacitors. *Microelectronics Journal*. Vol. 32, pp. 11-19.

Brinker, C.J. & Scherer, G.W. (1990). The Physics and Chemistry of Sol-gel Processing. Academic Press, Inc. pp. 788-789.

Callister, W. D. (2007). Materials Science and Engineering: An Introduction, Seventh Edition. John Wiley & Sons.

Campbell, F.C. (2010). Introduction to Composite Materials, Structural Composite Materials. ASM International. pp. 8

Carter, C.B. & Norton, M.G. (2013). Ceramic Materials: Science and Engineering, Second Edition. Springer. pp. 358.

Chao, F. & Liang, G.Z. (2009). Effects of Coupling Agent on the Preparation and Dielectric Properties of Novel Polymer-Ceramic Composites for Embedded Passive Applications. *Journal of Materials Science: Materials in Electronics*. Vol. 20, pp. 560-564.

Charles, J.H.K. (2005). Miniaturized Electronics. Johns Hopkins APL Technical Digest, Vol. 26, pp. 402.

Chisholm, N., Mahfuz, H., Rangari, V.K., Ashfaq, A. & Jeelani, S. (2004). Fabrication and Mechanical Characterization of Carbon/SiC-Epoxy Nanocomposites. *Composite Structures*. Vol. 67, pp. 115.124.

Cho, S.D., Lee, J.Y., Hyun, J.G. & Paik, K.W. (2004). Study on Epoxy/$BaTiO_3$ Composite Embedded Capacitor Films (ECFs) for Organic Substrate Applications. *Materials Science and Engineering B*. Vol. 110, pp. 233-239.

Choa, S.D., Lee, J.Y., Hyuna, J.G., Paik, K.W. (2004). Study on Epoxy/$BaTiO_3$ Composite Embedded Capacitor Films (ECFs) For Organic Substrate Applications. *Materials Science and Engineering B*. Vol. 110, pp. 233-239.

Choi, Y.K., Sugimoto, K., Song, S.M., Gotoh, Y., Ohkoshi, Y. & Endo, M. (2005). Mechanical and Physical Properties of Epoxy Composites Reinforced by Vapour Grown Carbon Nanofiber. *Carbon*. Vol. 43, pp. 2199-2208.

Chua, T.P., Mariatti, M., Azizan, A. & Rashid, A.A. (2010). Effects of Surface-Functionalized Multi-Walled Carbon Nanotubes on the Properties of Poly(Dimethyl Siloxane) Nanocomposites. *Composites Science and Technology*. Vol. 70, pp. 671-677.

Cozzolino, M.J., Ewell, G.J. (2002). Microelectronic Failure Analysis. ASM International. pp. 133-147.

Cui, B. (2011). Recent Advances in Nanofabrication Techniques and Applications. InTech. pp. 505-532.

Das, R.N., Egitto, F.D., Lauffer, J.M. & Markovich, V.R. (2008). Laser Micromachining of Barium Titanate ($BaTiO_3$)-Epoxy Nanocomposite-Based Flexible/Rollable Capacitors: New Approach for Making Library of Capacitors. *IEEE Transactions on Electronics Packaging Manufacturing*. Vol. 31, pp. 97-103.

Deschanvres, A., Raveau, B. & Tollemer, T. (1967). Substitution of Copper for a Bivalent Metal in Titanates of Perovskite Type. *Bulletin de la Société Chimique de France*. pp. 4077-4081.

Deshmukh, G.S, Peshwe, D.R., Pathak, S.U. & Ekhe, J.D. (2011). A Study on Effect of Mineral Additions on the Mechanical, Thermal and Structural Properties of Poly (Butylene Terephthalate) (PBT) Composites. *Journal of Polymer Research*. Vol. 18, pp. 1081-1090.

Deshpande, R.P. (2012). Capacitors: Technology and Trends. Tata McGraw-Hill, pp. 1.

Devaraju, N.G., Kim, E.S. & Lee, B.I. (2005). The Synthesis and Dielectric Study of $BaTiO_3$/Polyimide Nanocomposite Films. *Microelectronic Engineering*. Vol. 82, pp. 71-83.

Doane, D.A & Franzon, P.D. (1993). Multichip Module Technologies and Alternatives: The Basics. New York: Van Nostrand Reinhold. pp. 232.

Dodiuk, H. & Goodman, S.H. (2013). Handbook of Thermoset Plastics, Third Edition. William Andrew. pp. 192.

Dufton, P.W. (2000). Lightweight Thermoset Composites: Materials in Use, Their Processing and Applications. iSmithers Rapra. pp. 10.

Dunn, D.J. (2003). Adhesives and Sealants: Technology, Applications and Markets. iSmithers Rapra. pp. 27.

Duran, P., Gutierrez, D., Tartaj, J. & Moure, C. (2002). Densification Behaviour, Microstructure Development and Dielectric Properties of Pure $BaTiO_3$ Prepared by Thermal Decomposition of (Ba,Ti)-Citrate Polyester Resins. *Ceramics International*. Vol. 28, pp. 283-292.

Emslie, A.G., Bonner, F.T. & Peck, L.G. (1958). Flow of a Viscous Liquid on a Rotating Disk. *Journal of Applied Physics.* Vol.29, pp. 858-862.

Erjavec, J. (2013). Hybrid, Electric and Fuel-Cell Vehicles, Second Edition. Cengage Learning. pp. 81.

Etika, K.C., Liu, L., Hess, L.A & Grunlan, J.C. (2009). The Influence of Synergetic Stabilization of Carbon Black and Clay on the Electrical and Mechanical Properties of Epoxy Composites. *Carbon*. Vol. 47, pp. 3128-3136.

Fariz, A.R. (2013). Investigation of Magnesium Doped Calcium Copper Titanate ($CaCu_3Ti_4O_{12}$) on Ca and Cu Site Prepared by Solid State Reaction Method. MSc Thesis, Universiti Sains Malaysia.

Fayomi, C.J.B, Sawan, M. & Roberts, G.W. (2004). Reliable Circuit Techniques for Low-Voltage Analog Design in Deep Submicron Standard CMOS: A Tutorial. *Analog Integrated Circuits and Signal Processing*. Vol. 39, pp. 21-38.

Feng, M., Huang, X., Tang, H. & Liu, X. (2014). Effects of Surface Modification on Interfacial and Rheological Properties of CCTO/PEN Composite Films. *Colloids and Surfaces A: Physicochem. Eng. Aspects*. Vol. 441, pp. 556-564.

Foo, E. (2012). Fabrication and Properties of Silica-Epoxy Thin Film Composite. MSc Thesis. Universiti Sains Malaysia.

Fowler, R.J. (1994). Electricity: Principles and Applications, Fouth Edition. New York: Macmillan/McGraw-Hill.

Gao, L.X., Li, L., Qi, X.R., Wei, W.X., Hai, J.L., Gao, W.Q. & Gao, Z.W. (2013). Enhancement on Electric Responses of $BaTiO_3$ Particles with Polymer-Coating. *Polymer Composites*. Vol. 34, pp. 897-903.

Gerke, R.D. (2005). Embedded Passives Technology An Overview. Report by NASA. pp. 9.

Gorzkowski, E.P., Pan, M.J., Bender, B. & Wu, C.C.M. (2007). Glass–Ceramics of Barium Strontium Titanate for High Energy Density Capacitors. *Journal of Electroceramics*. Vol. 18, pp. 269-276.

Goyanes, S.N., Marconi, J.D., Konig, P.G., Martin, M.D. & Mondragon, I. (2000). Dynamic Properties of Epoxy Composites Filled with Quartz Powder. *Journal of Alloys and Compounds*. Vol. 310, pp. 374-377.

Haertling, G.H. (1999). Ferroelectric Ceramics: History and Technology. *Journal of the American Ceramic Society*. Vol. 82, pp. 797-818.

Halimatudahliana, Ismail, H. & Nasir, M. (2002). The Effect of Various Compatibilizers on Mechanical Properties of Polystyrene/Polypropylene Blend. *Polymer Testing*. Vol. 21, pp. 163-170.

Han, C.D. (1981). Multiple Flow in Polymer Processing. Academic Press, Inc. pp 124.

Han, D.F., Zhang, Q.M., Luo, J., Tang, Q. & Du, J. (2012). Optimization of Energy Storage Density in ANb_2O_6–$NaNbO_3$–SiO_2 (A=[(1-x)Pb, xSr]) Nanostructured Glass–Ceramic Dielectrics. *Ceramics International*. Vol. 38, pp. 6903-6906.

He, L., Neaton, J., Cohen, M., Vanderbilt, D., & Homes, C. (2002). First-Principles Study of the Structure and Lattice Dielectric Response of $CaCu_3Ti_4O_{12}$. *Physical Review B*. Vol. 65, pp. 1-11.

Helmi, A.K., Hazizan, M.A. & Shuhadah, M.S. (2013). Hybrid Multiwalled Carbon Nanotubes/Minerals as Potential Fillers for Polymer Composites. *Advanced Materials Research*. Vol. 620, pp. 236-240.

Hepburn, D.M., Kemp, I.J. & Shields, A.J. (2000). Mica. *IEEE Electrical Insulation Magazine*. Vol. 16, pp. 19-24.

Hirano, H., Kadota, J., Yamashita, T. & Agari, Y. (2012). Treatment of Inorganic Filler Surface by Silane-Coupling Agent: Investigation of Treatment Condition and Analysis of Bonding State of Reacted Agent. *World Academy of Science, Engineering and Technology*. Vol. 6, pp.177-181.

Holand, W. & Beall, G.H. (2012). Glass Ceramic Technology, Second Edition. Wiley-American Ceramic Society.

Homes, C.C., Vogt, T., Shapiro, S.M., Wakimoto, S. & Ramirez, A.P. (2001). Optical Response of High-Dielectric Constant Perovskite-Related Oxide. *Science*. Vol. 293, pp. 673-676.

Huang, X., Xie, L., Wu, C. & Jiang, P. (2011). Core-Shell Structured Poly(Methyl Methacrylate)/$BaTiO_3$ Nanocomposites Prepared by In Situ Atom Transfer Radical Polymerization: A Route To High Dielectric Constant Materials with the Inherent Low Loss of the Base Polymer. *Journal of Materials Chemistry*. Vol. 21, pp. 5897-5906.

Hwu, J.M., Yu, W.H., Yang, W.C., Chen, Y.W. & Chou, Y.Y. (2005). Characterization of Dielectric Barium Titanate Powders Prepared by Homogeneous Precipitation Chemical Reaction for Embedded Capacitor Applications. *Materials Research Bulletin*. Vol. 40, pp. 1662-1679.

Ibrhium, L.Q., Ismail, M.M. & Aldabbagh, B.M. (2013). Dielectric Constant of nano-CCTO/Epoxy Composite. *Journal of Applied Physics*. Vol. 5, pp. 49-54.

Ioannou, G., Patsidis, A. & Psarras, G.C. (2011). Dielectric and Functional Properties of Polymer Matrix/ZnO/$BaTiO_3$ Hybrid Composites. *Composites Part A*. Vol. 42, pp. 104-110.

Jain, P. & Rymaszewski, E.J. (2003). Thin Film Capacitors for Packaged Electronics. Springer. pp. 11.

Jeefferie, A.R., Yuhazri, M.Y., Nooririnah, O., Haidir, M.M., Sihombing, H., Mohd Salleh, M.A. & Ibrahim, N.A. (2010). Thermomechanical and Morpological Interrelationship of Polypropylene/Multiwalled Carbon Nanotubes (PP/MWCNTs) Nanocomposites. *International Journal of Basic & Applied Sciences*. Vol. 10, pp. 22-27.

Julie, J.M., Sabar, D.H. & Zainal, A.A. (2006). The Effect of Compaction Pressure on the CCTO Formation and Dielectric Properties via Solid State Technique. In: Proceeding of the 6th National Seminar on Neutron and X-Ray Scattering. pp. 79-81.

Keithley, J.F. (1999) The Story of Electrical and Magnetic Measurements From 500 BC to the 1940s. John Wiley & Sons. pp. 21.

Kim, S.H., Koo, C.Y., Cheon, J.H., Ha, J., Lee, J.W., Lee, I.H., Kim, W.S. & Brian, L. (2009). High Dielectric PLZT Thin Film for Embedded Capacitors. *Journal of the Korean Physical Society*. Vol. 54, pp. 840-843.

Kochetov, R., Andritsch, T., Lafont, U., Morshuis, P.H.F. & Smit, J.J. (2009). Thermal Conductivity of Nano-Filled Epoxy Systems. In: CEIDP '09. IEEE Conference on Electrical Insulation and Dielectric Phenomena, Virginia Beach, US. pp. 658-661.

Kord, B. (2011). Effect of Calcium Carbonate as Mineral Filler on the Physical and Mechanical Properties of Wood Based Composites. *World Applied Sciences Journal*. Vol. 13, pp. 129-132.

Kroschwitz, J.I., Bailey, B., Carter, C.P., Thomas, S., Gonzalez, D. & Murrell, S. (2004). Encyclopedia of Polymer Science and Technology. Hoboken, USA: Wiley-Interscience. pp. 9.

Lampman, S. (2003). Engineering Plastics: An Introduction. Characterisation and Failure Analysis of Plastics. ASM International. pp. 3-27.

Lawrence, C.J. (1988). The Mechanics of Spin Coating of Polymer Films. *Physics of Fluids*. Vol. 31, pp. 2786-2795.

Lee, A.M. (1990). International Encyclopedia of Composites. New York: VCH Publishers, Inc. pp. 102-115.

Lee, K.J. (2005). Fabrication and Reliability Assessment of Embedded Passives in Organic Substrate. MSc Thesis, Georgia Institute of Technology.

Lee, S., Hyun, J.G., Kim, H. & Paik, K.W. (2007). A Study on Dielectric Constants of Epoxy/$SrTiO_3$ Composite for Embedded Capacitor Films (ECDs). *IEEE Transactions on Advanced Packaging*. Vol. 30, pp. 428-433.

Leong, Y.W., Mohd. Ishak, Z.A. & Ariffin, A. (2004). Mechanical and Thermal Properties of Talc and Calcium Carbonate Filled Polypropylene Hybrid Composites. *Journal of Applied Polymer Science*. Vol. 91, pp. 3327-3336.

Leszczynska, A., Njuguna, J., Pielichowski, K. & Banerjee, J.R. (2007). Thermally Stable and Flame Retardant Polymer Nanocomposites. *Thermochimica Acta*. Vol. 454, pp. 75-96.

Li, J.C., Ba, D.C. & Song, Y.L. (2010). Organic Nanostructured Thin Film Devices and Coatings for Clean Energy. CRC Press. pp. 189-201.

Li, Y.C, Tjong, S.C. & Li, R.K.Y. (2011). Dielectric Properties of Binary Polyvinylidene Fluoride/Barium Titanate Nanocomposites and their Nanographite Doped Hybrids. *Polymer Letters*. Vol. 5, pp. 526-534.

Lin, I.N., Yang, W.C. & Hu. C.T. (2004). Base-Metal-Electroded $BaTiO_3$ Capacitor Materials with Duplex Microstructures. *Journal of the American Ceramic Society*. Vol. 87, pp. 851-858.

Liu, L. & Grunlan, J.C. (2007). Clay Assisted Dispersion of Carbon Nanotubes in Conductive Epoxy Nanocomposites. *Advanced Functional Materials*. Vol. 17, pp. 2343-2348.

Lu, J. (2008). High Dielectric Constant Polymer Nanocomposites For Embedded Capacitor Applications. Ph.D Thesis, Georgia Institute of Technology.

Lu, J., Moon, K.S., Kim, B.K. & Wong, C.P. (2007). High Dielectric Contant Polyaniline/Epoxy via In Situ Polymerization for Embedded Capacitor Applications. *Polymer*. Vol. 48, pp. 1510-1516.

Lu, J. & Wong, C.P. (2008). Nanoparticle-based High-k Dielectric Composites: Opportunities and Challenges. Nanopackaging: Nanotechnologies and Electronics Packaging. Ed. J. Morris, D. Mallik, Springer-Verlag New York Inc.

Luo, S., Sun, R., Zhang, J., Yu, S., Du, R. & Zhang, Z. (2009). Synthesis and Characterization of Nano $BaTiO_3$/epoxy Composites for Embedded Capacitors. In: International Conference on Electronic Packaging Technology & High Density Packaging. IEEE. pp. 865-859.

Luo, S., Yu, S., Sun, R. & Wong, C.P. (2014). Nano Ag-Deposited $BaTiO_3$ Hybrid Particles as Fillers for Polymeric Dielectric Composites: Toward High Dielectric Constant and Suppressed Loss. *Applied Materials & Interfaces*. Vol. 6, pp. 176-182.

Mandal, S. & Alam, S. (2011). Dynamic Mechanical Analysis and Morphological Studies of Glass/Bamboo Fiber Reinforced Unsaturated Polyester Resin-Based Hybrid Composites. *Journal of Applied Polymer Science*. Vol. 125, pp. 382-387.

Mandal, S., Alam, S., Varma, I.K. & Maiti, S.N. (2008). Studies on Bamboo/Glass Fiber Reinforced USP and VE Resin. *Journal of Reinforced Plastics and Composites*. Vol. 29, pp. 43-51.

Manfred, W. & Markus, W. (2010). Phenols. Phenolic Resins: A Century of Progress. Springer- Verlag Berlin Heidelberg. pp. 9-24.

Manik, S.K. & Pradhan, S.K. (2006). Microstructure Characterization of Ball-Mill-Prepared Nanocrystalline $CaCu_3Ti_4O_{12}$ by Rietveld Method. *Physica E: Low-dimensional Systems and Nanostructures*. Vol. 33, pp. 160-168.

Marcovich, N.E., Reboredo, M.M. & Aranguren, M.I. (1999). Moisture Diffusion in Polyester-Woodflour Composites. *Polymer*. Vol. 40, pp. 7313-7320.

Margem, F.M., Monteiro, S.N., Neto, J.B., Rodriguez, R.J.S. & Soares, B.G. (2010). The Dynamic-Mechanical Behavior of Epoxy Matrix Composites Reinforced with Ramie Fibers. *Revista Matéria*. Vol. 15, pp. 167-175.

McGrath, L.M., Parnas, R.S., King, S.H., Schroeder, J.L, Fischer, D.A. & Lenhart, J.L. (2008). Investigation of the Thermal, Mechanical and Fracture Properties of Alumina Epoxy Composites. *Polymer*. Vol. 49, pp. 999-1014.

Miyagawa, H., Misra, M., Drzal, L.T. & Mohanty, A.K. (2005). Fracture Toughness and Impact Strength of Anhydride-cured Biobased Epoxy. *Polymer Engineering & Science*. Vol. 45, pp. 487-495.

Muhammad Firdaus, S. (2014). Fabrication and Characterization of Nano-Sized Filler Filled Epoxy Composites for Electronic Application. MSc Thesis. Universiti Sains Malaysia.

Nan, G. (2006). Pellicles and Films Making from Polymer Solution. *Buletinul Universiti Petrol*. Vol. 8, pp. 99-102.

Ng, C.H. (2013). Properties of Various Types of Mineral and Ceramic Fillers in Epoxy Composite. Bachelor's Thesis. Universiti Sains Malaysia.

NPCS Board of Consultant & Engineers. (2007). Phenolic Resins Technology Handbook. Niir Project Consultancy Services.

Nurdina, A.K. (2010). Studies on the Properties of Single and Hybrid Mineral Fillers Filled Polypropylene Composites. MSc Thesis. Universiti Sains Malaysia.

Oleksy, M., Karolina, S.R., Heneczkowski, M., Oliwa, R. & Jesionowski, T. (2014). Epoxy Resin Composite Based on Functional Hybrid Fillers. *Materials*. Vol. 7, pp. 6064-6091.

Owen, S. (1993). Epoxy Resins-Water Borne. Surface Coatings: Raw Materials and Their Usage. Chapman & Hall. Vol. 1, pp. 193-197.

Pabst, W. & Gregorová, E. (2007). Characterization of Particles and Particle Systems. *Pabst & Gregorová (ICT Prague)*. pp. 4.

Paipetis, A. & Kostopoulos, V. (2012). Carbon Nanotube Enhanced Aerospace Composite Materials: A New Generation of Multifunctional Hybrid Structural Composites. Springer Science & Business Media. pp. 160.

Park, J.M., Kim, D.S., Lee, J.R. & Kim, T.W. (2003). Nondestructive Damage Sensitivity and Reinforcing Effect of Carbon Nanotube/Epoxy Composites using Electro-Mechanical Technique. *Journal of Materials Science and Engineering: C*. Vol. 23, pp. 971-975.

Park, S.J. (2014). Matrices for Carbon Fiber Composites. Carbon Fibers. Springer. pp. 74.

Particle Sciences. (2010). Technical Brief, Vol. 3. [Online]. [Accessed 28th December 2014]. Available from World Wide Web: http://www.particlesciences.com/docs/technical_briefs/TB_2010_3.pdf.

Peter A. Sandborn (2003). A review of the Economics of Embedded Passives. International Electronic Packaging Technical Conference and Exhibition.

Pfahl, R.C. & McElroy, J. (2005). The 2004 International Electronics Manufacturing Initiative (iNEMI) Technology Roadmaps. In: Conference on High Density Microsystem Design and Packaging and Component Failure Analysis. IEEE. pp. 1-7.

Poh, C.L., Mariatti, M., Ahmad Fauzi, M.N., Ng, C.H., Chee, C.K. & Chuah, T.P. (2014). Tensile, Dielectric and Thermal Properties of Epoxy Composites Filled with Silica, Mica and Calcium Carbonate. *Journal of Materials Science: Materials in Electronics*. Vol. 25, pp. 2111-2119.

Pongdhorn, S., Uthai, T. & Kannika, H. (2004). Effect of Curing System on Reinforcing Efficiency of Silane Coupling Agent. *Polymer Testing*. Vol. 23, pp. 397-403.

Prakash, B.S. & Varma, K.B.R. (2007). Dielectric Behaviour of CCTO/epoxy and Al-CCTO/epoxy Composites. *Composites Science and Technology*. Vol. 67, pp. 2362-2368.

Prall, K.M. (2000). The Viscoelastic Behavior of Pigmented Latex Coating Films. Ph.D Thesis. University of Maine.

Rahaman, M.N. (2007). Ceramic Processing. CRC Press. pp. 242-243.

Ramajo, L., Castro, M.S. & Reboredo, M.M. (2007) Effect of Silane as Coupling Agent on the Dielectric Properties of $BaTiO_3$-epoxy Composites. *Composites Part A: Applied Science and Manufacturing*. Vol. 38, pp. 1852-1859.

Ramajo, L., Ramírez, M.A., Bueno, P.R., Reboredo, M.M. & Castro, M.S. (2007). Differences Between the Dielectric Properties of $CaCu_3Ti_4O_{12}$-Epoxy And $BaTiO_3$-Epoxy Composites. In: Congreso SAM/CONAMET 2007. Vol. 4, pp. 1240-1244.

Ramajo, L.A., Ramirez, M.A. & Bueno, P.R. (2008). Dielectric Behaviour of $CaCu_3Ti_4O_{12}$-Epoxy Composites. *Materials Research*. Vol. 11, pp. 85-88.

Ramirez, A.P., Subramanian, M.A., Gardel, M., Blumberg, G., Li, D., Vogt, T. & Shapiro, S. (2000). Giant Dielectric Constant Response in a Copper-Titanate. *Solid State Communications*. Vol. 115, pp. 217-220.

Ramkumar, S., Ghaffarian, R. & Varanasi, A. (2006). Lead-free 0201 Manufacturing, Assembly and Reliability Test Results. *Microelectronics Reliability*. Vol. 46, pp. 244-262.

Rao, Y. (2001). High Dielectric Constant Material Development and Electrical Simulation of Embedded Capacitors. Ph.D Thesis, Georgia Institute of Technology.

Rao, Y., Ogitani, S., Kohl, P., Wong, C.P. (2002). Novel Polymer–Ceramic Nanocomposite Based on High Dielectric Constant Epoxy Formula for Embedded Capacitor Application. *Journal of Applied Polymer Science*. Vol. 83, pp. 1084-1090.

Rao, Y. & Wong, C.P. (2004). Material Characterization of a High-Dielectric-Constant Polymer–Ceramic Composite for Embedded Capacitor for RF Applications. *Journal of Applied Polymer Science*. Vol. 92, pp. 2228-2231.

Ratna, D. (2005). Epoxy Composites: Impact Resistance and Flame Retardancy. Shawburry Shrewsbury, UK: Smithers Rapra Technology. Vol. 16.

Sahu, N., Parija, B. & Panigrahi, S. (2009). Fundamental Understanding and Modeling of Spin Coating Process : A review. *Indian Journal of Physics*. Vol. 83, pp. 493-502.

Salmah, H., Koay, S.C. & Hakimah, O. (2012). Surface Modification of Coconut Shell Powder Filled Polylactic Acid Biocomposites. *Journal of Thermoplastic Composite Material*. Vol. 26, pp. 809-819.

Sandborn, P.A. (2003). The Economics of Embedded Passives, Integrated Passive Component Technology. Wiley-IEEE Press. pp. 1-31.

Sarjeant, W. J., Zirnheld, J., MacDougall, F.W., Bowers, J.S., Clark, N., Clelland, I.W., Price, R.A., Hudis, M., Kohlberg, I., McDuff, G., McNab, I., Parler Jr, S.G. & Prymak, J. (1999). Capacitors-Past, Present and Future. Handbook of Low and High Dielectric Constant Materials and Their Applications. Academic Press. Vol. 2, pp. 423-491.

Sarojadevi, M. & Bhuvana, S. (2009). Structure Property Relationships in Processable Heat Resistant Poly(amide-imide-imide)s for High Temperature Applications. Polyimides and Other High Temperature Polymers: Synthesis, Characterization and Applications. Vol. 5, pp. 93-117.

Sarojadevi, M., Hariharanand, R. & Amutha, N. (2009). Synthesis and Properties of Novel Bismaleimides, Polyaspartimides and Organosoluble Polyimides. Polyimides and Other High Temperature Polymers: Synthesis, Characterization and Applications. CRC Press. Vol 5, pp. 43-70.

Schonhorn, H. (1985). Adhesion and Adhesives: Interactions at Interfaces. *Journal of Plastic Film and Sheeting*. Vol. 1, pp. 163-179.

Seema, A., Dayas, K.R., Varghese, J.M. (2007). PVDF-PZT-5H Composites Prepared by Hot Press and Tape Casting Techniques. *Journal of Applied Polymer Science*. Vol. 106, pp. 146-151.

Sharif, N.S.A. (2010). Effect of Lanthanum Oxide (La_2O_3) Addition on the Properties of Calcium Copper Titanate ($CaCu_3Ti_4O_{12}$). MSc Thesis. Universiti Sains Malaysia.

Shi, D. (2006). Introduction to Biomaterials. World Scientific. pp. 201.

Shireesha, G., Manjunatha, C., Jain, A. & Radhakrishna, M.C. (2013). Preparation and Characterization of Poly(vinylidenefluoride)–$CdSiO_3$ Nanocomposite Thin Films. In: Workshop on Advanced Materials Manufacturing Management and Thermal Studies, Tumkur.

Shriprakash, B. & Varma, K.B.R. (2007). Dielectric Behavior of CCTO/epoxy and Al-CCTO/epoxy Composites. *Journal of Composite Science and Technology*. Vol. 67, pp. 2363-2368.

Siemann, U. (2005). Solvent Cast Technology- A Versatile Tool for Thin Film Production. *Progress in Colloid & Polymer Science*. Vol. 130, pp. 1-14.

Sirdeshmukh, D.B., Sirdeshmukh, L. & Subhadra, K.G. (2006). Micro- and Macro-Properties of Solids: Thermal, Mechanical and Dielectric Properties. New York: Springer-Verlay Berlin Heidelberg. pp.199-504.

Stephen, A.D. (2001). Survey of Instrumentation and Measurement. John Wiley & Sons, pp. 277-290.

Subramanian, M.A., Li, D., Duan, N., Reisner, B. A. & Sleight, A. W. (2000). High Dielectric Constant in $ACu_3Ti_4O_{12}$ and $ACu_3Ti_3FeO_{12}$ Phases. *Journal of Solid State Chemistry*. Vol. 151, pp. 323-325.

Sun, Y., Zhang, Z. & Wong, C.P. (2006). Study and Characterization on the Nanocomposite Underfill for Flip Chip Applications. *IEEE Transactions on Components and Packaging Technologies*. Vol. 29, pp. 190-197.

Suriati, G., Mariatti, M. & Azizan, A. (2012). Improvement of Properties of Silver Filled Epoxy Composites via Processing Method. *Moldavian Journal of the Physical Sciences*. Vol. 11, pp. 94-105.

Susumu, N., Masuo, K. & Toru, M. (1998). Dynamic Viscoelastic Properties and Thermal Properties of Ni Powder-Epoxy Resin Composite. *Journal of Applied Polymer Science*. Vol. 69, pp. 2593-2598.

Tee, D.I., Mariatti, M., Azizan, A., See, C.H. & Chong, K.F. (2007). Effect of Silane-based Coupling Agent on the Properties of Silver Nanoparticles Filled Epoxy Composites. *Composites Science & Technology*. Vol. 67, pp. 2584-2591.

Teh, P.L. (2008). Development of Core Layer Materials Using Particulate Filled Epoxy Composites. Ph.D Thesis. Universiti Sains Malaysia.

Teh, P.L., Jaafar, M., Akil, H.M., Seetharamu, K.N., Wagiman, A.N.R. & Beh, K.S. (2008). Thermal and Mechanical Properties of Particulate Fillers Filled Epoxy Composites for Electronic Packaging Application. *Polymers for Advanced Technologies*. Vol. 19, pp. 308-315.

Thomas, P., Varughese, K.T., Dwarakanath, K. & Varma, K.B.R. (2010). Dielectric Properties of Poly(vinylidene fluoride)/$CaCu_3Ti_4O_{12}$ Composites. *Composites Science and Technology*. Vol. 70, pp. 539-545.

Thomas, P., Ravindran, R.S.E. & Varma, K.B.R. (2013). Structural, Thermal and Electrical Properties of Poly(Methyl Methacrylate)/$CaCu_3Ti_4O_{12}$ Composite Sheets Fabricated via Melt Mixing. *Journal of Thermal Analysis and Calorimetry*. Vol. 115, pp. 1311-1319.

Tiwari, A., Mishra, A.K., Kobayashi, H. & Turner, A.P.F. (2012). Intelligent Nanomaterials. Wiley-Scrivener Publishing LLC. pp. 803.

Tjong, S.C. & Mai, Y.W. (2010). Physical Properties and Applications of Polymer Nanocomposites, First Edition. Woodhead Publishing in Materials. pp. 119-120.

Todd, M.G. & Shi, M.G. (2003). Characterising The Interphase Dielectric Constant of Polymer Composite Materials: Effect of Chemical Coupling Agents. *Journal of Applied Physics*. Vol. 94, pp. 4551-4557.

Tsangaris, G.M., Kouloumbi, N. & Kyvelidis, S. (1996). Interfacial Relaxation Phenomena in Particulate Composites of Epoxy Resin with Copper or Iron Particles. *Materials Chemistry and Physics*. Vol. 44, pp. 245-250.

Tummala, R. (2001). Fundamentals of Microsystems Packaging, Third Edition. New York: McGraw-Hill Publications.

Tuncer, E., Sauers, I., James, D.R., Alvin, R., Ellis, M., Paranthaman, P., Tolga, A.T., Sathyamurthy, S., Karren, L.M., Li, J. & Goyal, A. (2007). Electrical Properties of Epoxy Resin Based Nano-Composites. *Nanotechnology*. Vol. 18, pp. 25703-25706.

Ulrich, R., Schaper, L., Nelms, D. & Leftwich. M. (2000). Comparison of Paraelectric and Ferroelectric Materials for Applications as Dielectrics in Thin Film Integrated Capacitors. *The International Journal of Microcircuits and Electronic Packaging*. Vol. 23, pp. 172.

Ulrich, R., Schaper, L. (2003). Integrated Passive Component Technology. New York: IEEE Press/ Wiley-Interscience.

Ulrich, R. & Brown, W. (2006). Materials for Microelectronic Packaging. Wiley-IEEE Press. pp. 29-76.

Urbaniak, M. (2010). A Relationship Between the Glass Transition Temperature and the Conversion Degree in the Curing Reaction of the EPY® Epoxy System. *Polimery*, Vol. 56, pp. 240-243.

Vijatović, M.M., Bobić, J.D. & Stojanović, B.D. (2008). History and Challenges of Barium Titanate: Part II. *Science of Sintering*. Vol. 40, pp. 235-244.

Vijayakumari, G. (2009). Engineering Physics, Second Edition. Vikas Publishing House. pp. 373.

Voo, R. (2012). Properties of Various Nano Fillers Filled Epoxy Thin Film Nano Composites. MSc Thesis, Universiti Sains Malaysia.

Voo, R., Mariatti, M. & Sim, L.C. (2012). Thermal Properties and Moisture Absorption of Nanofillers-Filled Epoxy Composite Thin Film for Electronic Application. *Polymers for Advanced Technologies*. Vol. 23, pp. 1620-1627.

Wang, R. (2007). Self Assembly of Hybrid Structures on Nano Templates. Ph.D Thesis. Wayne State University.

Weber, U., Greuel, G., Boettger, U., Weber, S., Hennings, D. & Waser, R. (2001). Dielectric Properties of $Ba(Zr,Ti)O_3$-Based Ferroelectrics for Capacitor Applications. *Journal of the American Ceramic Society*. Vol. 84, pp. 759-766.

Wei, L.Y., Zainal, A.M.I. & Azlan, A. (2006). Polypropylene Hybrid Composites Based on Talc and Calcium Carbonate. *Frontal Polymer Research*. pp. 189-246.

Weon, J.I. & Sue, H.J. (2006). Mechanical Properties of Talc- and $CaCO_3$-Reinforced High-Crystallinity Polypropylene Composites. *Journal of Materials Science*. Vol. 41, pp. 2291-2300.

Whittie, S., Moy, P., Schoch, A., Lenhart, J. & Weerasooriya, T. (2011). Strain Rate Response of Cross-Linked Polymer Epoxies under Uni-Axial Compression. Dynamic Behavior of Materials. In: Proceedings of the 2011 Annual Conference on Experimental and Applied Mechanics. Vol. 1, pp. 57.

Witucki, G.L. (1992). A Silane Primer: Chemistry and Applications of Alkoxy Silanes. In: 57th Annual Meeting of the Federation of Societies for Coatings Technology, Chicago, IL.

Wu, C.C., Chen, Y.C., Su, C.C. & Yang, C.F. (2009). The Chemical and Dielectric Properties of Epoxy/$(Ba_{0.8}Sr_{0.2})(Ti_{0.9}Zr_{0.1})O_3$ Composites for Embedded Capacitor Application. *Journal of European Polymer*. Vol. 45, pp. 1442-1447.

Wu, C.L., Zhang, M.Q., Rong, M.Z. & Friedrich, K. (2002). Tensile Performance Improvement of Low Nanoparticles Filled-Polypropylene Composites. *Composites Science and Technology*. Vol. 62, pp. 1327-1340.

Wu, S.M., Jahja, E., Yen, W.K. & Wang, J.W. (2007). Study of Discrete Capacitor Embedded Process and Characterization Analysis in Organic-Base Substrate. In: 9th Electronics Packaging Technology Conference (EPTC). IEEE. pp. 125-129.

Xanthos, M. (2005). Functional Fillers for Plastics. Wiley-VCH Verlag GmbH & Co. KGaA. Vol. 2, pp. 12.

Xie, S.H., Zhu, B.K., Li, J.B., Wei, X.Z. & Xu, Z.K. (2004). Preparation and Properties of Polyimide/Aluminium Nitride Composites. *Polymer Testing*. Vol. 23, pp. 797-801.

Xu, J., Moon, K.S., Pramanik, P., Bhattacharya, S. & Wong, C.P. (2007). Optimization of Epoxy-Barium Titanate Nanocomposites for High Performance Embedded Capacitor Components. *IEEE Transactions on Components and Packaging Technologies*. Vol. 30, pp. 248-253.

Yang, W., Yu, S., Sun., R. & Du, R. (2011). Nano- and Microsize Effect of CCTO Fillers on the Dielectric Behavior of CCTO/PVDF Composites. Acta Materialia. Vol. 59, pp. 5593-5602.

Yang, C., Song, H.S. & Liu, D.B. (2013). Effect of Coupling Agents on the Dielectric Properties of $CaCu_3Ti_4O_{12}$/PVDF Composites. *Composites Part B: Engineering*. Vol. 50, pp. 180-186.

Yimsiri, P. & Mackley, M.R. (2006). Spin and Dip Coating of Light-Emitting Polymer Solutions: Matching Experiment with Modeling. *Chemical Engineering Science*. Vol. 61, pp. 3496-3505.

Yoon, J.R., Han, J.W. & Lee, K.M. (2009). Dielectric Properties of Polymer-Ceramic Composites for Embedded Capacitors. *Transactions on Electrical and Electronic Materials*. Vol. 10, pp. 116-120.

Zhang, Y., Wang, Y., Deng, Y., Li, M., Bai, J. (2012). High Dielectric Constant and Low Loss in Polymer Composites Filled by Self-Passivated Zinc Particles. *Materials Letters*. Vol. 72, pp. 9-11.

Zhang, Z.F., Bai, X.F., Zha, J.W., Li, W.K. & Dang, Z.M. (2014). Preparation and Dielectric Properties of $BaTiO_3$/epoxy Nanocomposites for Embedded Capacitor Application. *Composites Science and Technology*. Vol. 97, pp. 100-105.

APPENDIX A: The Calculations of CCTO Filler and Matrix Content

Accordingly, the subsequent specimen production is based 30 g as total weight of a composite. Equation 1 simplifies the finding for this step.

$$m_e + m_h + m_f = 30\text{g} \tag{1}$$

where m_e = Weight of epoxy resin (g)

m_h = Weight of hardener or curing agent (g)

m_f = *Weight of ceramic filler (g)*

A formula is needed to convert filler loading in vol% to weight in gram as the filler loading was the variable to be studied and determined in the earliest stage of research. Carlsson and Pipes (1997) stated that the calculation should be started with a basic formula of volume fraction as shown in Equation 2. Derivation of Equation 2 summaries the conversion of filler loading from volume percent to weight in gram as illustrated in Equation 3.

$$V_f = \frac{\frac{m_f}{\rho_f}}{\frac{m_f}{\rho_f}+\frac{m_m}{\rho_m}} \tag{2}$$

$$V_f = \frac{\frac{m_f}{\rho_f}\times\rho_f\rho_m}{\left(\frac{m_f}{\rho_f}\times\rho_f\rho_m\right)+m\left(\frac{m_m}{\rho_m}\times\rho_f\rho_m\right)}$$

$$= \frac{m_f\rho_m}{m_f\rho_m+m_m\rho_f}$$

$$= \frac{m_f\rho_m}{m_f\rho_m+(m_T-m_f)\rho_f}$$

$$= \frac{\rho_m}{\rho_m+\left(\frac{m_T-m_f}{m_f}\times\rho_f\right)}$$

$$= \frac{1}{1+\frac{m_T - m_f}{m_f}\left(\frac{\rho_f}{\rho_m}\right)}$$

$$V_f = \left[\frac{m_T - m_f}{m_f}\left(\frac{\rho_f}{\rho_m}\right) + 1\right]^{-1} \quad (3)$$

where V_f = Volume fraction of filler (volume/volume)

$m_m = m_e + m_h$ = Weight of matrix (g)

ρ_f = Density of filler = 4.7 g/cm^3 (for CCTO) ; 6.08 g/cm^3 (for $BaTiO_3$)

ρ_m = Density of matrix = 1.16 g/cm^3 (for D.E.R.^{TM} 332)

m_T = Total weight of uncured mixture = 30 g

The simplified Equation 3 will be applied to convert filler loading from volume percent to weight (g). After determining the weight for every volume percent of filler loading, they will be subtituted into Equation 1, respectively to yield the weight of matrix system. Equation 4 explain the above sentences in formula form.

$$m_e + m_h = 30\text{g} - m_f \quad (4)$$

The following step is the determination of amount of epoxy resin and curing agent to be used in each filler loading. If 100 g of epoxy resin is going to be used, 32 g of curing agent should be added in. Therefore, the total weight of matrix is supposed to be 132 g. However, based on the predetermined dimensions or volume of the composite, the amount of epoxy resin and curing agent can be calculated using the following equations (Equation 5 and 6).

$$m_e = \frac{100}{132} \times (30 - m_f) \quad (5)$$

$$m_h = \frac{32}{132} \times (30 - m_f) \quad (6)$$

The following is a typical example of calculation for 5 vol% filler filled epoxy composite. The calculation was carried out using Equation 3, 4, 5 and 6. For information, 5 vol % is also equivalent to 0.05 v/v.

$$V_f = \left[\frac{m_T - m_f}{m_f}\left(\frac{\rho_f}{\rho_m}\right) + 1\right]^{-1}$$

$$0.05 = \left[\frac{30 - m_f}{m_f}\left(\frac{4.7}{1.16}\right) + 1\right]^{-1}$$

$$m_f = 5.10 \text{ g}$$

$$m_e + m_h = 30\text{g} - m_f$$

$$= (30 - 5.10) \text{ g}$$

$$= 24.90 \text{ g}$$

$$m_e = \frac{100}{132} \times 24.90$$

$$= 18.86 \text{ g}$$

$$m_h = \frac{32}{132} \times 24.90$$

$$= 6.04 \text{ g}$$

Each of the calculated values will be used to prepare the particular composites. Table 1 summaries the amounts of epoxy resin, curing agent and CCTO ceramics in terms of weight for each filler loading. The calculations for each filler loading are based on the same methods.

Table 1 : Content of the resulting composites at different filler loading

CCTO Filler Loading (vol %)	Content of Composites			
	Amount of CCTO (g)	**Amount of Epoxy Resin (g)**	**Amount of Curing Agent (g)**	**Total Weight of Uncured Mixture (g)**
0	0	22.73	7.27	30
5	5.10	18.86	6.04	30
10	8.72	16.12	5.16	30
15	11.43	14.07	4.50	30
20	13.54	12.47	3.99	30
30	22.09	13.57	4.34	40
40	24.89	11.45	3.66	40

APPENDIX B: Calculation for the Quantity of GPTMS Silane Coupling Agent at the Corresponding Filler Concentration

A weight ratio of GPTMS:CCTO at 1:10 had been applied in the present study (Equation 7). Note that the amount of fillers will remain the same (as mentioned in Appendix A). The calculation of the quantity of GPTMS will be based on the previous filler concentration. It was done according to Equation 8 and 9.

$$silane : CCTO = 1 : 10 \text{ (by weight)} \tag{7}$$

$$m_f = \frac{10}{11} \times m_{f+silane} \tag{8}$$

$$m_{silane} = \frac{1}{11} \times m_{f+silane} \tag{9}$$

where $m_{f+silane}$ = Total weight of filler and silane coupling agent (g)

m_f = Amount of GPTMS needed (g)

A simple step of calculation will be performed at a filler loading of 20vol % using Equation 8 and 9, as shown in the following.

$$m_f = \frac{10}{11} \times m_{f+silane}$$

$$13.54 = \frac{10}{11} \times m_{f+silane}$$

$$m_{f+silane} = 14.89 \text{ g}$$

$$m_{silane} = \frac{1}{11} \times m_{f+silane}$$

$$m_{silane} = \frac{1}{11} \times 14.89$$

$$= 1.35 \text{ g}$$

The quantity of GPTMS needed for 20 vol% filler loading is listed in Table 2.

Table 2 : Content of GPTMS for CCTO filler treatment

CCTO Filler Loading (vol %)	m_f (g)	$m_{f+silane}$ (g)	m_{silane} (g)
20	13.54	14.89	1.35

APPENDIX C: The Dilution of GPTMS Silane Coupling Agent by Ethanol

Due to relatively small amount of GPTMS, it needs to be diluted in a low-boiling-point solvent in order for all parts of filler to be completely wetted and coated by GPTMS. The selected silane-based coupling agent was delivered in liquid form and prior to application, it was diluted in ethanol to make up 1%, 5% and 10% solution, respectively.

To make up a 1%, 5% and 10% silane solutions in ethanol, a volume ratio of GPTMS : ethanol should be followed as stated in Equation 10.

$$silane : ethanol = 10 : 90 = 1 : 9 \text{ (by volume)} \tag{10}$$

Since the selected silane-based coupling agent has a known density of 1.07 g/ml, the volume of 1.35 g silane could be calculated based on Equation 11.

$$V_{silane} = \frac{m_{silane}}{\rho_{silane}} \tag{11}$$

where V_{silane} = Volume of GPTMS (ml)

ρ_{silane} = Density of GPTMS = 1.07 g/ml

The 1%, 5% and 10% silane solutions should be compromised of V_{silane} ml (or equivalent to m_{silane} g) of 3-glycidoxypropyltrimethoxysilane. After obtaining the amount of silane in terms of volume, a total volume of GPTMS and ethanol may be calculated based on Equation 12.

$$\frac{V_{silane}}{V_{silane+ethanol}} \times 100\% = 1\% / 5\% / 10\% \quad (12)$$

where $V_{silane+ethanol}$ = Total volume of GPTMS/ethanol solution (ml)

The quantity of ethanol needed in terms of volume to prepare a solution containing 1%, 5% and 10% of GPTMS might be obtained from the following equation (Equation 13).

$$V_{ethanol} = V_{silane+ethanol} - V_{silane} \quad (13)$$

where $V_{ethanol}$ = Amount of ethanol (ml)

The amount of ethanol in terms of volume could be converted to weight for the ease of measurement by applying Equation 14.

$$m_{ethanol} = \rho_{ethanol} \times V_{ethanol} \quad (14)$$

where $m_{ethanol}$ = Weight of ethanol needed for dilution of GPTMS (g)

In order to provide further understanding on the above calculations using Equation 11, 12, 13 and 14, the following example might help. By taking 20 vol% of CCTO and 1% of GPTMS as an example.

$$V_{silane} = \frac{m_{silane}}{\rho_{silane}}$$

$$V_{silane} = \frac{1.35}{1.07}$$

$$= 1.27 \text{ ml}$$

$$\frac{V_{silane}}{V_{silane+ethanol}} \times 100\% = 1\%$$

$$\frac{1.27}{V_{silane+ethanol}} \times 100\% = 1\%$$

$$V_{silane+ethanol} = 126.5 \text{ ml}$$

$$V_{ethanol} = V_{silane+ethanol} - V_{silane}$$

$$V_{ethanol} = 126.5 - 1.27$$

$$= 125.24 \text{ ml}$$

$$m_{ethanol} = \rho_{ethanol} \times V_{ethanol}$$

$$m_{ethanol} = 0.789 \times 125.24$$

$$= 98.81 \text{ g}$$

Table 3 represent a list of ethanol content required for the preparation of GPTMS for 20 vol% of CCTO filler.

Table 3 : The quantity of ethanol required for the preparation of 1%, 5% and 10% GPTMS solutions for 20 vol% of CCTO filler

Concentration of GPTMS	m_f (g)	m_{silane} (g)	V_{silane} (ml)	$V_{silane+ethanol}$ (ml)	$V_{ethanol}$ (ml)	$m_{ethanol}$ (g)
1 %	13.54	1.35	1.27	126.50	125.24	98.81
5 %	13.54	1.35	1.27	25.30	24.04	18.96
10 %	13.54	1.35	1.27	12.65	11.39	8.98

LIST OF PUBLICATIONS

Journals

Saidina, D.S., Mariatti, M. & Julie, M.J. (2014). Properties of Calcium Copper Titanate and Barium Titanate Filled Epoxy Composites for Electronic Applications: Effect of Filler Loading and Hybrid Fillers. *Journal of Materials Science: Materials in Electronics*. Vol. 25, pp. 4923-4932.

Saidina, D.S., Mariatti, M. & Juliewatty, J. (2015). Tensile and Dielectric Properties of Calcium Copper Titanate in Epoxy Composites. *Advanced Materials Research*. Vol. 1107.

Conference Proceeding

Saidina, D.S., Mariatti, M. & Juliewatty, J. (2014). Thermal Properties and Dynamic Mechanical Properties of Ceramic Fillers Filled Epoxy Composites. *Proceedings of the 23rd Scientific Conference of the Microscopy Society Malaysia (SCMSM2014)*. 10th-12th December 2014, Universiti Teknologi Petronas, Tronoh, Perak.